ISSN 1097-8135

Life Science Journal

Acta Zhengzhou University Overseas Edition

Volume 3 Number 1, January 2006

Life Science Journal

Volume 3 Number 1 January 2006

Life Science Journal

Acta Zhengzhou University Overseas Edition

Life Science Journal, the Acta Zhengzhou University Overseas Edition, is an international journal with the purpose to enhance our natural and scientific knowledge dissemination in the world under the free publication principle. The journal is calling for papers from all who are associated with Zhengzhou University – home and abroad. Any valuable papers or reports that are related to life science are welcome. Other academic articles that are less relevant but are of high quality will also be considered and published. Papers submitted could be reviews, objective descriptions, research reports, opinions/debates, news, letters, and other types of writings. All publications of *Life Science Journal* are under vigorous peer-review. Let's work together to disseminate our research results and our opinions.

CONTENTS

Cardiac Resynchronization Therapy for Congestive Heart Failure

Lexin Wang

School of Biomedical Sciences, Charles Sturt University, New South Wales, Australia

Abstract: Congestive heart failure (CHF) is a leading cause of morbidity and mortality worldwide. Many CHF patients have intraventricular conduction delays such as right or left bundle branch block or non-specific QRS widening on the body surface ECG. Intraventricular conduction delays cause dyssynchrony of the ventricles, leading to regional movement abnormalities and worsening of cardiac function. Recent clinical trials have indicated that cardiac resynchronization therapy improves cardiac function class, exercise tolerance, maximum oxygen consumption and quality of life in patients with moderate to severe heart failure. It is also associated with a significant reduction in mortality and hospital admissions for heart failure. [Life Science Journal. 2006;3(1):1-4] (ISSN: 1097-8135).

Keywords: heart failure; cardiac resynchronization therapy; cardiac electrophysiology

1 Introduction

Congestive heart failure (CHF) is a common cardiovascular disease and a leading cause of morbidity and mortality around the world. Despite major advances in pharmacological therapy in the past 2 decades, CHF is still associated with a high morbidity and mortality rate (The CONSENSUS Trial Study Group, 1987; Bristow, 2000). Recently, the effects of cardiac resynchronization therapy, or biventricular pacing, on heart failure have been investigated in a number of clinical trials (Leclercq, 1998; Alonso, 1999; Auricchio, 1999; Gras, 1998; Leclercq, 2000; Etienne, 2001; Lau, 2000; Cazeau, 2001; Braunschweig, 2000; Abraham, 2002 ; Higgins, 2003; Bristow, 2004; Cleland, 2005). The rationale for the resynchronization therapy is that many of the heart failure patients have intraventricular conduction delays, leading to poor coordination of ventricular contraction and relaxation (dyssynchrony) and worsening cardiac function (Farwell, 2000; Aaronson, 1997; Shenkman, 2002; Xiao, 1992; Littmann, 2000).

Results from major clinical studies have demonstrated that cardiac resynchronization therapy provides significant improvement in cardiac function, exercise tolerance and quality of life (Leclercq, 1998; Alonso, 1999; Auricchio, 1999; Gras, 1998; Leclercq, 2000; Etienne, 2001; Lau, 2000; Cazeau, 2001; Braunschweig, 2000). MIRACLE trial, one of the largest clinical trials on cardiac resynchronization therapy, presents some convincing evidence on the efficacy of cardiac resynchronization therapy in treating moderate to severe CHF (Abraham, 2002). However, no clear benefits on short-term mortality are observed in the study. Two recent trials, the COMPANION (Bristow, 2004) and CARE-HF (Cleland, 2005), have demonstrated that cardiac resynchronization therapy, with or without implantable defibrillator, not only improves patient's quality of life but also reduces the mortality in short- and medium-term. The primary aims of this paper are to review the most recent landmark clinical trials and evaluate the therapeutic effects of cardiac resynchronization on CHF.

2 Rationale of Cardiac Resynchronization Therapy

Intraventricular conduction delays, such as right or left bundle branch block (RBBB or LBBB), or non-specific wide QRS complex, occurs in more than 20% of patients with CHF (Farwell, 2000; Shenkman, 2002). Such conduction delays are the primary causes of dyssynchrony of the ventricles. They have a negative impact on the failing heart to eject blood and are major contributors of worsening clinical symptoms. QRS duration is closely related to the level of ejection fraction, the wider the QRS duration, the lower the ejection fraction (Shenkman, 2002). LBBB alone is associated with a 13% increase in the left ventricular end-systolic diameter and 40% reduction in left ventricular ejection fraction. Left ventricular dyssynchrony also enhances the severity of the mitral regurgitation in CHF patients (Xiao, 1992; Littmann, 2000; Saxon, 1998; Kerwin, 2000).

Furthermore, intraventricular conduction de-

lays have been found to correlate with an increased risk of death in CHF patients (Xiao, 1996; Shamim, 1999; Hesse, 2001). The highest 5-year mortality has been found in those with QRS duration between 120 – 140 ms (Shenkman, 2002). Both LBBB and RBBB are associated with elevated and equal all-cause mortality rates in a general population (Hesse, 2001).

The current indications for cardiac resynchronzation therapy are that patients are in New York Heart Association class Ⅲ or Ⅳ despite standard pharmacological therapy, with a left ventricular ejection fraction of less than 35 per cent and left ventricular end-diastolic dimension of at least 30 mm (Cleland, 2005). The duration of QRS complex must be more than 120 ms. Additional criteria to be met are an aortic pre-ejection delay of more than 140 ms, an interventricular mechanical delay of more than 40 ms or delayed activation of the posterolateral left ventricular wall (Higgins, 2003; Bristow, 2004; Cleland, 2005).

Currently, resynchronization is achieved by pacing or sensing the right atrium, pacing the right and left ventricles. This involves the positioning of pacing leads into the right atrium, right ventricle and the left ventricle, respectively (Wang, 2003). The positioning of left ventricular pacing lead is the key for a successful resynchronization therapy. This is achieved by inserting a pacing lead into one of the distal coronary venous branches where the left ventricle is paced from the epicardium. The pacing locations for the best hemodynamic outcomes are the lateral or posterolateral left ventricular walls (Wang, 2003).

There is a considerable variability in the presence, diameter, angulation and tortuosity of coronary veins (Meisel, 2001). For this reason the coronary veins must be studied by injecting contrast media into the coronary sinus before the positioning of left ventricular lead. Overall, the success rate for implantation of left-sided leads ranges from 75% to 93% (Leclercq, 1998; Alonso, 1999; Auricchio, 1999; Gras, 1998; Leclercq, 2000; Etienne, 2001; Lau, 2000; Cazeau, 2001; Braunschweig, 2000; Abraham, 2002; Higgins, 2003; Bristow, 2004; Cleland, 2005).

Color tissue Doppler imaging (TDI) has emerged as a noninvasive tool for selection of proper left ventricular pacing sites and for evaluation of myocardial contraction synchrony. TDI has been proven useful in detecting quantitatively the regional systolic and diastolic times and velocities within the myocardium (Hatle, 2000). TDI is able to accurately identify the ventricular site of most delayed activation (Ansalone, 2002). Pacing from these most delayed sites results in the greatest improvement in ventricular resynchronization and ventricular function (Ansalone, 2002).

Cardiac resynchronization therapy is generally well tolerated by patients. However, implantation and maintenance of biventricular pacing devices are associated with greater risks than a conventional pacing device. Apart from the common adverse effects seen in a pacemaker implantation, a very small proportion of patients (<0.1%) undergoing cardiac resynchronization procedure develop complete heart block that requires permanent cardiac pacing, or progressive hypotension or asystole during the procedures (Abraham, 2002).

Other major adverse effects include coronary sinus dissection (4%) and cardiac vein or coronary sinus perforation (2%) (Abraham, 2002). After implantation, approximately 6% – 11% of the patients require repositioning or replacement of the left ventricular lead due to lead dislodgement during long-term pacing (Abraham, 2002; Alonso, 2001). However, this complication does not result in the discontinuation of treatment in any patient.

3 Effects of Cardiac Resynchronization Therapy

The primary goals of any heart failure treatment are to improve the length or quality of the patient's life. Trials of cardiac resynchronization therapy have shown improvements in functional status of the heart, the distance patients can walk in 6 min, and hospital admission for heart failure (Braunschweig, 2000; Abraham, 2002; Higgins, 2003; Bristow, 2004; Cleland, 2005). Cardiac resynchronization therapy also reduces left ventricular end-systolic diameter, and increases stroke volume and thus, cardiac output and ventricular systolic function (Leclercq, 1998; Alonso, 1999; Auricchio, 1999; Gras, 1998). There is also an increase in the systolic and pulse pressure, and a decrease in pulmonary wedge pressure (Leclercq, 1998; Alonso, 1999; Auricchio, 1999; Gras, 1998). The acute hemodynamic benefits of the cardiac resynchronization are largely due to improved septal contribution to ventricular ejection, increased diastolic filling times, and reduced mitral regurgitation. Another important and unique benefit of resynchronization therapy is that biventricular pacing acutely enhances systolic function but modestly lowering myocardial oxygen consumption (Nelson, 2000). Most other heart failure therapy, however, increase energy cost of the myocardium while enhancing systolic function.

MUSTIC study (Linde, 2002) was a randomised, crossover clinical trial where patients un-

derwent 3 months' active pacing then switched to a non-pacing period of three months. It was found that patients' exercise capacity improved only during active pacing period, with a more than 23% increase in 6-min walking distance. The clinical symptoms were improved by 32% during active treatment and the maximal oxygen consumption was up by 8%.

MUSTIC study (Linde, 2002) also investigated the long-term effects of cardiac resynchronization therapy in patients with sinus rhythm and those with atrial fibrillation. At the end of the 12-month active pacing period, there was a significant improvement in 6-min walk distance, peak oxygen consumption and the quality of life. The NYHA class improved by 25% – 27% and the ejection fraction was up by 4% – 5% (Linde, 2002). Mitral regurgitation in these patients was almost halved at the end of the trial. These data indicate the clinical benefits of cardiac resynchronization can be maintained for at least 12 months.

MIRACLE trial randomized 228 patients to biventricular pacing therapy and 225 to a placebo control arm for six months (Abraham, 2002). All patients were in normal sinus rhythm and had an ejection fraction of less than 35%. Compared with the control group, patients assigned to cardiac resynchronization experienced an improvement in the distance walked in 6 min, NYHA functional class and quality of life (Abraham, 2002). The time on the treadmill exercise testing and the ejection fraction were also improved during active pacing periods. Furthermore, patients treated with cardiac resynchronization required less hospitalisation or intravenous medication for heart failure (Abraham, 2002). However, the clinical benefits were observed on only about two thirds of the patients received the resynchronization therapy. Furthermore, although the overall cardiac event rate was 40% lower in the cardiac resynchronization group, the mortality rate was similar between the pacing and control groups in the first 6 months of therapy (Abraham, 2002).

The CARE-HF trial is the largest trial so far, to assess the effect of cardiac resynchronization therapy on mortality rates in short- and medium-term (Cleland, 2005). A total of 813 patients were enrolled and followed for more than 29 months. At the end of the study, the mortality rate in the cardiac resynchronization therapy and medication group was 20% and 30%, respectively, indicating that resynchronization reduces mortality more than 2 years after the treatment. As compared with medical therapy, cardiac resynchronization reduced the interventricular mechanical delay, the end-systolic volume index and the area of the mitral regurgitant jet (Cleland, 2005). There was also a greater increase in ejection fraction, improvement in quality of life and symptoms in the resynchronization group (Cleland, 2005).

Another major trial, COMPANION, compared the effect of drug therapy, cardiac resynchronization, and cardiac resynchronzation plus implantable defibrillator on mortality and hospital admission in 1,250 patients (Bristow, 2004). Compared with the drug therapy group, the risk of the combined end point of death or hospitalization for heart failure was reduced by 34 percent in the resynchronization group and by 40 percent in the resynchronization-defibrillator group (Bristow, 2004). These results suggest that a combination of resynchronization therapy and implantable defibrillator offers further survival benefits for patients with severe CHF.

4 Conclusions

Cardiac resynchronization therapy offers a new approach for treating patients with ventricular dyssynchrony and moderate to severe heart failure. Clinical trials have demonstrated that this new therapy improves patient's symptoms, quality of life and short- to medium-term survival. However, up to 30% of patients who receive resynchronization devices will not show clinically significant responses to this therapy. Given the significant costs associated with the therapy, it is important to have further studies to establish measures of identifying the non-responders before the therapy is implemented.

Correspondence to:
Lexin Wang, MD, PhD.
School of Biomedical Sciences
Charles Sturt University
Wagga Wagga, NSW Australia.
Telephone:612-6933-2909
Fax:612-6933-2587
Email:lwang@csu.edu.au

References

1. Aaronson KD, Schwartz JS, Chen TM, et al. Development and prospective validation of a clinical index to predict survival in ambulatory patients referred for cardiac transplant evaluation. Circulation 1997; 95:2660 – 7.
2. Abraham WT, Fisher WG, Smith AL, et al. Cardiac resynchronization in chronic heart failure. N Engl J Med 2002; 346:1845 – 53.
3. Alonso C, Leclercq C, Victor F, et al. Electrocardiographic predictive factors of long-term clinical improvement with multisite biventricular pacing in advanced heart failure. Am J Cardiol 1999; 84:1417 – 21.
4. Alonso C, Leclercq C, d'Allonnes FR, et al. Six years

experience of transvenous left ventricular lead implantation for permanent biventricular pacing in patients with advanced heart failure: technical aspects. Heart 2001; 86:405 – 10.
5. Ansalone G, Giannantoni P, Rici R, et al. Doppler myocardial imaging to evaluate the effectiveness of pacing sites in patients receiving biventricular pacing. J Am Coll Cardiol 2002; 39:489 – 99.
6. Auricchio A, Stellbrink C, Block M, et al. Effect of pacing chamber and atrioventricular delay on acute systolic function of paced patients with congestive heart failure. Circulation 1999; 99:2993 – 3001.
7. Braunschweig F, Linde C, Gadler F, et al. Reduction of hospital days by biventricular pacing. Eur J Heart Fail 2000; 2:399 – 406.
8. Bristow MR. Beta-adrenergic receptor blockade in chronic heart failure. Circulation 2000; 101:558 – 69.
9. Bristow MR, Saxon LA, Boehmer J, et al. Cardiac-resynchronization therapy with or without an implantable defibrillator in advanced chronic heart failure. N Engl J Med 2004; 350:2140 – 50.
10. Cazeau S, Leclercq C, Lavergne T, et al. Effects of multisite biventricular pacing in patients with heart failure and intraventricular conduction delay. N Engl J Med 2001; 344:873 – 80.
11. Cleland JG, Daubert JC, Erdmann E, et al. Cardiac Resynchronization-Heart Failure (CARE-HF) Study Investigators. The effect of cardiac resynchronization on morbidity and mortality in heart failure. N Engl J of Med 2005; 352:1539 – 49.
12. Etienne Y, Mansourati J, Touiza A, et al. Evaluation of left ventricular function and mitral regurgitation during left ventricular-based pacing in patients with heart failure. Eur J Heart Fail 2001; 3:441 – 7.
13. Farwell D, Patel NR, Hall A, et al. How many people with heart failure are appropriate for biventricular resynchronization? Eur Heart J 2000; 21:1246 – 50.
14. Gras D, Mabo P, Tang T, et al. Multisite pacing as a supplemental treatment of congestive heart failure: preliminary results of the Medtronic Inc. InSync Study. Pacing Clin Electrophysiol 1998; 21:2249 – 55.
15. Hatle L, Sutherland GR. The Gruntzig lecture: regional myocardial function: a new approach. Eur Heart J 2000; 21:337 – 57.
16. Hesse B, Diaz LA, Snader CE, et al. Complete bundle branch block as an independent predictor of all-cause mortality: report of 7,073 patients referred for nuclear exercise testing. Am J Med 2001; 110:253 – 9.
17. Higgins SL, Hummel JD, Niazi IK, et al. Cardiac resynchronization therapy for the treatment of heart failure in patients with intraventricular conduction delay and malignant ventricular tachyarrhythmias. J Am Coll Cardiol 2003; 42:1454 – 9.
18. Kerwin WF, Botvinick EH, O'Connell JW, et al. Ventricular contraction abnormalities in dilated cardiomyopathy: effect of biventricular pacing to correct interventricular dyssynchrony. J Am Coll Cardiol 2000; 35:1221 – 7.
19. Lau CP, Yu CM, Chau E, et al. Reversal of left ventricular remodelling by synchronous biventricular pacing in heart failure. Pacing Clin Electrophysiol 2000; 23: 1722 – 25.
20. Leclercq C, Cazeau S, Le Breton H, et al. Acute hemodynamic effects of biventricular DDD pacing in patients with end-stage heart failure. J Am Coll Cardiol 1998;32: 1825 – 31.
21. Leclercq C, Cazeau S, Ritter P, et al. A pilot experience with permanent biventricular pacing to treat advanced heart failure. Am Heart J 2000; 140:862 – 70.
22. Linde C, Leclercq C, Rex S, et al. Long-term benefits of biventricular pacing in congestive heart failure: results from the MUltisite STimulation in cardiomyopathy (MUSTIC) study. J Am Coll Cardiol 2002; 40:111 – 8.
23. Littmann L, Symanski JD. Hemodynamic implications of left bundle branch block. J Electrocardiol 2000; 33:Suppl:115 – 21.
24. Meisel E, Pfeiffer D, Engelmann L, et al. Investigation of coronary venous anatomy by retrograde venography in patients with malignant ventricular tachycardia. Circulation 2001; 104:442 – 7.
25. Nelson GS, Berger RD, Fetics BJ, et al. Left ventricular or biventricular pacing improves cardiac function at diminished energy cost in patients with dilated cardiomyopathy and left bundle-branch block. Circulation 2000; 102:3053 – 9.
26. Saxon LA, Kerwin WF, Cahalan MK, et al. Acute effects of intraoperative multisite ventricular pacing on left ventricular function and activation/contraction sequence in patients with depressed ventricular function. J Cardiovasc Electrophysiol 1998; 9:13 – 21.
27. Shamim W, Francis DP, Yousufuddin M, et al. Intraventricular conduction delay: a prognostic marker in chronic heart failure. Int J Cardiol 1999; 70:171 – 8.
28. Shenkman HJ, Pampati V, Khandelwal AK, et al. Congestive heart failure and QRS duration: establishing prognosis study. Chest 2002; 122:528 – 34.
29. The CONSENSUS Trial Study Group. Effects of enalapril on mortality in severe congestive heart failure: results of the Cooperative North Scandinavian Enalapril Survival Study (CONSENSUS). N Engl J Med 1987; 316:1429 – 35.
30. Wang LX. Cardiac resynchronization therapy in congestive heart failure: the state of the art and perspectives. Exper Clin Cardiol 2003;7:212 – 5.
31. Xiao HB, Brecker SJ, Gibson DG. Effects of abnormal activation on the time course of the left ventricular pressure pulse in dilated cardiomyopathy. Br Heart J 1992; 68: 403 – 7.
32. Xiao HB, Roy C, Fujimoto S, et al. Natural history of abnormal conduction and its relation to prognosis in patients with dilated cardiomyopathy. Int J Cardiol 1996;53:163 – 70.
33. Nelson GS, Berger RD, Fetics BJ, et al. Left ventricular or biventricular pacing improves cardiac function at diminished energy cost in patients with dilated cardiomyopathy and left bundle-branch block. Circulation 2000; 102: 3053 – 59.

Received November 1, 2005

Low Level of B-type Natriuretic Peptide in Relation to Poor Prognosis in Patients with Advanced Left Ventricular Systolic Dysfunction

Tongwen Sun[1], Shuxiang Zhang[2], Guoying Su[2], Yanzhou Zhang[3], Li Li[1], Lexin Wang[1]

1. Emergency Center/Department of Cardiology, the First Affiliated Hospital of Zhengzhou University, Zhengzhou, Henan 450052, China

2. Department of International Exchange and Cooperation, Zhengzhou University, Zhengzhou, Henan 450001, China

3. Department of Cardiology, Renji Hospital Affiliated to Shanghai Jiaotong University, Shanghai 200001, China

Abstract: Background. B-type/brain natriuretic peptide (BNP) is released from the cardiac ventricles in response to increased wall tension. Elevated circulating BNP in heart failure (HF) usually indicates poor outcome and compensation. In advanced chronic HF, however, low level of BNP may reflect an impaired neurohormonal response. The primary aim of present study was to investigate the prognostic value of low BNP level in advanced heart failure patients. **Materials and Methods.** 50 advanced HF patients with New York Heart Association (NYHA) functional class Ⅲ and Ⅳ were enrolled in this study. Their blood BNP level were measured by Biosite Triage BNP test on admission and they were followed-up for 12±2 month after hospital discharge. **Results.** Cardiovascular mortality during follow-up was 24%. BNP levels were lower in patients who died (501±72 vs. 877 ± 89 ng/L, $P<0.01$). After adjusted for age, sex, duration of HF, left ventricular ejection fraction, serum creatinine level and drug therapy (including β-blocker, angiotensin-converting enzyme inhibitor, digoxin, diuretics and intravenous vasoactive medications), logistic stepwise regression analysis showed that lower BNP level (<520 ng/L) on admission was an independent predictor of cardiovascular mortality in advanced HF patients (OR = 1.21, 95% confidence interval 0.56−2.32, $P<0.01$). **Conclusions.** Cardiac natriuretic peptide system can no longer contribute adequately to neurohormonal compensation and that paradoxically low BNP level is an adverse prognostic marker in advanced HF. [Life Science Journal. 2006;3(1):5−8] (ISSN: 1097−8135).

Keywords: B-type /brain natriuretic peptide; heart failure; prognosis; mortality

1 Introduction

B-type/brain natriuretic peptide (BNP) is a peptide hormone released from cardiac ventricles in response to myocardial stretch or increased wall tension (Sun, 2005). Circulating levels of BNP are elevated in patients with heart failure (HF) and represent the activation of initially beneficial compensatory mechanisms (Sun, 2005). In addition, levels of BNP can be used to confirm the diagnosis and to aid in the assessment of prognoses in patients with HF (Sun, 2005; Lainchbury, 2003; Multinational, 2002; Anand, 2003; Anand, 2003; Tsutamoto, 1997). It is generally accepted that high level of BNP indicates an increased risk for a poor prognosis and that low circulating level reflect more stable compensation or effective treatment (Sun, 2005; Anand, 2003; Anand, 2003; Tsutamoto, 1997). However, some patients with symptomatic chronic HF can have "normal level" (<100 ng/L) of BNP (McGeoch, 2002; Tang, 2003). Recently, a small sample study suggested that lower BNP level could predict higher mortality in advanced HF patients because their neurohormonal systems can no longer maintain the higher levels needed for hemodynamic compensation (Miller, 2005; Packer, 2003). The primary objective of this study was to assess the association between BNP level and clinical outcomes in advanced HF patients with New York Heart Association (NYHA) class Ⅲ and Ⅳ.

2 Materials and Methods

2.1 Patients

A total of 50 patients with NYHA class Ⅲ and Ⅳ hospitalized for management of decompensated

chronic HF from August 2003 to December 2004 were enrolled in this study. Male 34, female 16, age 65 ± 9 (range from 24 to 78). The inclusion criteriaes were a history of HF more than 2 years and left ventricular ejection fraction (LVEF) less than 40%. The exclusion criteriaes were severe renal dysfunction, cancer and died during hospitalision. All the patients received intravenous diuretics and vasoactive agent during hospitalision. The discharged from hospital when symptoms were relief and stabilization. We followed up once every month during the first three months and then once every quarter. The total follow-up time was 12 ± 2 (range from 2 to 24) months. They were divided into two groups according to the results of follow-up.

2.2 Measurement of circulating BNP level

A point-of-care test of fluorescence immunoassay for the quantification of BNP was used (Biosite Diagnostics Inc, USA), 2 ml of intravenous blood was collected within 24 h of admission and BNP was determined within 20 minutes. The range of measurement was 5 – 5 000 ng/L.

2.3 Echocardiogram examination

A GE VIVID-7 echocardiograph (GE company, USA) were used. All the enrolled patients accepted echocardiograph examination by the same echocardiographer. Left ventricular ejection fraction (LVEF) and left ventricular end-diastolic dimension (LVEDd) were measured from the apical four-chamber view.

2.4 Statistical analysis

Numerical variable were presented by mean ± standard deviation (SD) and analyzed with student t test. Categorical variable were tested with χ^2 test analysis. All data were analyzed by SPSS 10.0 and a value of $P<0.05$ was considered statistically significant.

3 Results

The BNP levels and the LVEF of all the patients were 520 ± 270 ng/L (range from 78 to 3400 ng/L) and 26% ± 2% (range from 15% to 35%), respectively. The cardiovascular mortality rate was 24% during follow-up (12 patients died). There were no statistical difference about the clinical characteristics and therapy between the non-survival and the survival except for diastolic blood pressure (lower in the non-survival) and serum creatinine (higher in the non-survival) (Table 1). The BNP level was significantly lower in the non-survival than that in the survival (501 ± 72 ng/L vs. 877 ± 89 ng/L, $P<0.01$). After adjusted for age, sex, duration of HF, left ventricular ejection fraction, serum creatinine level and drug therapy (including β-blocker, angiotensin-converting enzyme inhibitor, digoxin , diuretics and intravenous vasoactive medications), logistic stepwise regression analysis showed that lower BNP level (< 520 ng/L) on admission was an independent predictor of cardiovascular mortality in advanced HF patients (OR = 1.21, 95% confidence interval 0.56 – 2.32, $P<0.01$).

Table 1. The comparison of clinical characteristics, therapy and BNP level between the non-survival and the survival

Group	Age	Male	Cause of HF		Duration of HF (m)	BP (mmHg)		HR (bpm)	LVEF
			DCM	ICM		SBP	DBP		
Non-survival (n=12)	67 ± 6	7	5	7	60 ± 10	121 ± 5	58 ± 2	78 ± 3	24 ± 2
Survival (n=38)	66 ± 5	25	13	25	54 ± 9	116 ± 6	65 ± 3▲	88 ± 4	25 ± 2

Group	BNP (ng/L)	Urine output (ml)	Serum creatinine (mg/dl)	Therapy				
				β-bolcker	ACEI	Nitrates	Digosin	Frusemide
Non-survival (n=12)	501 ± 72	1400 ± 360	2.1 ± 0.20	9	10	12	8	12
Survival (n=38)	877 ± 89▲	1300 ± 350	1.7 ± 0.13▲	27	29	38	25	38

▲$P<0.01$. BP: blood pressure; SBP: systolic blood pressure; DBP: diastolic blood pressure; LVEF: left ventricular ejection fraction; ACEI: angiotensin-converting enzyme inhibitor

4 Discussion

The physiological mechanism of HF is excessively activation of neuroendocine systems such as sympathetic nerve system (SNS), rennin-angiotensin-aldosterone-system (RAAS) and endothelin system(Sun, 2005). The physiological function of BNP includes vasodilation, natriuresis, diuresis, and inhibits both RAAS and SNS (Sun, 2005). The activation of natriuretic peptides system is a rational compensation (Sun, 2005; Lainchbury, 2003; Multinational Study Investigators, 2002; Anand, 2003; Tsutamoto, 1997). Recombined human BNP-nesiritide had been used for treatment in HF patients and had a better effect than positive inotropic therapy (Coclucci, 2000; The UMAC Invetigators, 2002; Abraham, 2005). Numerous clinical studies revealed that circulating BNP increased in HF patients and were positively related to mortality (Lainchbury, 2003; Multinational Study Investigators, 2002; Anand, 2003; Tsutamoto, 1997). It served as independent predictor of poor prognosis in cardiovascular disease (Anand, 2003; Tsutamoto, 1997). But we followed up 50 NYHA Ⅲ-Ⅳ patients with a HF history of more than 2 years for 12 months. Finally we concluded that the BNP level of non-survivals were significantly lower than that of survivals. Multiple variable analysis demonstrated that lower BNP level on admission was an independent risk factor of mortality. This was contrary to many previous studies (Anand, 2003; Tsutamoto, 1997).

In 2002, McGeoch and his coworkers (2002) found that among patients with LVEF of below 45% and receiving long-term treatment, 19% of them had a BNP level below 35 pmol/L (= 128 ng/L). In 2003, Tang and his coworkers (2003) studied 558 ambulatory patients with chronic, stable systolic HF (LVEF < 50%). They finally found that among the 498 symptomatic (NYHA functional class Ⅱ-Ⅲ) patients, 106 (21.3%) had plasma BNP levels in the "normal" diagnostic range (<100 ng/L); 60 patients were considered asymptomatic, and their plasma BNP levels ranged from 5 to 572 ng/L (median, 147 ng/L) (Tang, 2003). This suggested that natriuretic peptides system has been activated during the compensation stage of HF. However, in the decompensation stage of HF, a part of patients had "normal" BNP level (Tang, 2003). The author believed that it was the result of aggressive therapy. They did not follow-up for prognosis, but the author accepted the opinion of lower BNP level with a better clinical outcome (Tang, 2003). In 2005, Miller's study (2005) indicated that end-stage HF patients were treated with nesiritide, and the BNP level before and after nesiritide treatment were much lower in the non-survival than that in the survival. All the patients' BNP level were significantly increased after nesiritide treatment. Present study was partly coincidence with Miller' study.

The lower concentration of BNP may reflect a loss of the ability to synthesize and release BNP in amounts of sufficiency and maintain effective neurohormonal compensation; or the BNP clearance and/or degradation is up regulated in end-stage HF (Packer, 2003; Andreassi, 2001; Alimirez, 1999; Deschodt-Lanckman, 1989). Increased levels of the neutral endopeptidases that degrade BNP have been described in patients with end-stage renal dysfunction (Deschodt-Lanckman, 1989) and may be a common mechanism in patients with HF, given the relative severity of renal dysfunction observed in the patients in this study.

These observations support the hypothesis that at some point in the progression of advanced HF, neurohormonal systems in HF are unable to provide adequate levels of the natriuretic hormones to maintain hemodynamic compensation. This could be due to reduced synthesis and secretion, increased degradation, and/or clearance or other additional factors not yet clearly understood (Packer, 2003). Regardless of the cause, it suggests that the inability to maintain high cardiac natriuretic peptide levels in the setting of hemodynamic compromise is an adverse prognostic indicator (Packer, 2003).

The clinical value of present study is that, with the dramatically clinical use and study of measuring BNP, the clinical cardiologists should not over-depend on the results of BNP measurement in the diagnosis, monitoring therapy and risk stratification in patients with HF. They should evaluate the disorder comprehensively and tightly integrate with clinical findings. End-stage HF patients with lower BNP level reflects exhausion of natriuretic peptides. This also provides theoretical foundation for human recombined BNP-nesiritide used as an agent for HF treatment.

The samples of this study were relatively small, so the selection bias may exist. Furthermore, We did not measure atrial natriuretic peptide in this group of patients. So, the result of this study need large samples, multi-center, double blind clinical trials to confirm. The relationship between natriuretic peptides and pathogenesis, progression and prognosis of HF need further research to elucidate.

Correspondence to:
Tongwen Sun
Emergency Center/Department of Cardiology
The First Affiliated Hospital
Zhengzhou University
Zhengzhou, Henan 450052, China
Telephone: 86-13838516916
Fax: 86-371-6697-0906
Email: suntongwen@163.com

References

1. Abraham WT, Adams KF, Fonarow GC. et al. In-hospital mortality in patients with acute decompensated heart failure requiring intravenous vasoactive medications – an analysis from the acute decompensated heart failure national registry (ADHERE). J Am Coll Cardiol 2005;46(1):57–64.
2. Alimirez R, Protter AA. Clearance of human brain natriuretic peptide in rabbits, effect of the kidney, the natriuretic peptide clearance receptor, and peptidase activity. J Pharmacol Exp Ther 1999;289(2):976–80.
3. Anand IS, Fisher LD, Chiang YT, et al. Changes in brain natriuretic peptide and norepinephrine over time and mortality and morbidity in the Valsartan Heart Failure Trial(Val-HeFT). Circulation 2003;107(9):1278–83.
4. Andreassi MG, Silvia DR, Palmieri C, et al. Up-regulation of 'clearance' receptors in patients with chronic heart failure : a possible explanation for the resistance to biological effects of cardiac natriuretic hormone. Eur J Heart Fail 2001;3(4):407–14.
5. Coclucci WS, Elkayam U, Horton DP, et al. For the Nesritide Study Group. Intravenous nesiritide, a natruretic peptide, in the treatment of decompensated congestive heart failure. N Engl J Med 2000;343(3):246–53.
6. Deschodt-Lanckman M, Michaux F, DePrez E, et al. Increased serum levels of endopeptidase 24.11 ("enkephalinase") in patients with end-stage renal failure. Life Sci 1989;45(2):133–41.
7. Lainchbury JG, Campbell E, Frampton CM, et al. Brain natriuretic peptide and N-terminal brain natriuretic peptide in the diagnosis of heart failure in patients with acute shortness of breath. J Am Coll Cardiol 2003;42(3):728–35.
8. McGeoch G, Lainchburyb J, Townc GI, et al. Plasma brain natriuretic peptide after long-term treatment for heart failure in general practice. Eur J Heart Fail 2002;4(4):479–83.
9. Miller WL, Burnett JC Jr, Hartman KA, et al. Lower rather than higher levels of B-type natriuretic peptides (NT-pro-BNP and BNP) predict short-term mortality in end-stage heart failure patients treated with nesiritide. Am J Cardiol 2005;96(6):837–41.
10. Multinational Study Investigators. Rapid measurement of B-type natriuretic peptide in the emergency diagnosis of heart failure. N Engl J Med, 2002;347(3):161–7.
11. Packer M. Should B-type natriuretic peptide be measured routinely to guide the diagnosis and management of chronic heart failure. Circulation 2003;108(24):2950–3.
12. Sun TW, Zhang YZ. Brain natriuretic peptide and cardiac dysfunction. New Chin Med 2005;36(2):119–22.
13. Tang WH, Girod JP, Lee MJ, et al . Plasma B-Type natriuretic peptide levels in ambulatory patients with established chronic symptomatic systolic heart failure. Circulation 2003;108(24):2964–66.
14. The UMAC Invetigators(Vasodilatin in the Management of Acute Congestive Heart Failure). Intravenous nesiritide vs nitroglycerin for treatment of decompensated congestive heart failure: a randomized controlled trial. JAMA 2002;287(12):1531–40.
15. Tsutamoto T, Wada A, Maeda K , et al. Attenuation of compensation of endogenous cardiac natriuretic peptide system in chronic heart failure: prognostic role of plasma brain natriuretic peptide concentration in patients with chronic symptomatic left ventricular dysfunction. Circulation 1997;96(2):509–16.

Received October 21, 2005

Impact of Hepatitis G Virus Infection on Chronic Hepatitis C Egyptian Patients: Clinical, Virological and Ultrastructural Aspects

Maisa Omar[1], Nevine Fam[1], Samah Saad El-Din[1], *Hanem Ahmed[2], **Mahmoud Romeih[2], Hoda Yehia[3], Moataz Siam[4], Moataz Hassan[4], Mohamed Saber[2]

Microbiology[1], Biochemisty and Molecular biology[2], Electron Microscopy (Pathology)[3]. and Tropical Medicine[4] Departments, Theodore Bilharz Research Institute (TBRI) Giza, Egypt.

*Present address: * Food Science and Human Nutrition, Michigan State University, East Lansing, MI 48823, USA; ** Biochemistry and Molecular Biology Department, Michigan State University, East Lansing, MI 48823, USA*

Abstract: Hepatitis G virus (HGV) coinfection in chronic hepatitis C patients has recently been an active area of research as the impact of HGV infection on HCV chronic liver disease is still controversial. This study was conducted to investigate the prevalence of HGV infection in chronic HCV patients and to clarify its clinical, virological and histopathological impact at the ultrastructural level on chronic HCV liver disease. One hundred chronic HCV patients and 80 healthy blood donors were subjected to clinical, laboratory and ultrasonographic examination. Blood samples were examined for HCV and HBV markers, HCV serotyping, HCV quantitation of viral load and HGV RNA detection by nested Rt-PCR. Liver biopsy specimens were obtained from 25 patients and processed for light and electron microscopic (EM) examination. Chronic HCV patients were classified into 4 groups: chronic hepatitis (CH = 45); compensated cirrhosis (CC = 11); decompensated cirrhosis (DC = 22); and hepatocellular carcinoma (HCC = 22). The prevalence of HGV infection was significantly higher in chronic HCV patients (19%) versus blood donors (5%) $P<0.001$. HGV viraemia was significantly more common in patients with mild liver disease (CH + CC) than in patients with severe liver disease (DC + HCC) (23.2% versus 13.6%) $P<0.05$. No significant difference was detected between HGV-infected and non-infected patients regarding mean age, sex, liver biochemical tests, virologic markers and HCV serotype distribution. Decompensated cirrhosis was significantly less common in HGV coinfected persons (5.2%), than in those with isolated HCV infection (26%) $P<0.01$. Also the HCV RNA viral load in the former group was lower (median $2.1\times10^5\pm0.4$) than in the latter group (median $2.9\times10^5\pm0.5$) but the difference was statistically insignificant ($P>0.05$). Histopathologic examination of liver biopsy specimens by light and EM revealed no significant difference in the grade of periportal, portal and intralobular necroinflammation and in the stage of fibrosis. No virus particles or any characteristic morphological discrimination were detected between HCV patients with and without HGV infection. [Life Science Journal. 2006;3(1):9-17] (ISSN: 1097-8135).

Keywords: hepatitis G virus; clinical; virological and ultrastructural aspects; hepatitis G virus infection on chronic hepatitis C Egyptian patients

1 Introduction

Hepatitis G virus (HGV) and GB virus type C (GBV-C) were independently discovered as putative blood-borne causative viruses of non-A-E hepatitis (Simons, 1995; Linnen, 1996). Molecular characterization demonstrated that they were different isolates of the same virus and they represent a new genus in the family Flaviviridaea (Alter, 1996). HGV is not only phylogenetically closely related to hepatitis C virus (HCV), but it also has similar modes of transmission. It may infect the liver as an independent virus or as a coinfection with HCV (Abraham, 2003; Lisukova, 2003). It appears that it is even more efficiently transmitted by sexual and vertical exposure than is HCV (Stapleton, 2003).

Evidence of HGV infection is also found among people who have no acknowledged risk of blood-borne infection. The distribution of the virus varies geographically and information worldwide is incomplete. Infection rates among eligible blood donors range from 1% - 5% in developed countries (Chams, 2003)

Although HGV has been initially associated with fulminant hepatic failure, acute and chronic hepatitis (Abraham , 2003; Yoshiba , 1995), numerous studies failed to demonstrate its direct involvement in induction of significant hepatitis (Alter, 1997).

Coinfection with more than one virus may contribute to changes in the evolution of liver disease either negatively or favorably (Chams, 2003). The influence of HGV infection on HCV chronic liver disease is controversial. There was a growing consensus that coinfection has no apparent effect on the course or severity of chronic HCV liver disease and it does not alter the pathogenicity or replication of the virus(Shang, 2000; Petrova ,1999).

However, other investigators showed that acute and chronic hepatitis could be induced by HGV, and that coinfection worsens the liver histology of patients with chronic HCV (Moriyama, 2000; Xu, 2001).

Recent studies on the pathogenesis of HGV in human immunodeficiency virus (HIV)-infected patients yielded surprising results. Several studies found that HGV coinfection in HIV-positive people was associated with either a decrease in mortality or improved clinical outcome, compared to those without HGV infection (Stapleton, 2003; Williams, 2004). Moreover, it has been demonstrated in an in-vitro model of HGV and HIV coinfection, using interleukin-2 stimulated human peripheral blood mononuclear cells (PBMCs), that GBV-C/HGV led to inhibition of HIV replication by inducing cellular chemokines (RANTES, MIP-1, SDF-1) that inhibit HIV, and also by down-regulating the cellular expression of the HIV co-receptors CCR5 and CXCR4 (Xiang, 2005).

These findings plus the capability of both HCV and HGV to replicate in PBMCs(Stapleton, 2003; Mazur, 2001), raise the speculation of possible viral interference and claims re-evaluation of the effect of interaction of two closely-related viruses on their host. So the aim of the study was to determine the prevalence of HGV infection in chronic hepatitis C patients and to clarify its clinical, virological and histopathological impact at the ultrastructural level on chronic HCV liver disease.

2 Patients and Methods

Two groups were enrolled in the study: Group 1 included 100 chronic hepatitis C patients attending the Gastroenterology Unit of Theodore Bilharz Research Institute (TBRI) Giza, Egypt, during the period from August, 2002 until September, 2003. Chronic hepatitis was diagnosed on the basis of: elevated serum ALT and AST for more than 6 months, ultrasonographic and/or histopathologic evidence of chronic hepatitis or cirrhosis. Hepatitis C was diagnosed by HCV antibody and/or HCV RNA testing. Group 2 included 80 healthy, age-matched, volunteer blood donors from the Blood Bank of TBRI.

Patients' characteristics including age, sex, clinical examination with special stress on manifestations and decompensation of liver disease were recorded. Patients were examined by ultrasonography and upper endoscopy.

Liver biopsy specimens were obtained from 25 patients who were feasible for biopsy and were processed for light and electron microscopic (EM) histopathologic examination.

Patients were further classified based on clinical data and available histopathology into 4 subgroups: chronic hepatitis (CH = 45); compensated cirrhosis (CC = 11); decompensated cirrhosis (DC = 22); and hepatocellular carcinoma (HCC = 22). Patients with clinical features of portal hypertension were assumed to have cirrhosis even if a liver biopsy was not done. Decompensated cirrhosis was defined as the presence of complications related to portal hypertension such as ascites, encephalopathy, decreased synthetic functions reflected by decreased albumin concentration and prolonged prothrombin time. HCC was either based on histopathological diagnosis or on the presence of a hepatic focal lesion by imaging associated with elevated alpha-fetoprotein.

Blood samples collected from patients and blood donors were subjected to: complete blood picture, serum bilirubin, ALT, AST, alkaline phosphatase, albumin, globulins, prothrombin time and concentration and alpha-fetoprotein.

Serum samples were stored in several aliquots at −70℃ until tested for viral markers of HCV, HBV and HGV.

2.1 Serologic assays

Assay for HCV antibody was performed by third generation enzyme immunoassay (EIA) (anti-HCV version 4 Murex-Biotech Ltd., UK). Serum HBs antigen (HBsAg) and HBc antibody (HBcAb) were tested by EIA (Murex version 3, Murex-Biotech Ltd., UK). HCV serotyping was performed by Murex HCV serotyping 1-6 EIA (Murex-Biotech Ltd., UK).

2.2 Detection of HCV RNA viral load by PCR

RNA extraction was performed by the acid guanidinium thiocyanate and phenol-chlorofom single-step method (Chomezynski, 1987). Nested RT-PCR was used for quantitation of HCV RNA viral load using 2 sets of primers within the 5' non-

coding region. Amplification products were analyzed using 2% agarose gel electrophoresis (Van Doorn, 1994).

2.3 Detection of HGV RNA by PCR

RNA extraction was performed by the acid guanidinium thiocyanate and phenol-chloroform method(Chomezynski, 1987). Reverse transcriptase reaction and PCR were carried out using PTC-200 from MJ Research Inc. according to Schauder, (1995). All experiments included HGV positive and negative control. The oligonucleotide primer pairs used were: 5′-CGG CCA GGT GGA TG-3′ (position 100 sense), 5′-CGA CGA GCC TGA CGT CGGG-3′(position 285 antisense).

The RT reaction and PCR were performed in 100(L reaction volume containing 50(LRNA dilution, 2.5U recombinant Taq DNA polymerase (Promega, Madison, WI), 3U avian myeloblastosis virus (AMV) reverse transcriptase (Promega, Madison, WI), 1.5U RNase, 100 μm each of 4 deoxy-ribonuclease triphosphate, 0.2 mM each of primer, 50 mM KCl, 1.5 mM $MgCl_2$, 0.01% gelatin and 10 mM Tris-HCl pH 8.3. The RT reaction was performed at 42℃ for 45 min followed by 5 min at 94℃. The PCR was subjected for 30 cycles each of 94℃ (denaturating) for 1 min, 55℃ (annealing) for 1 min and 72℃ (extension) for 1 min and finally one cycle at 72℃ for 10 min. Amplification products were analyzed using 2% agarose gel electrophoresis according to the method described by Van Doorn (1994).

2.4 Light and electron microscopic processing of liver biopsy specimens

For light microscopic examination, liver biopsy specimens were fixed in 10% buffered formalin and processed for the preparation of 4 μm thick paraffin sections that were stained by haematoxylin and eosin and Masson trichrome stains. The specimens were graded and staged semiquantitatively from 0－4 according to Desmet et al (1994), assuming that grade 1 activity is scored (1－3), grade 2 (4－8), grade 3 (9－12) and grade 4 (13－18) of the Knodell score Knodell et al (1981).

For EM examination, a small piece of liver biopsy about 3 mm^3 was divided into 1 mm^3 pieces and fixed in 4% glutaraldehyde buffered with 0.2 M sodium cacodylate, washed twice in equal volumes of sodium cacodylate 0.2 M and sucrose 0.4 M at 4 ℃, postfixed in 2% osmium tetroxide for 1 hour then washed in distilled water and dehydrated in ascending alcohol concentration, embedded in Epon and polymerized at 60℃ for 48 hours. Semithin sections stained with methylene blue azur II and ultrathin sections double stained with uranyl acetate and lead citrate were performed using an Ultracut R ultramicrotome. Examination of the stained ultrathin sections was done using a Philips EM 208 S electron microscope.

2.5 Statistical Analysis

Analyses were conducted using Student's t-test and test of proportion. The level of statistical significance was set at $P = 0.05$. Histological variables were analysed according to Wilcoxon variance analysis.

3 Results

The prevalence rate of HGV infection was significantly higher in chronic HCV patients (19%) versus blood donors (5%) $P<0.001$. Four of the 19 HGV-positive patients were also coinfected with HBV. The overall prevalence rate of HGV infection was 12.7% (23/180). Among the 23 HGV-positive cases, isolated HGV infection was detected in 2 (8.7%) while coinfection with HCV was found in 21 (91.3%) $P<0.000\ 1$ (Table 1).

The distribution of HGV infection in chronic HCV patients according to severity of liver disease is shown in Table 2. CH and CC were categorized as mild liver disease, while DC and HCC were considered as severe liver disease. HGV viraemia was significantly more common among patients with mild liver disease (23.2%) than among those with severe liver disease (13.6%) $P<0.05$.

Demographic, virologic and clinical data of chronic HCV patients were compared according to the presence or absence of HGV infection (Table 3). There was no significant difference between HGV-infected and non-infected patients regarding mean age, sex distribution, ALT serum levels, virologic markers, or HCV serotype distribution. HCV RNA viral load was lower in patients with than without HGV infection, however the difference was statistically insignificant ($P>0.05$).

Analysis of disease categories denoting severity of liver disease showed that decompensated cirrhosis was significantly less common in HGV coinfected persons (5.2%), than in those with isolated HCV infection (26%) $P < 0.01$. HCV serotyping showed that serotype 4 was the most prevalent (96%), 71% of patients had single type 4 and 25% had mixed serotypes (4+1/4+2), while 4% had serotype 1.

Liver histopathologic examination of 25 cases (8 HGV positive and 17 HGV negative) by light microscopy disclosed the presence of 22 (88%) cases of chronic hepatitis and 3 (12%) well differentiated cases of HCC of the trabecular pattern. Grading and staging of chronic hepatitis liver biopsies from HGV coinfected patients compared to isolated

HCV infection showed no statistically significant difference in periportal, portal and intralobular necroinflammation and in the stage of fibrosis (Table 4). Also there was no difference between the two groups regarding the presence of steatosis, bile duct damage and lymphoid aggregations.

Table 1. Prevalence rates of HGV infection in chronic hepatitis C patients and blood donors: isolated infection, coinfection with HCV

Group	No Tested	HGV RNA Positive N (%)	Isolated HGV infection	Coinfection of HGV&HCV
Group1 (Chronic HCV)	100	19(19)**	–	19
Group 2 (Blood donors)	80	4 (5)	2	2
Total N (%)	180	23(12.7)	2(8.7)	21(91.3)***

* *P*<0.001: HGV prevalence in group 1 versus group 2
** *P*<0.0001: HGV coinfection with HCV versus isolated HGV infection

Table 2. Distribution of HGV-positive viraemia in chronic HCV patients according to severity of liver disease

Character	Mild Liver Disease (n=56)		Severe Liver Disease (n=44)	
	CH (45)	CC (11)	DC (22)	HCC (22)
HGV-RNA positive	10	3	1	5
Total N (%)	13 (23.2)*		6 (13.6)	

*P<0.05 for mild versus severe liver disease in HGV/HCV coinfection.
CH: Chronic hepatitis; CC: Compensated cirrhosis; DC: Decompensated cirrhosis; HCC: Hepatocellular carcinoma.

Table 3. Demographic, virological and clinical data of chronic hepatitis C patients according to the presence or absence of HGV RNA

Characteristic	HGV +ve (n=19)		HGV −ve (n=81)		P value
Age (mean(SD)	44±8.5		43±6.2		NS
Sex (M:F)	13:6		63:18		NS
Mean ALT level (IU/L)	60±31		65±34		NS
Virological features					
HCV RNA (copies/ml)					
Mean×10^5(SD)	19	2.1 (0.4)	81	2.9(0.5)	NS
HCV serotype 4	13	68.4%	58	71.6%	NS
Mixed serotype (1+4/2+4)	5	26.3%	20	24.6%	NS
HCV serotype1	1	5.3%	3	3.7%	NS
HBs antigen +ve	4	21.0%	0	–	–
HBc antibody +ve	11	57.9%	38	46.9%	NS
Disease categories					
Chronic hepatitis	10	52.6%	35	43.2%	NS
Compensated cirrhosis	3	15.7%	8	9.9%	NS
Decompenstated cirrhosis	1	5.2%	21	26.0%	0.01
Hepatocellular carcinoma	5	26.3%	17	20.9%	NS

Table 4. Grading and staging of chronic hepatitis liver biopsies in HGV coinfection compared to isolated HCV infection

Characteristic	1	2	3	4	Mean±SD	P value
Grading						
HGV Coinfection	0	4	2	2	9.75±4.65	
HCV	0	7	4	3	9.5±4.128	NS
Staging						
HGV Coinfection	3	2	1	2	3.25±0.70	
HCV	6	3	3	2	3.14±0.663	NS

EM examination of the ultrathin liver sections revealed no virus or virus-like particles in the nuclei or in the cytoplasm of hepatocytes. There was evident proliferation of the smooth and rough endo-

plasmic reticulum associated with distended cisternae, as well as electron dense opaque mitochondria of different sizes (Figure 1). Moderate sized collagen fibrils were observed intercellularly and in perisinusoidal spaces and collagen like fibrils were seen extended in the cytoplasm between the organelles of the hepatocytes. Extravasation of RBCs together with infiltration by macrophages and lymphocytes were disclosed between hepatocytes. Many large and moderate-sized fat locules were observed filling the hepatocytes, pushing the nuclei aside and compressing the neighbouring cells (Figures 2,3). Apoptotic cells were detectable showing either peripheral chromatin condensation beneath the nuclear membrane or dense chromatin aggregates in the nucleus, together with condensed cytopasmic organelles. No characteristic morphological discrimination could be found between HCV infected specimens and those coinfected with HGV (Figures 1 – 3).

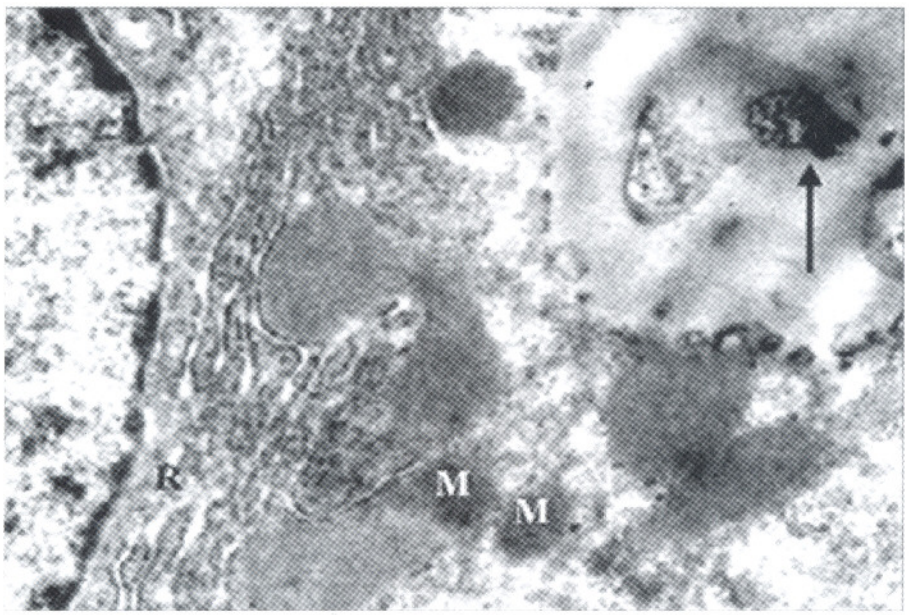

Figure 1. Electronmicrograph from a case of HCV showing a hepatocyte with proliferated endoplasmic reticulum (R) and opaque mitochondria (M) (A degenerated hepatocyte with apoptotic nucleus (arrow) is observed) (×10 000)

4 Discussion

To determine the prevalence of HGV viraemia and its impact on chronic HCV patients in our region, we studied 100 chronic HCV patients and 80 volunteer blood donors. The prevalence of HGV in chronic hepatitis C patients was significantly higher (19%) compared to blood donors (5%). This was comparative with the infection rates reported in researches on Egyptian HCV patients where prevalence rates were 18.5%, 14% and 11.5% (Heiba, 1999; El-Zayadi, 1999; Hassoba, 1997). These rates were also not markedly different from other studies from different geographic areas that reported HGV RNA viraemia among chronic HCV patients in the range from 17% to 23% (Martinot, 1996; Wang , 1998; Handajani, 2000; Li, 2001; Bjorkman, 2001).

HGV infection is closely associated with HCV infection both in areas of endemicity and in areas of no endemicity for HCV (Tanaka, 1998). This was confirmed in this study as among 23 HGV-positive cases, the association of HCV and HGV infections versus isolated HGV infection was 91.3% versus 8.7%. This probably reflects common exposure and transmission patterns rather than an interdependent relation. Moreover, this high association may be attributed to the reduced clearance of HGV viraemia among HCV-infected patients, as most immunocompetent individuals who become infected with HGV clear the virus, while fewer than 25% of HCV-infected patients spontaneously clear infection (Stapleton, 2004).

The rate of HGV viraemia in blood donors detected in this study (5%), was consistent with that reported in epidemiological studies of the general population and blood donors in Africa and South America (5% – 10%) (Desmet, 1994). In contrast it was lower than that reported among 82 apparently healthy, Egyptian blood donors (12%) (Hassoba, 1997). This difference could be due to

variabilities in the characteristics of population of blood donors as the age group, social standard and special habits. In addition, there is evidence that HGV can be transmitted intrafamilialy, by non-parenteral routes as saliva and semen, by accupuncture or sharp objects and it has an age-related prevalence(Semprini, 1998; Chen,1999; Seifreid, 2004).

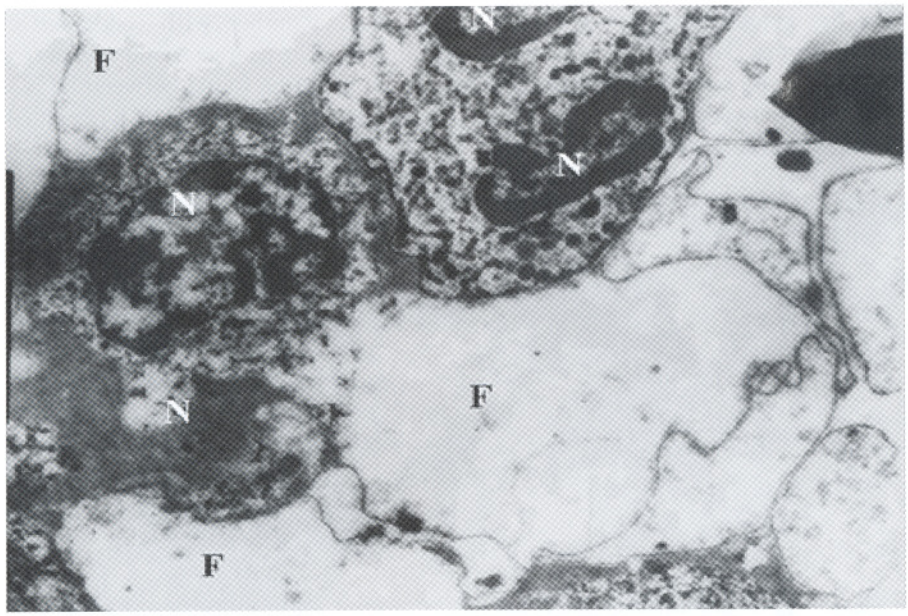

Figure 2. Electronmicrograph from a case of HCV coinfected with HGV showing fat vacuoles (F) compressing 2 apoptotic binucleated (N) hepatocytes (×5 000)

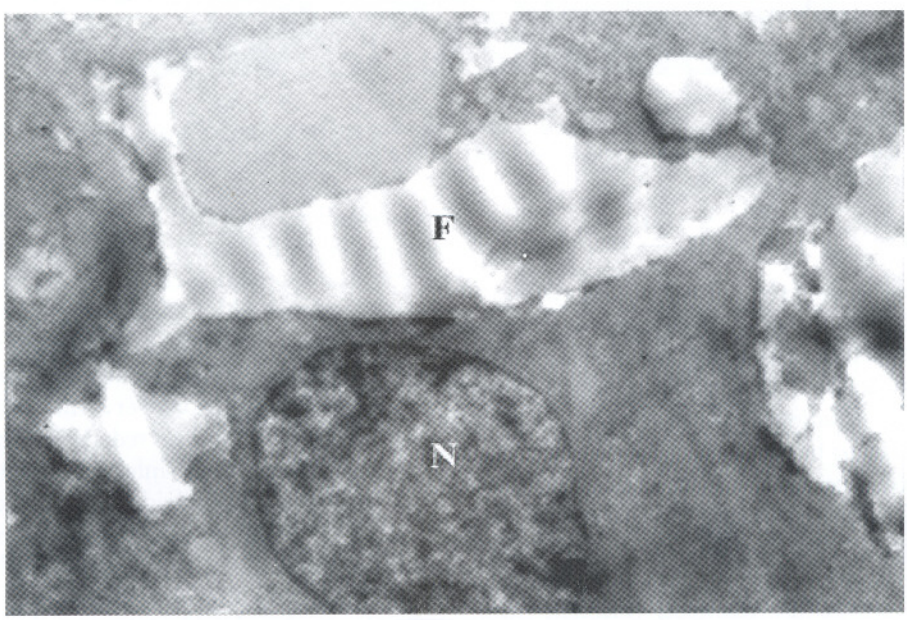

Figure 3. Electronmicrograph from a case of HCV showing fat vacuoles replacing the cytoplasmic organelles of a hepatocyte (×7 000)

Egypt is a country known for its high seroprevalence of HCV (Hassan, 2001). The common exposure patterns of HCV and HGV may account for the overall high HGV viraemia among Egyptian blood donors that exceeds that reported from Japan (0.8%), USA (1.7%), China (2%), Indonesia (2.7%) and Korea (1.8%) (Alter, 1997; Wang, 1998; Handajani, 2000; Li, 2001; Jeon, 2003).

Numerous studies performed on HGV led to the exclusion of its role as a significant aetiologic agent of hepatitis. However coinfections with other viruses may contribute to changes in the progress and severity of liver disease patients (Chams, 2003). From the point of view of some authors, several facts must be considered before dismissing the possible pathogenic role for HGV in HCV chronic liver disease. First, the lack of detectable core protein, which may explain the absence of excess inflammation in HCV coinfected patients. Second, the presence of a highly conserved E2 region and formation of an anti-HGV-E2 antibody that is indicative of an effective immune response in the host leading to clearance of viral RNA. Third, HGV isolates from widely separated geographic areas have been thought to be highly conserved, until the recent description of 5 major genotypes and 5 subclasses of genotype 1, which suggests the possibility of a relationship between specific genotypes and pathogenicity. Fourth, the virus occurs and appears to replicate *in vitro* in PBMCs and not in hepatocytes. It also inhibits replication of HIV in coinfected cell cultures (Williams, 2004; Hattori, 2003; Liu, 2003; George, 2003).

In this study, analysis of HGV-positive versus negative patients in chronic HCV patients showed no significant difference between patient groups regarding age, sex, virologic markers or serotype distribution. Furthermore, no association was found between the presence of HGV viraemia and the severity of liver disease in terms of serum ALT levels or histopathologic examination in both severity of inflammation and degree of fibrosis. These findings agree with other workers on hepatitis C patients who also failed to detect a significant effect of coinfection with HGV on the indices of liver disease including biochemical, histologic and response to interferon therapy (Heiba, 1999; Wang, 1998; Slimane, 2000; Par, 2004).

However, our finding that HGV infection was significantly less prevalent in patients with severe disease (DC and HCC), than in those with mild liver disease (CH and CC) is noteworthy. It does not only deny the role of HGV in aggravating liver disease, but also raises the question of a possible beneficial role of HGV in chronic HCV patients through viral reciprocal inhibition. Because both HCV and HGV are capable of replicating in lymphocytes (Stapleton, 2003; Mazur, 2001), it is reasonable to speculate that viral interference might occur. In this study we found that the concentration of HCV RNA was lower in patients coinfected with HCV and HGV than in those with HCV infection only. Although the difference was not statistically significant, it is suggestive of the possible reciprocal relationship between the two viruses. A reverse relation was found to exist between HCV RNA concentration and HGV infection in a study on chronic HCV patients coinfected with HGV. HCV copy numbers in patients with HGV coinfection was significantly lower than that in patients without HGV (Yan, 2000). In contrast, such relation was not found in other studies (Chu, 2001). Further studies on viral load quantitation by more accurate methods, as real time PCR, are required to clarify this issue.

Also in favor of the possible beneficial role of HGV is the recent finding of the inhibitory effect of HGV on replication of HIV in the *in-vitro* models of coinfection. It has been demonstrated that this is achieved by the down-regulation of expression of major HIV coreceptors, by the increase in specific chemokines and by alteration in the Th cytokine production by PBMCs (Mazur, 2001). It was found that HGV may help maintain cytokine profiles associated with long-term non progression among HIV-positive patients and that HGV coinfection correlated with an intact Th1 cytokine profile among those patients (Nunnari, 2003). Since Th cytokines are involved in the pathogenesis of disease, so HGV may potentially influence other comorbid infections in a beneficial mode (Stapleton, 2004).

Results of histopathologic examination in this study revealed no difference in the inflammatory scores or fibrosis stage that could be attributed to HGV coinfection. These findings were consistent with other authors who showed that coinfection did not affect the liver lesion nor induced a more aggressive disease (Shang, 2000; Strauss, 2002; Petrik, 1998; Goldstein, 1997). Regarding the presence of lymphoid aggregation, steatosis and bile duct damage, the lesions mostly encountered in HCV infection, we did not detect a significant difference between the two groups, although other authors observed more severe bile duct damage in HGV coinfected persons (Xu, 2001; Chu, 2001). EM examination also confirmed that there were no detectable specific ultrastructural morphological features in coinfected patients. Also, no virus particles were detected in hepatocytes of the coinfected patients. This is supportive with the suggestion that HGV may be a non hepatotropic virus. The replication site of HGV *in vivo* is still unknown. The virus appears to be primarily a lymphotropic virus rather than hepatotropic (Tucker, 2000). Evidence denoting that the negative strand of HGV could not be detected in the liver, suggest that the virus does not replicate in the liver (Laras, 1999).

In contrast, HGV replication was identified in the cytoplasm of hepatocytes of 10 donor livers. It was detected by in situ hybridization with HGV RNA probes and immunologic staining for HGV- E2 protein. However there was no evidence of liver disease in those HGV infected healthy liver donors despite viral replication in hepatocytes (Halasz, 2000).

Generally speaking, the EM studies on HGV infections are very few in the literature. In a study by Xu et al (2000), they observed that the ultrastructural changes in one case of acute single HGV infection were: shrinkage of liver cells, extension of rough endoplasmic reticulum, proliferation of collagen fibrils but they did not comment on the presence or absence of virus particles.

5 Conclusion

HGV infection is common in chronic HCV patients. It does not appear to aggravate the liver disease at the histopathologic and the ultrastructural levels, but the finding that it was less prevalent in clinically severe liver disease than in those with mild disease, plus the lower HCV RNA concentration in coinfected patients raise the speculation of a possible beneficial role. But much more *in-vitro* and *in-vivo* studies are required to answer the question related to interaction of both viruses.

Acknowledgments

This work was funded by Hepatitis Research Project number 74D of the Microbiology Department of TBRI.

Correspondence to:
Mahmoud Romeih
Associate Prof of Biochemistry and Molecular Biology
Biochemistry and Molecular Biology Department
Theodor Bilharz Research Institute
Giza, Egypt
Email: romeih@msu.edu; romeihm@yahoo.com

References

1. Abraham P, John T, Raghuraman S, et al. GB virus C/hepatitis G virus and TTV infections among high risk renal transplant recipients in India. J Clin Virol 2003; 28: 59 – 69.
2. Alter J. The cloning and clinical implications of HGV and HGBV-C. N Engl J Med 1996; 334: 1536 – 7.
3. Alter J. A reassessment of the literature on the hepatitis G virus. Transfusion 1997; 37: 569 – 72.
4. Bjorkman P, Widell A, Veress B, et al. GB virus C/Hepatitis G virus infection in patients investigated for chronic liver disease and in the general population in Sweden. Scand J Inf Dis 2001; 33: 611 – 7.
5. Chams V, Fournier-Wirth C, Chabanel A, et al. Is GB virus-C alias "hepatitis G" involved in human pathology. Trans Clin Biol 2003; 10: 292 – 306.
6. Chomezynski P, Sacchi N. Single step method of RNA isolation by acid guanidine thiocyanate-phenol-chloroform extraction. Annal Biochem 1987; 162: 156 – 9.
7. Chen BP, Rumi MG, Colombo M, et al. TT virus is present in a high frequency of Italian hemophilic patients transfused with plasma-derived clotting factor concentrates. Blood 1999; 94: 4333 – 6.
8. Chu C, Hwang S, Luo J, et al. Clinical, virological, immunological and pathological significance of GB virus C / hepatitis G infection in patients with chronic hepatitis C. Hepatol Res 2001; 19: 225 – 36.
9. Desmet VJ, Michael GM, Hoofnagle JH, et al. Classification of chronic hepatitis: Diagnosis, grading and staging. Hepatol 1994; 19: 1513 – 20.
10. El-Zayadi A, Abe K, Selim O, et al. Prevalence of GBV-C/hepatitis G virus viremia among blood donors, health care personnel, chronic non-B non-C hepatitis, chronic hepatitis C and hemodialysis patients in Egypt. J Virol Meth 1999; 80: 53 – 8.
11. George SL, Xiang J, Stapleton JT. Clinical isolates of GB virus type C vary in their ability to persist and replicate in peripheral blood mononuclear cell culture. Virology 2003; 3(16): 161 – 201.
12. Goldstein NS, Underhill J, Gordon SC, et al. Comparative histologic features of liver biopsy specimens from patients coinfected with hepatitis G and C viruses with chronic hepatitis C virus alone: an age-, sex-, disease duration-, and transmission-matched controlled study of chronic hepatitis. Am J Clin Pathol 1997; 108: 616 – 8.
13. Hassan M, Zaghlool A, El-Serag B, et al. The role of hepatitis C in hepatocellular carcinoma. J Clin Gastroenterol 2001; 33: 123 – 6.
14. Heiba A, Abou Al-Ola O, Al-Husseiny M, et al. Frequency and clinical correlation of dual infections with the hepatitis G and C viruses. Egypt J Med Microbiol 1999; 8: 21 – 6.
15. Hassoba H, Terrault N, El-Gohary A. Antibody to GBV-C second envelope glycoprotein (anti-GBV-CE2): Is a marker for immunity. J Med Virol 1997; 53: 354 – 60.
16. Handajani R, Soetjipto, Lusida MF, et al. Prevalence of GB virus infection among various populations in Surabaya, Indonesia, and identification of novel groups of sequence variants. J Clin Microbiol 2000; 38: 662 – 8.
17. Hattori J, Ibe S, Nagai H, et al. Prevalence of infection and genotypes of GBV-C/HGV among homosexual men. Microbiol Immunol 2003; 47: 759 – 63.
18. Halasz R, Sallberg M, Lundholm S, et al. The GBV-C replicates in hepatocytes without causing liver disease in healthy blood donors. J Inf Dis 2000; 182 (6): 1756 – 60.
19. Jeon MJ, Shin JH, Suh SP, et al. TT virus and hepatitis G virus infections in Korean blood donors and patients with chronic liver disease. World J Gastroenterol 2003; 9: 741 – 4.
20. Knodell RG, Ishak KG, Black WC, et al. Formulation and application of a numerical scoring system for assessing histological activity in asymptomatic chronic active hepatitis. Hepatol 1981; 1 :431 – 5.
21. Linnen J, Wages J Jr, Zhang-Keck Y, et al. Molecular

cloning and disease association of hepatitis G virus: a transfusion-transmissible agent. Science 1996;271: 505 – 8.
22. Lisukova E. HG-viral infection in adults. Ter Arkh 2003;75: 23 – 7.
23. Li S, Zeng L, Luo D, et al. Hepatitis G viral RNA co-infection in plasma and peripheral blood mononuclear cells in patients with hepatitis C. J Tongji Med Univ 2001; 21:238 – 9.
24. Liu F, Teng W, Fukuda Y, et al. A novel subtype of GB virus C/HGV genotype 1 detected uniquely in patients with haemophilia in Japan. J Med Virol 2003; 71: 385 – 90.
25. Laras A, Zacharakis G, Hadziyannis J . Absence of the negative strand of GBV-C/HGV RNA from the liver. J Hepatol 1999;30: 383 – 8.
26. Moriyama M, Matsumura H, Shimuzu T, et al. Hepatitis G virus influences the liver histology of patients with chronic hepatitis C. Liver 2000; 20: 397 – 404.
27. Mazur W, Mazurek U, Jurkaz M, et al. Positive and negative strands of HCV RNA in sera and peripheral blood mononuclear cells of chronically haemodialyzed patients. Med Sci Monit 2001;7:108 – 15.
28. Martinot MP, Marcellin M, Pouteau C, et al. HGV infection in French patients with chronic hepatitis C. Hepatol 1996;24:4 – 10.
29. Nunnari G, Nigro L, Palermo F, et al. Slower progression of HIV-infection in persons with GBV coinfection correlates with an intact T-helper1-cytokine profile. Ann Int Med 2003;139:26 – 30.
30. Petrova EP, Chokshi S, Naoumov NV, et al. TT virus (TTV) and hepatitis G virus (HGV) – two examples of human viruses with no clear disease association. Infect Dis Rev 1999;1:93 – 6.
31. Par A, Takacs M, Bjornas J, et al. Viral coinfections in hepatitis C: HBV, GBV-C/HGV and TTV. Orv Hetil 2004;145:987 – 92.
32. Petrik J, Guella L, Wight D, et al. Hepatic histology in hepatitis C virus carriers coinfected with hepatitis C virus. GUT 1998;42:103 – 6.
33. Simons JN, Pilot-Matias TJ, Leary TP, et al. Identification of two flavivirus-like genomes in the GB hepatitis agent. Proc Natl Acad Sci USA 1995;92:3401 – 5.
34. Stapleton JT. GB virus type C/Hepatitis G virus. Semin Liver Dis 2003;23:137 – 48.
35. Shang Q, Zhang G, Yu J. The effect of hepatitis G virus infection on clinical features and liver pathologic lesions of chronic hepatitis C. Zhonghua Shi Yan He Lin Chuang Bing Du Xue Za Zhi 2000;14:250 – 2.
36. Schauder GG, Dawson GJ, Simons JN, et al. Molecular and serological analysis in the transmission of the GB hepatitis agents. J Med Virol 1995;46:81 – 90.
37. Stapleton J, Williams C, Xiang J. GB virus type C: a beneficial infection? J Clin Microbiol 2004;42:3915 – 9.
38. Semprini AE, Persico T, Thiers V, et al. Absence of hepatitis C virus and detection of hepatitis G virus/GB virus C RNA sequences in the semen of infected men. J Infect Dis 1998;177:848 – 54.
39. Seifreid C, Weber M, Bialleck H, et al. High prevalence of GBV-C/HGV among relatives of HGV-positive blood recipients and in patients with aplastic anaemia. Transfusion 2004;44:268 – 74.
40. Slimane SB, Albrecht JK, Fang FW, et al. Clinical, virological and histopathological implications of GB virus-C / hepatitis G virus infection in patients with chronic hepatitis C virus infection. J Viral Hepatol 2000;7:51 – 5.
41. Strauss E, Gayotto LC, Fay F, et al. Liver histologyin coinfection of hepatitis C and hepatitis G virus. Rev Inst Med Trop S Paulo 2002;44:1 – 10.
42. Tanaka E, Tacke M, Kobayashi M, et al. Past and present hepatitis G virus infections in areas where hepatitis C is highly endemic and those where it is not endemic. J Clin Microbiol 1998;36:110 – 4.
43. Tucker TJ, Smuts HE, Eades C. Evidence that GBV-C/HGV is primarily a lymphotropic virus. J Med Virol 2000;61:52 – 8.
44. Van Doorn LJ. Molecular biology of the hepatitis C virus. J Med Virol 1994;43: 345 – 56.
45. Williams CF, Klinzman D, Yamashita TE, et al. Persistent GB virus C infection and survival in HIV-infected men. N Engl J Med 2004;350:981 – 90.
46. Wang H, Sun Y, Chang J. The coinfection of hepatitis C virus with hepatitis G virus and its reaction to interferon treatment. Zhonghua Shi Yan He Lin Chaung Bing Du Xue Za Zhi 1998;12:377 – 79.
47. Xu JZ, Yang ZG, Le MZ, et al. A study on the pathogenicity of hepatitis G virus. World J Gastroenterol 2001;7:547 – 50.
48. Xiang J, George SL, Wunschmann S, et al. GB virus type C infection inhibits HIV-1 replication by increasing RANTES. MIP-1α, MIP-1β and SDF-1. Lancet 2004; 363: 2040 – 6.
49. Yoshiba M, Okamoto H, Mishiro S. Detection of the GBV-C hepatitis virus genome in serum from patients with fulminant hepatitis of unkown etiology. Lancet 1995;346:1131 – 2.
50. Yan J, Dennin RH. A high frequency of GBV-C/HGV coinfection in hepatitis C in Germany. World J Gastroenterol 2000;6(6):833 – 41.

Received October 25, 2005

The Protein Expression of NDRG1 in Esophageal Squamous Cell Carcinoma and Its Relationship with Clinical Pathology Factors

Fucheng He[1], Yunhan Zhang[2], Dongling Gao[2], Kuisheng Chen[2], Huixiang Li[2], Lan Zhang[2], Sanshen Zhang[3]

1. The First Affiliated Hospital of Zhengzhou University, Zhengzhou, Henan 450052, China
2. Henan Key Laboratory of Tumor Pathology, Zhengzhou, Henan 450052, China
3. Tumor Hospital of Anyang, Anyang, Henan 455000, China

Abstract: Aim. To study the expression of N-myc downstream regulated gene 1(NDRG1) in esophageal squamous cell carcinomas(ESCC). **Methods.** The S-P immunohistochemical method was employed to detect the expression of NDRG1 in 49 cases of esophageal squamous cell carcinoma, mucosa adjacent to cancer and normal mucosa. **Results.** There were no differences in the positive expression rate of NDRG1 protein in cancerous tissues, mucosa adjacent to cancer and normal mucosa($P>0.05$), but protein expression levels were different. In normal mucosa, mucosa adjacent to cancer and cancerous tissues, the expression rate in low expression level(+) were: 8.2%, 65.3%, 81.6%; the expression rate of high expression level(++) were: 87.7%, 13.0%, 8.1%, respectively, and they had significantly differences($P<0.01$). There were no differences of NDRG1 protein expression in different differentiation levels of esophageal carcinoma and with or without lymph node metastasis of esophageal carcinoma. **Conclusion.** The expression of NDRG1 is lower in esophageal squamous cell carcinoma, and this may be related to the occurence of esophageal squamous cell carcinoma. [Life Science Journal. 2006; 3(1): 18 - 22] (ISSN: 1097 - 8135).

Keywords: esophageal squamous cell carcinoma; N-myc downstream regulated gene 1; immunohistochemistry; protein expression

1 Introduction

Esophageal squamous cell carcinoma(ESCC) is a common malignant tumor which seriously destroys people's health. A better understanding of the molecular events involved in the development of esophageal cancer will be helpful to its early diagnosis, treatment and prognosis. N-myc downstream regulated gene 1 (NDRG1) was found by different laboratories (van Belzen, 1997; Zhou, 1998) and was demonstrated to be related to cell differentiation(van Belzen, 1997; Guan, 2000). It caused great interest about the relationship between NDRG1 and cancers. Researchers found that the expression of NDRG1 was higher in human normal tissues, such as kidney, prostrate, colon, etc, and lower in prostrate cancer and colon cancer (Lachat, 2002). Treatment with differentiation agents to tumor cell lines can increase the expression of NDRG1 in colon cancer and prostrate cancer cells (Park, 2003; Piquemal, 1999). To date, the exact biological function of NDRG1 remains obscure. Scholars consider that it was related to cell differentiation and necessary but not sufficient for p53-induced apoptosis (Stein, 2004). There is little report about the expression of NDRG1 in esophageal carcinoma, so we detceted the protein expression in esophageal carcinoma to probe the role of NDRG1 in its occuring and developing in order to provide some clues for diagnosis and differentiation treatment of esophageal carcinoma.

2 Materials and Methods

2.1 Materials

Human esophageal tissue specimens of surgical resection were obtained from 49 patients with esophageal cancer at Anyang Tumor Hospital during the period from September to November,

2004. There were 25 men and 24 women ranging age from 40 to 76 years with a mean of 58.3 years. 21 cases had regional lymph node metastasis. The tumor tissue, tissue adjacent to cancer and normal mocusa were collected in each case. The diagnosis of squamous carcinoma was made according to the WHO's criteria, 2000. All patients had no chemical and radial therapy history before surgical operation.

All specimens were fixed in 4% polyformalin, embedded in paraffin and stained by routine HE for routine HE analysis and histochemistry. 49 cases of carcinoma were divided into three levels according to tumor differentiation grade: high differentiation in 14 cases, moderate differentiation in 23 cases, and poor differentiation in 12 cases.

2.2 Methods

Immunohistochemistry S-P method was used to detect NDRG1 protein. NDRG1 goat polyclonal antibody was purchased from SANTA CRUZE Corporation, US. and immunostaining S-P kit was purchased from ZYMED Corporation, US. Immunohistochemistry was performed as follows (1) Four-micron sections of human tissues were deparaffinized by xylene, dehydrated in graded alcohol. Endogenous peroxidase activity was blocked with 3% H_2O_2 in methanol at room temperature for 15 min. (2) To retrieve the immunoreactivity, tissue sections were boiled twice in 10 mM sodium citrate, pH 6.0 for 5 min in an 800W microwave oven. (3) Then, non-specific staining was blocked by incubating in normal non-immune serum at room temperature for 10 min. (4) The goat anti-NDRG1 was added to adjacent tissue sections and incubated overnight at 4℃. (5) Biotin-conjugated second antibody was added to the sections and incubated at room temperature for 10 min. (6) S-P complex was added at room temperature for 10 min and DAB was used for the color reaction, and then the slides were counterstained with hematoxylin. The tissue sections were washed with PBS (0.01M, pH 7.4) between each step. Positive and negative controls were simultaneously used to ensure the specificity and reliability of staining. The positive result showed yellow or brown coloration in cytoplasm and /or plasma membranes.

The degree of NDRG1 staining was estimated by semi-quantitative evaluation and categorized by the extent and intensity of staining as follows (Shen, 1995):

(1) The extent of positive cells was estimated as 0 = positive staining cells $\leqslant$5%, 1 = positive staining cells in 6% − 30%, 2 = positive staining cells in 31% − 70%, 3 = positive staining cells in 71% − 100%.

(2) The intensity of staining was scored as 0 = achromatic, 1 = light yellow, 2 = yellow, 3 = brown. Combined staining score was used to evaluate the results of NDRG1 staining. The extent of positive cells was multiplied by the intensity of staining and scored as follows: (−) = 0, (+) = 1 − 3, (++) = 4 − 6. Results of the immunohistochemistry were judged based on the intensity of staining and the grading of the NDRG1 was done by two independent persons without prior knowledge of the patient outcome.

2.3 Stastistical analysis

The results were calculated by analysis SPSS software 11.0. χ^2 test was used to analysis the difference between groups. $P < 0.05$ was considered stastistically significance. All reported P values were two-sides.

3 Results

3.1 The expression of NDRG1 protein in esophageal normal mucosa, atypical hyperplasia mucosa and squamous cell carcinoma

The NDRG1 protein was light yellow to brown localized in the cytoplasm and cell membrance. The nuclear stain was not observed. In normal esophageal mucosa, the surface epithelial cells mainly stained and the majorities were yellow micro-granules located in the cytoplasm. The basal cells and atypical hyperplasia cells didn't be stained. The esophageal carcinoma cell stained lighter than normal mucosa epithelial cell. The expression results of NDRG1 protein was summarized in Table 1 and showed in Figures 1 − 3.

Table 1. Comparison of NDRG1 protein expression in all groups

Group	Cases	Expression of NDRG1			Percentage (%)
		−	+	++	
Normal esophageal mucosa[A]	49	2	4	43	95.9
Atypical hyperplasia mucosa[B]	23	5	15	3	78.3
Esophageal carcinoma[C]	49	5	40	4	89.8

A to B; A to C, $P<0.01$; B to C, $P>0.05$

The results in Table 1 showed that the positive expression rate of NDRG1 protein had no differences in cancerous tissue, mucosa adjacent to cancer tissue and normal esophageal mucosa. But the protein expression levels were different. In normal mucosa, the positive expression rate in low expression level (+) were: 8.2%, 61.3%, 81.8%; the expression rate in higher expression level (++) were: 87.7%, 13%, 8.1%, and they had significant difference ($P<0.01$). These results showed

that the expression level of NDRG1 protein in normal esophageal mucosa was higher than atypical hyperplasia mocusa and esophageal carcinoma. The lower expression of NDRG1 in atypical hyperplasia mucosa was concerned with the unexpression of NDRG1 in basal cells.

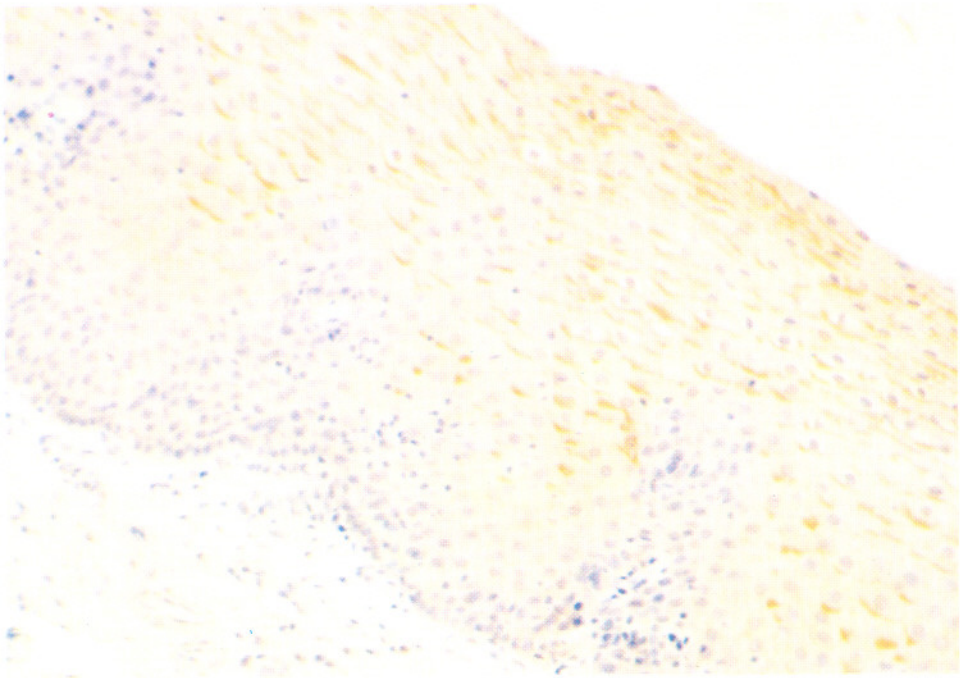

Figure 1. The expression of NDRG1 protein in normal esophageal tissue (S-P method, ×200)

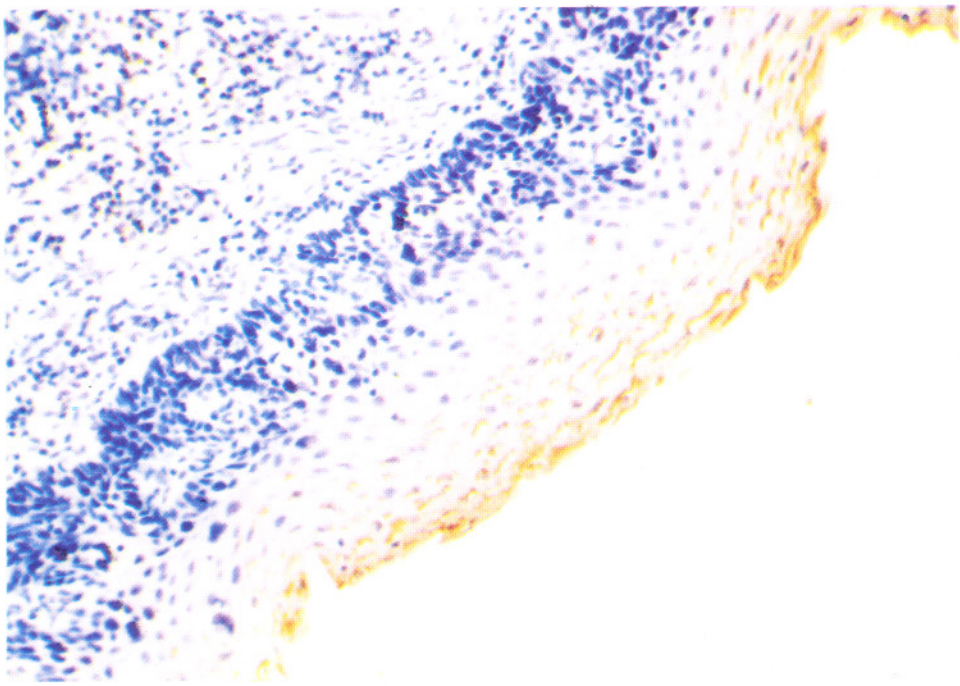

Figure 2. The expression of NDRG1 protein in esophageal atypical hyperplasia mucosa(S-P method, ×200)

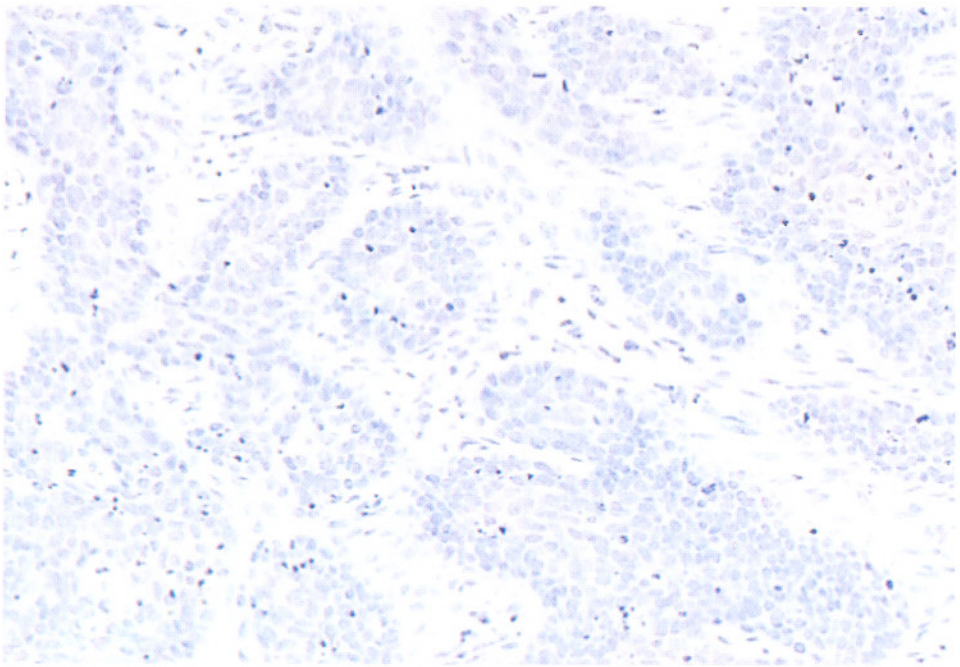

Figure 3. The expression of NDRG1 protein in ESCC(S-P method, ×200)

3.2 The relationship of NDRG1 protein expression and histological differentiations

The results of NDRG1 expression in esophageal carcinoma showed that there were no differences in different differentiation levels of esophageal squamous carcinomas ($P > 0.05$). The results were showed in Table 2.

Table 2. NDRG1 protein expression and histological differentiations in ESCC

Group	Cases	Expression of NDRG1			Percentage (%)
		−	+	++	
High differentiation	14	2	10	2	85.7
Moderate differentiation	23	2	19	2	91.3
Poor differentiation	12	1	10	1	91.7

Three groups compared, $P > 0.05$.

3.3 The relationship between NDRG1 protein expression and lymph node metastasis of esophageal carcinoma

The results showed that the expression of NDRG1 was lower and not concerned with the lymph node metastasis ($P > 0.05$). The results were showed in Table 3.

4 Discussion

NDRG1 has been mapped on chromosome 8q24.2 (van Belzen, 1997, 1998) and had a length of approximately 60 kb. NDRG1 contains 16 exons and 15 introns and NDRG1 mRNA has a length of 3 kb which contained an 1182 bp coding region, and its coding product contained 394 amino acids. Most studies showed that NDRG1 was involved in cellular growth (Kokame, 1998; Taketomi, 2003; Agarwala, 2000), cell differentiation (Piquemal, 1999; Qu, 2002; Piquemal, 1999), tumor genesis, metastasis (Kyuno, 2003) and poor clinical outcome of some tumor (Li, 2003).

Table 3. The relationship of NDRG1 protein and lymph node metastasis in ESCC

Group	Cases	Expression of NDRG1			Percentage (%)
		−	+	++	
Metastasis group	21	2	17	2	90.5
Non-metastasis group	28	3	23	2	89.1

Two groups compared, $P > 0.05$.

Our study showed that NDRG1 protein was mainly expressed on the surface of epithelial cells, and not expressed in basal cells. This result was in accordance with Lauchet P's (2002) result to digestive tract mucosa and urinary system mucosa. We found that the expression of NDRG1 protein was lower in esophageal squamous carcinoma cells. The positive rate was significantly lower than that of normal mucosa, and some squamous carcinoma even didn't express the NDRG1 protein. This showed NDRG1 was low expressed in esophageal carcinoma. Similar results were also found in colon cancer, prostrate cancer and renal cancer (Li,

2003). In addition, van Belzen et al (1997) reported that compared to normal colon mucosa, NDRG1 mRNA expression was decreased in colon adenomas and adenocarcinoma. The high expression of NDRG1 can inhibit tumor growth (Kurdistani, 1998; Kyuno, 2003). So our results may suggest that NDRG1 gene might play an important role in carcinogenesis and development of esophageal carcinoma.

Our study also found that there were no differences of NDRG1 expression between each differentiation levels of ESCC, which indicated that NDRG1 expression wasn't correlated to tumor differentiation level. Similar results also found in Wang Zhan's (2004) research on colon cancers.

There was little research on NDRG1 and tumor metastasis. Guan(2000) reported that NDRG1 stable transfection of SW620 metastatic colon cancer cell line with Drg1 cDNA induced morphological changes and down-regulated metastatic colon cancer cells to nearly undetectable levels when compared with primary colon cancer. Bandyopadhyay (2003) research also indicated that over expression of NDRG1 could inhibit the metastasis of prostrate cancer. But our results indicated there was no difference between lymph node metastasis group and no lymph metastasis group, suggesting that NDRG1 expression had no relation with ESCC metastasis. The reasons need further research.

Our results may provide some clues for ESCC carcinogenesis, prognosis and differentiation therapy.

Acknowledgments

This subject is supported by National Science Foundation of China, No 30470779.

Correspondence to:

Yunhan Zhang
Henan Key Laboratory of Tumor Pathology
Zhengzhou, Henan 450052, China
Telephone: 86-371-6665-8175
Email: yhzhang@zzu.edu.cn

References

1. Agarwala KL, Kokame K, Kato H, et al. Phosphorylation of RTP, an ER stress-responsive cytoplasmic protein. Biochem Biophys Res Commun 2000;272(2): 641 – 7.
2. Bandyopadhyay S, Pai SK, Gross SC, et al. The Drg-1 gene suppresses tumor metastasis in prostate cancer. Cancer Res 2003,15;63(8):1731 – 6.
3. Guan RJ, Ford HL, Fu Y, et al. Drg-1 as a differentiation-related, putative metastatic suppressor gene in human colon cancer. Cancer Res 2000; 60(3): 749 – 55.
4. Kokame K, Kato H, Miyata T. Nonradioactive differential display cloning of genes induced by homocysteine in vascular endothelial cells. Methods 1998; 16(4): 434 – 43.
5. Kurdistani SK, Arizti P, Reimer CL, et al. Inhibition of tumor cell growth by RTP/rit42 and its responsiveness to p53 and DNA damage. Cancer Research 1998; 58(19): 4439 – 44.
6. Kyuno J, Fukui A, Michiue T, et al. Identification and characterization of Xenopus NDRG1. Biochem Biophys Res Commun 2003; 309(1): 52 – 7.
7. Lachat P, Shaw P, Gebhard S, et al. Expression of NDRG1, a differentiation related gene, in human tissues. Histochem Cell Biol 2002;118(5):399 – 408.
8. Li J, Kretzner L. The growth-inhibitory Ndrg1 gene is a myc negative target in human neuroblastomas and other cell types with overexpressed N- or C-myc. Mol Cell Biochem 2003; 250(1): 91 – 105.
9. Masuda K, Ono M, Okamoto M, et al. Downregulation of Cap43 gene by von Hippel-Lindau tumor suppressor protein in human renal cancer cells. Int J Cancer 2003; 105(6): 803 – 10.
10. Park DJ, Vuong PT, de Vos S, et al. Comparative analysis of genes regulated by PML/RAR and PLZF/RAR in response to retinoic acid using oligonucletide arrays. Blood 2003;102(10),3727 – 36.
11. Park H, Adams MA, Lachat P, et al. Hypoxia induces the expression of a 43-kDa protein (PROXY-1) in normal and malignant cells. Biochem Biophys Res Commun 2000; 276(1): 321 – 8.
12. Piquemal D, Joulia D, Balaguer P, et al. Differential expression of the RTP/Drg1/Ndr1 gene product in proliferating and growth arrested cells. Biochim Biophys Acta 1999; 1450(3): 364 – 73.
13. Qu X, Zhai Y, Wei H, et al. Characterization and expression of three novel differentiation-related genes belong to the human NDRG gene family. Mol Cell Biochem 2002;229(1): 35 – 44.
14. Shen H. Study on the quantitative method of immunohistochemistry (Ⅲ). Zhongguo Zuzhi Huaxue Yu Xibao Huaxue Zazhi 1995; 4(1):89 – 91.
15. Stein S, Thomas EK, Herzog B, et al. NDRG1 is necessary for p53-dependent apoptosis. J of Biological Chemistry 2004;279(47):48930 – 40.
16. Taketomi Y, Sugiki T, Saito T, et al. Identification of NDRG1 as an early inducible gene during in vitro maturation of cultured mast cells. Biochem Biophys Res Commun 2003; 306(2): 339 – 46.
17. van Belzen N, Dinjens WN, Diesveld MP, et al. A novel gene which is up-regulated during colon epithelial cell differentiation and down-regulated in colorectal neoplasms. Lab Invest 1997; 77(1): 85 – 92.
18. van Belzen N, Dinjens WN, Eussen BH, et al. Expression of differentiation-related genes in colorectal cancer: possible implications for prognosis. Histol Histopathol 1998; 13(4): 1233 – 42.
19. Wang Zhen, Wang Fang, Wang Wei-Qi, et al. Correlation of N-myc downstream-regulated gene 1 overexpression with progressive growth of colorectal neoplasm. World J Gastroenterol 2004 ;10(4):550 – 4.
20. Zhou D, Salnikow K, Costa M. Cap43, a novel gene specifically induced by Ni^{2+} compounds. Cancer Research 1998; 58(10):2182 – 9.

Received October 8, 2005

A Theoretical Approach to the Overall Control of the Nervous System in Human Beings

Sum-Wah Lam

Russian Military Medical Academy, P. O. Box 806, Tuen Mun Central Post Office, Hong Kong SAR, China

Abstract: The First Law of the Overall Control of the Nervous System in Human Beings (The Law of Health and Disease): The shape and arrangement of our cerebral cortex controls our physiology as well as psychology. The Second Law of the Overall Control of the Nervous System in Human Beings (The Brain Functions Controlled Law): Postures as a habit can control the shape and arrangement of our cerebral cortex, which would in turn control our physiology and our psychology. The Third Law of the Overall Control of the Nervous System in Human Beings (The Hormonal Secretions Controlled Law): Whenever there is a change in the shape and arrangement of our cerebral cortex, there will be a change in the quantity of different major and orphan hormones, especially to those hormones which have direct or indirect relationship with the pituitary gland and the hypothalamus. [Life Science Journal. 2006;3(1):23-28] (ISSN: 1097-8135).

Keywords: overall control; nervous system; human beings

Contents

(A) Introduction

The term "Nervous disorder" implies that someone is suffering from psychiatric sickness, which results in both physiological and psychological changes. In other words, all these physiological and psychological changes are originated in part or in whole from the change in the shape and arrangement of one's cerebral cortex and its associated organs. This has an enormous implication to health and disease. Three laws are proposed by the author to portray how we can control the shape and arrangement of our cerebral cortex and its associated organs. Law 1 states that the shape and arrangement of our cerebral cortex and its associated organs control our physiology as well as our psychology. Law 2 states that postures as a habit can maintain or change the shape and arrangement of our cerebral cortex and its associated organs. Law 3 states that whenever there is a change in the shape and arrangement of our cerebral cortex and its associated organs, there is always a change in the quantity of different major and organ hormones secreted. These three laws are proposed by the author to be the Laws of the Overall Control of the Nervous System in Human Beings. Below are the theoretical frameworks of these three laws.

(B) The First Law of the Overall Control of the

Nervous System in Human Beings (Law of Health and Disease): The shape and arrangement of our cerebral cortex and its associated organs control our physiology as well as our psychology.

Below are some of the facts, which support the first law:

Systematic changes (asymmetrical in nature) in hemispheric organization are associated with pathological disturbances of mood (Flor-Henry, 1983). Deglin and Nikolaenko (1975) found that at the end of laterised induced seizure, sensori-motor cortical functions are transiently depressed. Laterization to the dominant hemisphere was produced profound intellectual retardation while laterization to non-dominant hemisphere lead to distinct intensification of emotional manifestations. Golden et al (1980) found that CT scan showed that the density of left hemisphere was greater than that of the right for a number of chronic schizophrenics. Sowell et al (2000) found brain abnormalities in MRI in mapping of the cerebral cortex and its associated organs). Niemann et al(2000) demonstrated that a smaller left hippocampus and left temporal horn in schizophrenic patients. Gur et al(2000) found ventricular enlargement in schizophrenics. Crespo-Facorro et al (2000) showed there were regional frontal abnormalities in schizophrenia patients. Flashman et al(2000) found there was a smaller brain size associated with schizophrenics. Garver DL, Nair TR, Christensen JD, Holcomb JA, and Kingsbury, SJ (2000) demonstrated that there was instability in brain and ventricle for psychotic patients. Hirayasu et al(2000) conducted a study on the hippocampal and superior temporal gyrus volume on schizophrenics and found they are different from normal subjects. Sanfilipo M, Lafargue T, Rusinek H, Arena L, Loneragan C, Lautin A, Lautin A, and Feiner D et al(2000) found there were volumetric differences in the measurement of the frontal and temporal lobe regions in schizophrenics. Downhill et al(2000) showed that there were difference in the shape and size of the corpus callosum in schizophrenics. These are some of the findings on the relationship between the shape and arrangement of the cerebral cortex and its associated organs, and schizophrenics. Findings on the relationship between the shape and arrangement of patients with anxiety, mania, sexual disorder, and other psychopathology are many. In fact, Sowell et al(2000) did a literature review on the abnormalities in shape and arrangement of the cerebral cortex and its associated organs as demonstrated by magnetic resonance images.

All these demonstrate that the cause of physiological and psychological disorders is rooted in the change in shape and arrangement of the cerebral cortex and its associated organs. Therefore, if we can control the shape and arrangement of different parts of the cerebral cortex and its associated organs, we can control our physiology as well as our psychology.

(C) The Second Law of the Overall Control of the Nervous System Human Beings (The Brain Functions Controlled Law): Postures as a habit, through tension and relaxation of our voluntary muscles, can maintain or change the shape and arrangement of our cerebral cortex, which would mean postures as a habit, can control our physiology as well as our psychology (Our voluntary muscular system controls the shape and arrangement of our cerebral cortex).

Below are some of the facts, which support the second law:

(1) Theories on therapeutic exercise contain much information on the relationship between exercise and therapy on certain diseases. As a result, exercise prescription is possible (Oshida, 2000; Kimura, 2000; Sunami, 2000; van der Velde, 2000; Phillips, 2000; van Tulder, 2000). During the process of exercise therapy, certain muscles are relaxed or at tension repeatedly. Therapy is possible because the voluntary muscular system controls the shape and arrangement of the cerebral cortex and hence can control the functions of the nervous system.

(2) Yoga exercise is a well-established discipline, which has a very long history. Practitioners of the Yoga exercise can maintain both their mind and body healthy, through certain postures as a habit. For many people with physiological or psychological defects, Yoga exercise provides a means of therapy (Kamei, 2000; Tooley, 2000; Bera, 1998; Raghuraj, 1998; Murugesan, 2000; Ramaratam, 2000; Hudson, 1998; Farrell, 1999; Gotter, 1999; Singh, 1999). This is possible because Yoga exercise can change the shape and arrangement of one's cerebral cortex and hence can change one's physiology and psychology, which can be used as a means of therapy.

(3) Dunkell's Theory (1977) on sleep postures as a habit has portrayed that there is a closed relationship between sleep postures and personality. This is only possible if a particular type of sleep posture will lead to a particular kind of shape and arrangement of one's cerebral cortex.

It is recorded in ancient Chinese sex books that different postures as a habit in the process of sexual

intercourse provide means of therapy to certain diseases. People who practice such postures can become healthier (Wilson, 1989; Stanway, 1988).

(4) It is known that the body language, the postures of sitting and walking, reflects our psychology and physiology (Pell, 1989; Leiber, 1992; Kurz, 1981; Russell, 1979; Babic, 1978; Bijeljac-Babic, 1978; Lundgren, 1994). It is also known that improper postures will result in chronic disease, for example, low back pain (Hartvigsen, 2002; Clark, 1996; Kauppila, 1996; Chilvers, 1996). The above phenomena can be explained by saying that our postures are controlled by the shape and arrangement of our cerebral cortex and the voluntary muscular system controls the shape and arrangement of our cerebral cortex.

(5) Alexander technique also provides means of therapy to certain diseases by having certain postures as a habit. This involves particular types of posture, which is only possible if the voluntary muscles control the shape and arrangement of the cerebral cortex and hence can change the physiology and psychology of the practitioner (Gelb, 1981; Huxley, 1940; Huxley, 1986; Jeffers, 1988; Barlow, 1984; Maisel, 1974; Lewis, 1986; Alexander, 1932; and Hayne, 1987).

(D) The Third Law of the Overall Control of the Nervous System in Human Beings (The Hormonal Secretions Controlled Law): Whenever there is a change in posture as a habit, which involves voluntary muscles, there is always associated with a change in the quantity of endocrine secretions, especially to those hormones which have direct or indirect relationship with the pituitary gland and the hypothalamus.

Below are some of the facts:

Postures as a habit during different physical activities and rest can alter the quantity of hormonal secretions (Brooke-Wavell, 2001; McMahon, 1985; Moreau, 2001; Wheeler, 1984; Heitkamp, 1996; Bunt, 1986; Cumming, 1986; Mathur, 1986; Ronkainen, 1986; Houmard, 1990; Mathur, 1986), to quote a few.

(E) Discussion

(1) How our physiology and psychology are controlled?

CT and MRI scan films show that many serious psychiatric sicknesses show peculiar patterns of shape and arrangement with the cerebral cortex and its associated organs. These indicate that the shape and arrangement of our cerebral cortex and its associated organs are relevant to our physiology as well as psychology. In fact, numerous diseases, which etiologies are unknown at present, for example, all types of hormonal diseases, such as diabetes mellitus, thyrotoxicosis, various kinds of cancer, and many other benign and malign diseases are originated from having problems with the shape and arrangement of our cerebral cortex and its associated organs. The mechanism in controlling one's disease and well-being is that when the geometric shape of some convolutions in the cerebral cortex change, there are always a change in the degree of one's physiological and psychological variables. By this mechanism, physiological and psychological variables can shift from one extreme to another. This explains how homeostasis can be disturbed and maintained, i.e. depending on the shape and arrangement of one's cerebral cortex and its associated organs. The First Law of the Overall Control of the Nervous System in Human Beings explains the causes of numerous diseases which have no answers at the moment, such as various kinds of cancer, various kinds of heart diseases, schizophrenia and other psychiatric sicknesses, which the diseases causes are unknown. All human physiology and psychology are controlled by the shape and arrangement of their cerebral cortex and its associated organs.

(2) How to control the shape and arrangement of our cerebral cortex, so as to control our physiology as well as our psychology?

If the author's first postulate is right, how to control the shape and arrangement of the human cerebral cortex will come next so as to solve physiological and psychological problems. If we can control the shape and arrangement of our cerebral cortex and its associated organs, we can control most aspects of our physiology and psychology. Law 2 of the overall control of the nervous system in human beings portrays how our physiology and psychology can be controlled. In fact, the shape and arrangement of our cerebral cortex and its associated organs are controlled by our voluntary muscular system, i.e. by having postures as a habit. In fact, our ancestors have developed many methods to control the shape and arrangement of our cerebral cortex, though they did not know why they work and could not explain them on scientific grounds, such as postures as a habit in exercise, sleep, sexual intercourse, sitting, walking, or any kind of sports or device which voluntary muscular movements or postures as a habit are involved. In fact, all known cases of malign and benign diseases that can be cured without having any known medical treatment

must have some changes in the shape and arrangement of his or her cerebral cortex and its associated organs to make him or her healthy again by chance or by accident. These cases are not miracles. In addition, by analyzing one's different postures it is possible to know his/her physiology or psychology, which is useful in diagnosis or prognosis of certain physical and mental diseases. Furthermore, it is possible to tell one's physiology and psychology at different times by analyzing his/her handwriting at different stages of his/her life. The author also found that musculature on our face, the shape of the eye brows and the lines on our hands change as a result of changing in habits of certain postures in different times of our life which reflect a change in our psychology and physiology.

There are many ways to prove that our voluntary muscular system controls functions of the brain. One of the immediate consequence is that decussation of nerve fibers in the brain stem can be interpreted. It usually needs a signal from the cerebral cortex to execute a voluntary movement. It is also known that the left-brain controls the right side of the muscular system, and *vice versa*. In fact, when a signal is executed from the left-brain for a voluntary movement on the right side, the muscles on the right side will exert a signal to the right brain so as to set a balance on the left side of the muscular system. The reverse is also true, which is essential in maintaining homeostasis. This can be easily proved in a laboratory where facilities for measurement of electrical activities are available.

It is recorded clinically that many diseases, including the communicable diseases, tuberculosis, and the non-communicable diseases, various kinds of cancer, can be cured without the intake of medicine or having other known medical treatments. Scientists should not believe in miracles. The mechanism on these is simple, as there must be some changes on the shape and arrangement of the patients' cerebral cortex for them to get recovered. In fact, numerous malignant and benign diseases are given arisen because there were changes in the shape and arrangement of the cerebral cortex. It is also under the same mechanism which people with malignant and benign diseases can be cured without having medical treatments.

Laws of the overall control of the nervous system explain the etiology of many non-communicable diseases and some communicable diseases. They explain how many psychiatric sicknesses are given rise, including epilepsy, schizophrenia, affective disorder, hysteria, obsessional states, and finally sexual disorder. They explain how we can get cured in many sicknesses without the intake of medicine and receiving any known medical treatment. They also explain how physiological brain-washing is possible. By the application of these hypotheses mental giants such as Einstein and other great thinkers can be produced in a sleep laboratory. Dunkell (1977) found that people with different sleep postures have different personality. But how about if we ask people to change their sleeping positions as a habit? Shall we expect a change in his/her personality as well? I believe and support the statement that there will be a change in personality from the first type to the second type. If not, all information from Dunkell's book will be invalid. Therefore, sleep postures as a habit can portray one's tendency for different diseases. Budda did sleep in some particular position as a habit, and he was also famous for his ability to control his physiology and psychology. I believe that Budda was the first person, who knew some of the ways to control human physiology and psychology, by sleeping or sitting in some particular positions. My Laws can link up the gap between oriental and western medicine. I believe that Buddhism is a treasure source of information on how to control human physiology and psychology through different postures.

Therefore, if we can control the shape and arrangement of one's cerebral cortex, we can control his or her sicknesses. Unfortunately, no controlled experiment on this has been done and the author thinks a study on the relationship between shape and arrangement of the cerebral cortex and its associated organs, and psychopathological variables is necessary.

In the coming few decades, scientists can devise means to alter or change patient's shape and arrangement of their cerebral cortex and its associated organs by means of electrical methods, such as the Electro-convulsive Therapy, Yoga exercise, breathing exercise, chemical convulsants, or any voluntary movement which muscles are involved, so as to cure diseases. This is very important in the treatment of all kinds of sickness symptoms, no matter physical or psychological, mild or serious.

(3) Effects on change in the shape and arrangement of our cerebral cortex on the quantity of hormonal secretions.

When there are changes in postures as habit, such as having a particular kind of sports, exercise, there are always changes in quantity of different hormonal secretions, as demonstrated by Law 3 of the overall control of the nervous system in human beings. One of the very factors how Yoga exercise is effective in controlling our physiology as well as

our psychology is that Yoga exercise has profound influence on the quantity of different hormonal secretions. The shape of our skull is another factor, which can determine our physiology and psychology, as the shape and arrangement of our cerebral cortex always depends on the shape of our skull. As far as to healing diseases are concerned, we certainly can control our postures as a habit to deal with the benign and malignant diseases.

(F) Inter-relationship between the three laws

The shape and arrangement of our cerebral cortex control our physiology and psychology (Law 1) and the shape and arrangement of our cerebral cortex in turn is controlled by our postures as a habit (Law 2). Postures as a habit controls our physiology and psychology, this is possible because the shape and arrangement of our cerebral cortex controls the secretions, in terms of quantity, of different major and organ hormones (Law 3).

Correspondence to:
Sum-Wah Lam
P.O. Box 806, Tuen Mun Central Post Office
Hong Kong SAR, China
Telephone: 852-8119- 8135
Fax: 852-3014-5724
Email: drswlam@gmail.com

References

1. Aaronson ST, Siham R, Biber MP, et al. Brain state and body position. Arch Gen Psychiatry 1982;39:330－5.
2. Alexander FM. The Use of Self. Dutton, New York, 1932.
3. Babic R, Green E, Bessineton JC, et al. Body language and tonic postural action. Agressologie 1978; 19(B): 51－2.
4. Barlow W. The Alexander Principle. Arrow, 1984.
5. Bera TK, Gore MM, Oak JP. Recovery from stress in two different postures and in Shavasana-a yogic relaxation posture. Indian J Physiol Pharmacol 1998;42(4):473－8.
6. Berbard T. Hatha Yoga. London: Rider, 1968.
7. Bijeljac-Babic R. Body language and communication. Agressologie 1978; 19(6):349－51.
8. Brooke-Wavell K, Prelevic GM, Bakridan C, et al. Effects of physical activity and menopausal hormone replacement therapy on postural stability in postmenopausal women-a cross sectional study. Maturitas 2001; 37(3):167－72.
9. Bunt JC, Boileau RA, Bahr JM, et al. Sex and training differences in human growth hormone levels during prolonged exercise. J App Physiol 1986 Nov; 61(5): 1796－801.
10. Cartwright RD. Effect of sleep position on sleep apnea severity. Sleep 1984;7(2):110－4.
11. Chilvers CD, Parker AH, Guillen G. Low back pain. NZ Med J 1996;109(1028):324.
12. Clark AJ . Back pain without apparent cause. CMAJ 1996; 155(7):861－2.
13. Crespo-Facorro B, Kim J, Andreasen NC, et al. Regional frontal abnormalities in schizophrenia: a quantitative gray matter vs. and cortical surface size study. Biol Psychiatry 2000. July 15; 48(2):110－9.
14. Cumming DC, Brunsting LA 3rd, Strich G. Reproductive hormone increases in response to acute exercise in men. Med Sci Sports Exerc 1986; 18(4): 369－73.
15. Deglin VL, Nikolaenko NN. Role of the dominant hemisphere in the regulation of emotion states. Human Physiology 1975; 1(3).
16. De Koninck J, Gagnon P, Lallier. Sleep positions in the young adult and their relationship with subjective quality of sleep. Sleep 1983;6(1):52－9.
17. Domino G, Bohn SA. Hynagogic exploration: sleep positions and personality. J Clin Psychol 1980:36;760－2.
18. Downhill JE, Buchsbaum MS, Wei T, et al. Shape and size of the corpus callosum in schizophrenia and schizotypal personality disorder. Schizophr Res 2000 May 5; 42 (30): 193－208.
19. Dunkell S. Sleep Positions. New York, William Morrow, 1977.
20. Farrell SJ, Ross AD, Sehgal KV. Eastern movement therapies. Phys Med Rehabil Clin N Am 1999 Aug; 10 (3): 617－29.
21. Felson B. Computerized Cranial Tomography. New York: Grune and Stratton, 1977.
22. Flashman LA, McAllister TW, Andreasen NC, et al. Smaller brain size associated with unawareness of illness in patients with schizophrenia. Am J Psychiatry 2000; 157 (7): 1167－9.
23. Flor-Henry P. Cerebral Basis of Psychopathology. Bristol: John Wright, 1983.
24. Garver DL, Nair TR, Christensen JD, et al. Brain and ventricle instability during psychotic episodes of the schizophrenias. Schizophr Res 2000; 44(1): 11－23.
25. Gelb M. Body Learning: An Introduction to the Alexander Technique. Aurum Press, 1981.
26. Golden CJ, Graber B, Coffman J, et al. Brain density deficits in chronic schizophrenia. Psychiatry Res 1980.
27. Gotter AC . Western movement therapies. Phys Med Rehabil Clin N Am 1999 Aug; 10(3): 603－16.
28. Gur RE, Turetsky BI, Cowell PE, et al. Temporolimbic volume reductions in schizophrenia. Arch Gen Psychiatry 2000 Aug; 57(8): 769－75.
29. Hartvigen J, Leboeuf-Yde C, Lings S, Does sitting at work cause low back pain? Ugeskr Laeger 2002 Feb 4; 164(6): 759－61.
30. Hayne CR. Total back care. Dent, 1987.
31. Heitkamp HC, Huber W, Scheib K. Beta-Endorphin and adrenocorticotrophin after incremental exercise and marathon running-female responses. Eur J Appl Physiol Occup Physiol 1996; 72(5－6): 417－24.
32. Hewitt J. Teach Yourself Yoga. London: English University Press, 1960.
33. Hirayasu Y, Shenton ME, Salisbury DF, et al. Hippocampal and superior temporal gyrus volume in first-episode schizophrenia. Arch Gen Psychiatry 2000; 57 (6): 618－9.
34. Hobson JA, Spagna T, Malenka R. Ethology of sleep with time-lapse photograph: Postural immobility and sleep cycle phase in man. Science 1978; 201: 1251－3.

35. Houmard JA, Costill DL, Mitchell JB, et al. Testosterone, cortisol, and creatine kinase levels in male distance runners during reduced training. Int J Sports Med 1990 Feb; 11(1):41 – 5.
36. Hudson S. Yoga aids in back pain. Aust Nurs J 1998 Apr; 5(9):27.
37. Huxley A. Ends and Means. Chatto and Windus, 1940.
38. Huxley A. Eyeless in Gaza. Grafton, 1986.
39. Jeffers S. Feel the fear and do it anyway. Century, 1988.
40. Kamei T, Toriumi Y, Kimura H, et. al. Decrease in serum cortisol during Yoga exercise is correlated with alpha wave activation. Percept Mot Skills 2000; 90(3 Pt 1): 1027 – 32.
41. Kauppila LI. Studying low back pain. Spine 1996; 21 (4):527.
42. Kimura, Y. Exercise therapy for hypertension. Nippon Rinsho 2000; 58 Suppl 2:56 – 9.
43. Kimura Y, Iwasaka T. Complication of exercise therapy. Nippon Rinsho 2000;58 Suppl: 226 – 8.
44. Kurokawa K, Nakamura K, Sumiyoshi T, et al. Ventricular enlargement in schizophrenia spectrum patients with prodromal symptoms of obsessive-compulsive disorder. Psychiatry Res 2000; 99(2):83 – 91.
45. Kurz C. Language and behaviour, two means of communication. Soins Psychiatr 1981; (12):2.
46. Leiber B. Body language: "Language to be seen". Kinderkrankenschwester 1992; 11(3):94 – 5.
47. Lewis, D. The Alpha Plan. Methuen, 1986.
48. Lundgren BF. Your body language reveals you! Vardfacket 1994; 18(10):4 – 6.
49. Maisel E. The Alexander Technique: Essential Writings of F. M. Alexander. Thames and Hudson, 1974.
50. Mathur DN, Toriola AL, Dada OA. Serum cortisol and testosterone levels in conditioned male distance runners and non-athletes after maximal exercise. J Sports Med Phys Fitness 1986; 26(3): 245 – 50.
51. Mathur RS, Neff MR, Landgrebe SC, Time-related changes in the plasma concentrations of prolactin, gonadotropins, sex hormone-binding globulin, and certain steroid hormones in female runner after a long-distance race. Fertil Steril 1986; 46(6): 1067 – 70.
52. McMahon M, Palmer RM. Exercise and hypertension. Med Clin North Am 1985; 69(1):57 – 70.
53. Moreau KL, Degarmo R, Langley J, et al. Increasing daily walking lowers blood pressure in postmenopausal women. Med Sci Sports Exerc 2001; 33(11): 1825 – 31.
54. Murugesan R, Govindarajulu N, Bera TK. Effect of selected yogic practices on the management of hypertension. Indian J Physiol Pharmacol 2000;44(2): 207 – 10.
55. Niemann K, Hammers A, Coenen VA, et al. Evidence of a smaller left hippocampus and left temporal horn in both patier first episode schizophrenias and normal control subjects. Psychiatry Res 2000; 99(2): 93 – 110.
56. Oshida Y. Practice of exercise therapy for diabetes mellitus. Nippon Rinsho 2000; 58 Suppl: 391 – 6.
57. Pell AR . Body language. Indiana Med 1989; 82(9): 749.
58. Phillips BA, Mastaglia FL . Exercise therapy in patients with myopathy, 2000. Curr Opin Neurol 2000; 13(5): 547 – 52.
59. Raghuraj P, Ramakrishnan AG, Nagendra HR, et al. Effect of two selected yogic breathing techniques of heart rate variability. Indian J Physiol Pharmacol 1998; 42 (4): 467 – 72.
60. Ramaratam S, Sridharan K. Yoga for epilepsy(Cochrane Review). Cochrane Database Syst Rev 2000; (3): CD001524.
61. Ronkainen HR, Pakarinen AJ, Kauppila AJ. Adrenocortical function of female endurance runners and joggers. Med Sci Sports Exerc 1986; 18(4):385 – 9.
62. Russell RL, Stile WB. Categories for classifying language in psychotherapy. Psychol Bull 1979; 86(2):404 – 19.
63. Sanfilipo M, Lafargue T., Rusinek H, Arena L, Loneragan C, Lautin A, Lautin A, and Feiner D, et. al. Cognitive performance in schizophrenia: relationship to regional brain volumes and psychotic symptoms. Psychiatry Res 2002; 116(1 – 2): 1 – 23.
64. Singh R. Role of yogic exercises/meditation in aircrew stress management. Aviat Space Environ Med 1999; 70 (9):939.
65. Sivananda S. Practice of Yoga. Sivanandanagar, U. P. Ddivine Life Society, 1970.
66. Sodee DB. Correlations in Diagnostic Imaging. New York: Appleton Century Crofts, 1979.
67. Solis H. Fernandez-Guardiala & Valverde, R. Neuropharmacologic and Neuroendocrine inter-relations of Human Sleep. In: The Function of Sleep. New York: Academic Press, 1979.
68. Sowell ER, Toga AW, Asarnow R. Brain abnormalities observed in childhood-onset schizophrenia: a review of structural magnetic resonance imaging literature. Ment Retard Dev Disabil Res Rev 2000; 6(3):180 – 5.
69. Sowell ER, Levitt J, Thompson PM, et al. Brain abnormalities in early-onset schizophrenia spectrum disorder observed statistical parametric mapping of structural magnetic resonance imaging of volume differences in brain structure. Am J Psychiatry 2000; 157(9): 1475 – 84.
70. Stanway A. The Loving Touch. Barcelona: Guild Publishing, 1988.
71. Sunami Y, Kiyonaga A, Tanaka H. The basic concept of exercise therapy. Nippon Rinsho. 2000; 58 suppl:216 – 20.
72. Thomson, John A. An Introduction to Clinical Endocrinology. New York: Churchill Living Stone, 1976.
73. Tooley GA, Armstrong SM, Norman TR, et al. Acute increases in night-time plasma melatonin levels following a period of meditation. Biol Phychol 2000; 53(1): 69 – 78.
74. van de Velde G, Mierau D. The effect of exercise on percentile rank aerobic capacity, pain, and self-rate disability in patients with chronic low-back pain: a retrospective chart view. Arch Phys Med Rehabil 2000; 81(11):1457 – 63.
75. Vivekananda S. Raja Yoga, or Conquering the Internal Nature. Calcutta: Advavita Ashrama, 1950.
76. Wheeler GD, Wall SR, Belcastro AN, et al. Reduced serum testosterone and prolactin levels in make distance runners JAMA 1984; 252(4):514 – 6.
77. Wilson G. The Sensual Touch. London: Guild Publishing, 1989.

Received November 16, 2005

Flow Cytometric Detection of Intracellular Cytokines and Chemokines in Acute T Lymphoblastic Leukemia Cells

Jifeng Yu[1], Liching Zhang[2], Hui Sun[3], Ling Sun[3], Qiutang Zhang[3]

1. BD Biosciences Pharmingen, San Diego, CA 92121, USA

2. General Atomics-Diazyme, San Diego, CA, USA

3. The First Affiliated Hospital, Zhengzhou University, Zhengzhou, Henan, 450052 China

Abstract: Intracellular cytokines/chemokines IL-1α, IL-2, IL-3, IL-4, IL-5, IL-6, IL-8, IL-10, IL-12, IL-16, IFN-γ, TNF-α, GM-CSF, MCP-1, MCP-3, MIP-1α and RANTES in T lymphocytes from normal donors ($n=8$) and patients with primary acute T lymphoblastic leukemia (T-ALL) ($n=35$) was detected following a 6-hr stimulation with PMA and calcium ionophore A23187. Significantly decreased percentages of cytokine/chemokine positive cells in T-ALL leukemic blasts were observed for IL-2, IL-16, IFN-α, TNF-γ and GM-CSF. In contrast, significantly increased percentage of cytokines/chemokines positive cells in T-ALL leukemic blasts was observed for IL-4, IL-8, IL-12 and MIP-1α. No significant differences were observed between T-ALL leukemic blasts and normal T lymphocytes for IL-1α, IL-3, IL-5, IL-6, IL-10, MCP-1, MCP-3 and RANTES. Also, the T-ALL patients can produce some cytokines/chemokines positive cells that normal donors usually do not produce under the PMA stimulation, such as IL-12 and MIP-1α. In 23 cases of T-ALL patients with the leukemic blast phonotyping of $CD3^-$ $CD7^+$, a minor population of $CD3^+$ $CD7^+$ T cells was also observed in 16 patients. Compared with T lymphocytes from normal donors, the $CD3^+$ $CD7^+$ cell populations in these T-ALL patients revealed significant higher percentages of IL-4, IL-8, IL-12 and MIP-1α cytokines/chemokines positive cells as well as significant lower percentages of IL-2, IL-16, IFN-α, TNF-γ and GM-CSF cytokines/chemokines positive cells. Compared with the $CD3^-$ $CD7^+$ leukemic blasts from these patients, the $CD3^+$ $CD7^+$ cell populations revealed significant higher percentages of IL-2, IL-4 and IL-12, IL-16 and IFN-α cytokines positive cells. No significant differences of IL-1α, IL-3, IL-5, IL-6, IL-8, IL-10, TNF-γ, GM-CSF, MCP-1, MCP-3, MIP-1α and RANTES positive percentages are found between the $CD3^-$ $CD7^+$ and $CD3^+$ $CD7^+$ cell populations. Detection of cytokines/chemokines in leukemic blasts may prove useful for predicting and monitoring response to therapies in which cytokines could be used as potential immunomodulators or therapeutic targets. [Life Science Journal. 2006;3(1):29 - 34] (ISSN: 1097 - 8135).

Keywords: acute T lymphoblastic leukemia; cytokine/chemokine; intracellular staining; flow cytometry

1 Introduction

T-cell acute lymphoblastic leukemia (T-ALL) is a malignant disease resulting from the clonal proliferation of T lymphoid precursors. It accounts for about 15% of all ALL cases in children and 20%-25% in adults (Rivera, 1995; Uckun, 1998). T-ALL is thought to originate inside the thymus and leukemic cells express phenotypic features corresponding to distinct maturational stages of thymocyte development: early (stage Ⅰ), intermediate (stage Ⅱ), or late (stage Ⅲ) (Heerema, 1998; Foa, 1986). Because leukemia cells may retain certain features of their normal counterparts, their characterization with respect to cytokine responsiveness can provide valuable information about the differentiation state of malignant cells and their dependence on the microenvironment. Cytokines/chemokines and its roles in the T-ALL leukemic cells have been studied by many researchers (Dibirdik, 1991; Masuda, 1991; Karawajew, 2000; Scupoli, 2003). It showed the effects of IL-7, IL-4, and IL-2 regarding the induction of proliferation in childhood T-lineage acute lymphoblastic leukemia (T-ALL), and their potential as growth factors has been pointed out (Dibirdik, 1991; Masuda, 1991). Inhibition of *in vitro* spontaneous apoptosis by IL-7 correlates with Bcl-2 up-regulation, cortical/mature immunophenotype, and better early cytoreduction of childhood T-cell acute lymphoblastic leukemia has been observed (Karawajew, 2000; Scupoli, 2003). However, many cytokines/chemokines have not been studied with T-ALL leukemic cells. Therefore, in the current study we investigated 17 different cytokines/chemokines intracellular expression profiles in leukemic blasts as well as in the non-leukemic cells

from 35 patients with T-ALL. Our data demonstrated that many different cytokines/chemokines could be detected in leukemic blasts with intracellular staining by flow cytometry after *in vitro* stimulation. Compared with T lymphocytes from normal donors, a significant decrease of cytokine/chemokine production in T-ALL was observed for IL-2, IL-16, IFN-α, TNF-γ and GM-CSF. In contrast, a significant increase of cytokines/chemokines production in T-ALL was observed for MIP-1α and IL-8. Furthermore, independent analysis of leukemic blasts and non-leukemic cells of T-ALL patients revealed differences in cytokines/chemokines production.

2 Materials and Methods

2.1 Patients and normal donors

All of the 35 patients with T-ALL fulfilled the French-American-British (FAB) Cooperative Group criteria (Bennett, 1981). Age range of patients was 14 – 52 years with 23 males and 12 females. Eight normal donors with age range of 20 – 40 years were included in this study as the normal controls.

2.2 Cells preparation

Peripheral blood samples were collected, after informed consent, from 35 adult patients with newly diagnosed T-ALL. Immunophenotype analysis of T-ALL blasts was performed by direct immunofluorescence and flow cytometry with a FACScan instrument(Becton-Dickinson, San José, CA, USA). Peripheral blood mononuclear cells (PBMC) were isolated with Ficoll-Hypaque. Before use, the cells' viability consistently exceeded 90% in each sample, as assessed by propidium-iodide (PI) dye exclusion. Then PBMC was stimulated with PMA (phorbol 12-myristate 13-acetate, Sigma) 50 ng/ml and Calcium Ionophore A23187 (Sigma) 1μg/ml in the presence of BD GolgiStop™ protein transport inhibitor 2 mM at 37°C, 7% CO_2 for 6 hours. Stimulated cells were stained surface with CD3 or CD3 and CD7, combining intracellular with anti-cytokine/chemokine monoclonal antibodies (See Table 1). Data was acquired on a FACScan instrument (Becton-Dickinson, San José, CA, USA) and analyzed with CELLQUEST software.

Values were expressed as mean ± SD. Differences (P values) were evaluated using the 2-tailed Student's t-test. Differences were considered statistically significant for $P<0.05$.

Table 1 Anti-cytokine/chemokine monoclonal antibodies used in this study

mAb	Clone name	Format
Il-1α	364-3B3-14	PE*
IL-2	MQ1-17H12	PE
IL-3	BVD3-1F9	PE
IL-4	MP4-25D2	PE
IL-5	JES1-39D10	PE
IL-6	MQ2-13A5	PE
IL-8	G265-8	PE
IL-10	JES3-9D7	PE
IL-12	C11.5	PE
IL-16	14.1	PE
IFN-γ	4S.B3	PE
TNF-α	MAb11	PE
GM-CSF	BVD2-21C11	PE
MCP-1	5D3-F7	PE
MCP-3	9H11	PE
MIP-1α	11A3	PE
RANTES	2D5	PE
CD3	HIT3a	PE-Cy5
CD7	M-T701	FITC**

* PE: Phycoerythrin. ** FITC: Flourescein isothiocyanate. # All monoclonal antibodies are from BD Biosciences Pharmingen.

Table 2. Comparison of cytokine producing cells between normal donor T cells and T-ALL leukemic blasts.

	Normal T lympho (N=8)	T-ALL Blasts (N=35)	*P* Value
IL-1α	0.3±0.1	0.3±0.2	>0.05
IL-2	52.8±7.4	15.5±13.3	<0.001
IL-3	0.5±0.3	0.3±0.2	>0.05
IL-4	3.2±1.3	5.8±5.3	>0.05
IL-5	0.4±0.3	0.4±0.2	>0.05
IL-6	0.5±0.1	0.8±0.7	>0.05
IL-8	9.7±2.6	47.8±33.5	<0.05
IL-10	0.3±0.1	0.4±0.2	>0.05
IL-12	0.2±0.1	2.0±2.4	<0.05
IL-16	91.9±3.8	30.9±36.0	<0.001
IFN-γ	19.8±7.1	8.2±6.1	<0.001
TNF-α	33.2±7.5	10.4±10.4	<0.001
GM-CSF	12.3±4.0	5.2±4.5	<0.01
MCP-1	0.3±0.1	0.3±0.2	>0.05
MCP-3	0.5±0.3	0.4±0.2	>0.05
MIP-1α	4.3±2.1	28.2±23.4	<0.05
RANTES	0.3±0.1	0.3±0.2	>0.05

3 Results

In the T-ALL patients, two different kinds of immunophenotyping of the leukemic blasts were observed in this study. Among these 35 T-ALL patient circulating leukemic blasts, 23 patients' blasts

had the phenotyping of $CD3^-$ $CD7^+$, while 12 patients' blasts had the phenotyping of $CD3^+$ $CD7^+$ (Figure 1). In the 23 patients' blasts with the $CD3^-$ $CD7^+$ phenotyping, a minor $CD3^+$ $CD7^+$ cell population was observed in 16 patients (Figure 2). After staining with different fluorescence conjugated antibodies, intracellular cytokines/chemokines were analyzed in these different cell populations using different flow cytometric gating strategies.

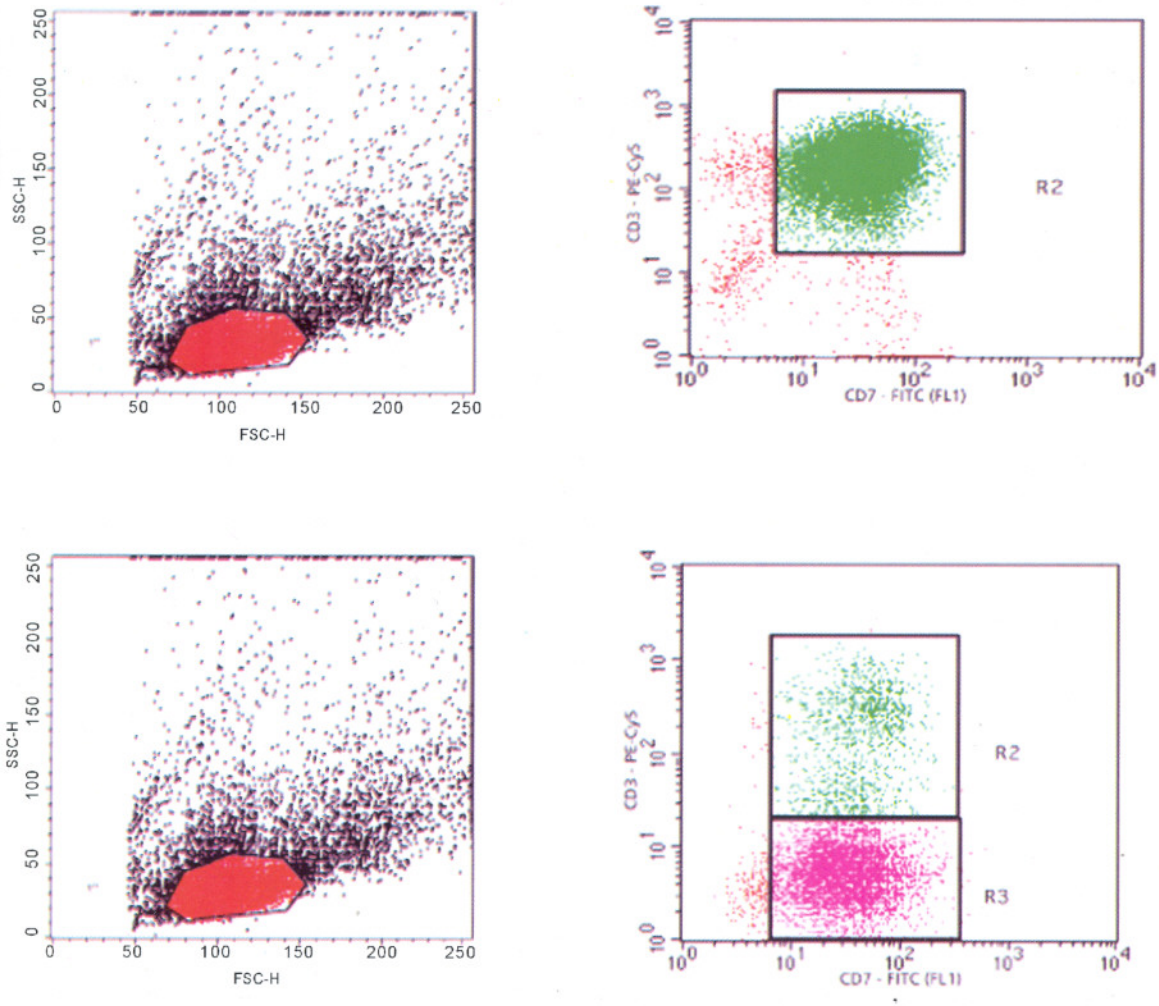

Figure 1. Legend: Two different phenotypings of leukemic blasts were observed in this study, $CD3^+$ $CD7^+$ and $CD3^-$ $CD7^+$. The upper panel showed the leukemic blasts with $CD3^+$ $CD7^+$ gated on the lymphocytic cells population and analysed with CD3 PE-Cy5 (Y-axis) and CD7 FITC (X-axis). The lower panel showed leukemic blasts with $CD3^-$ $CD7^+$ phenotyping.

Leukemic blasts produce many different cytokines/chemokines that can be detected with intracellular staining by flow cytometry. By gating on the leukemic blast populations, we analyzed different cytokines/chemokines production. We found that leukemic blast could produce many different cytokines/chemokines that could be detected with intracellular staining by flow cytometry, although the variation was quite big between different patients. Compared with normal donor T lymphocytes, significant decreased percentages of cytokine/chemokine positive cells in T-ALL leukemic blasts were observed for IL-2, IL-16, IFN-α, TNF-γ and GM-CSF. In contrast, significant increased percentage of cytokines/chemokines positive cells in T-ALL leukemic blasts was observed for IL-4, IL-8, IL-12 and MIP-1α. No significant differences were observed between T-ALL leukemic blasts and normal T lymphocytes for IL-1α, IL-3, IL-5, IL-6, IL-10, MCP-1, MCP-3 and RANTES (Table 2). Also, the cytokines/chemokines profiles from T-ALL patients were quite different from normal donors. Under the PMA stimulation condition, all normal donors produced detectable amount of IL-2, IL-4, IL-16, IFN-γ, TNF, GM-CSF and IL-8 positive cells, but no detectable IL-1α, IL-3,

IL-5, IL-6, IL-10, IL-12, MCP-1, MCP-3 and RANTES positive cells. However, the T-ALL patients could produce some cytokines/chemokines positive cells that normal donors usually do not produce under the PMA stimulation, such as IL-12 and MIP-1α.

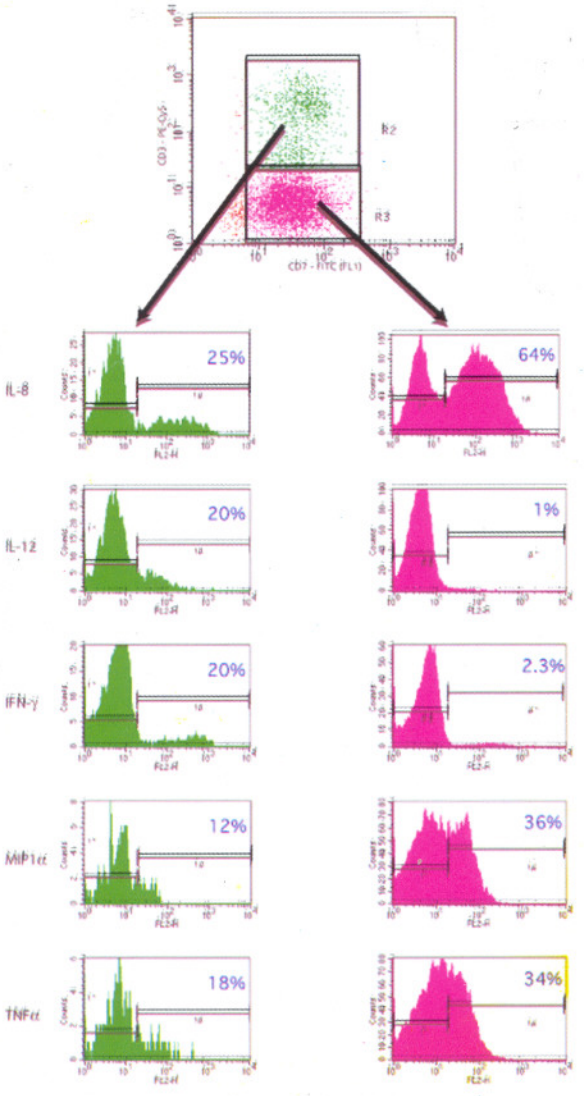

Figure 2. legend: In the 16 patients' blasts with the $CD3^-CD7^+$ phenotyping, a minor $CD3^+CD7^+$ cell population was observed. Independent analysis of the $CD3^+CD7^+$ and $CD3^-CD7^+$ cell populations revealed different profiles in cytokines/chemokines positive cell percentages. These are the typical histograms of different cytokines/chemokines from non-leukemic cells (green) and the leukemic blasts (pink).

In 23 cases of T-ALL patients with the leukemic blast phonotyping of $CD3^-CD7^+$, a minor population of $CD3^+CD7^+$ T cells was also observed in 16 patients. We considered this minor $CD3^+CD7^+$ population as the non-leukemic cells or the normal T cell in these T-ALL patients. Independent analysis of this $CD3^+CD7^+$ T cell population revealed differences in cytokines/chemokines positive cell percentages when compared to either the $CD3^-CD7^+$ leukemic blasts from the same patient or T lymphocytes from normal donors. Compared with T lymphocytes from normal donors, the $CD3^+CD7^+$ cell populations in these T-ALL patients revealed significantly higher percentages of IL-4, IL-8, IL-12 and MIP-1α cytokines/chemokines positive cells as well as significantly lower percentages of IL-2, IL-16, IFN-α, TNF-γ and GM-CSF cytokines/chemokines positive cells (Table 3). Compared with the $CD3^-CD7^+$ leukemic blasts from these patients, the $CD3^+CD7^+$ cell populations revealed significantly higher percentages of IL-2, IL-4 and IL-12, IL-16 and IFN-α cytokines positive cells. No significant differences of IL-1α, IL-3, IL-5, IL-6, IL-8, IL-10, TNF-γ, GM-CSF, MCP-1, MCP-3, MIP-1α and RANTES positive percentages were found between the $CD3^-CD7^+$ and $CD3^+CD7^+$ cell populations (Table 4).

Table 3. Comparison of cytokine producing cells between normal donor T cells and non-leukemic cells ($CD3^+CD7^+$) from T-ALL patients with leukemic blasts of phenotyping $CD3^-CD7^+$.

	Normal T lympho (N=8)	T-ALL $CD3^+CD7^+$ (N=16)	*P* value
IL-1α	0.3±0.1	0.3±0.1	>0.05
IL-2	52.8±7.4	11.6±7.1	<0.001
IL-3	0.5±0.3	0.3±0.1	>0.05
IL-4	3.2±1.3	6.2±4.5	<0.05
IL-5	0.4±0.3	0.4±0.2	>0.05
IL-6	0.5±0.1	0.4±0.2	>0.05
IL-8	9.7±2.6	31.2±19.0	<0.01
IL-10	0.3±0.1	1.0±1.6	>0.05
IL-12	0.2±0.1	7.8±17.1	<0.05
IL-16	91.9±3.8	41.1±30.2	<0.001
IFN-γ	19.8±7.1	9.7±11.7	<0.05
TNF-α	33.2±7.5	8.3±9.5	<0.001
GM-CSF	12.3±4.0	5.4±5.7	<0.05
MCP-1	0.3±0.1	0.9±1.6	>0.05
MCP-3	0.5±0.3	0.3±0.2	>0.05
MIP-1α	4.3±2.1	15.5±13.2	<0.05
RANTES	0.3±0.1	2.7±8.3	>0.05

4 Discussion

Cytokines/chemokines are very important factors in human immuno-regulation. Cytokines/chemokines producing cells detection can provide

critical information for cell-cell interaction in human body. There are different methods to detect cytokines/chemokines producing cells, such as ELISPOT, flow cytometry, immuno-radioactive assay, etc. Intracellular cytokines/chemokines staining by flow cytometry combining with cell surface staining with different monoclonal antibodies not only can detect cytoklines/chemokines producing cells, but also can provide further information such as which of cell subpopulation can produce what kind of cytokines/chemokines. It is known that different cell populations can produce different cytokines. Detection of the cytokines/chemokines producing cells would provide further information for understanding the function of cyteokines/chemokines producing cells in immunoregulation.

Table 4. Comparison of cytokine producing cells between leukemic blasts ($CD3^-$ $CD7^+$) and non-leukemic cells ($CD3^+$ $CD7^+$) from T-ALL patients with leukemic blast phenotyping $CD3^-$ $CD7^+$.

	T-ALL $CD3^+$ $CD7^+$ (n=16)	T-ALL $CD3^-$ $CD7^+$ (n=16)	*P* value
IL-1α	0.3±0.1	0.4±0.2	>0.05
IL-2	11.6±7.1	3.6±7.0	<0.05
IL-3	0.3±0.1	0.5±0.2	>0.05
IL-4	6.2±4.5	3.7±3.2	<0.05
IL-5	0.3±0.2	0.4±0.2	>0.05
IL-6	0.4±0.2	2.4±6.5	>0.05
IL-8	31.2±19.0	39.1±32.2	>0.05
IL-10	1.0±1.6	0.5±0.1	>0.05
IL-12	7.8±17.1	0.6±0.4	<0.05
IL-16	41.1±30.2	19.0±25.2	<0.05
IFN-γ	9.7±11.7	1.0±0.7	<0.05
TNF-α	8.3±9.5	13.0±10	>0.05
GM-CSF	5.4±5.7	7.5±8.6	>0.05
MCP-1	0.9±1.6	1.2±2.5	>0.05
MCP-3	0.3±0.2	0.5±0.2	>0.05
MIP-1α	15.5±13.2	16.6±25.5	>0.05
RANTES	2.7±8.3	0.6±0.5	>0.05

T-ALL is a special type of leukemia involving the T-cell clonal expansion of leukemia cells. We utilized the well-established cytokines/chemokines intracellular staining methods as well as the reagents from BD Biosciences to detect cytokines/chemokines producing cells in T-ALL leukemic patients. The different leukemic blasts not only have different morphology and immunophenotyping, but also have different patterns of cytokine/chemokine producing cells. Although the role of many different cytokines/chemokines in the leukemia still remains mostly unknown, the detection of cytokine/chemokines producing cells both in the leukemic blasts and non-leukemic cells would provide important information regarding the cytokines/chemokines production.

Our data demonstrated the abnormal cytokines/chemokines production pattern in the T-ALL patients, compared with normal T lymphocytes. T-ALL leukemic blasts have the significant lower producing ability for IL-2, IL-16, IFN-α, TNF-γ and GM-CSF. In contrast, T-ALL leukemic blasts have the significant lower producing ability for IL-4, IL-8, IL-12 and MIP-1α. Interestingly, the T-ALL patients can produce some cytokines/chemokines positive cells that normal donors usually do not produce under the PMA stimulation, such as IL-12 and MIP-1α. These abnormalities of cytokine/chemokine production could due to the clonal expansion of the T-lymphoid precursors.

Combined with surface staining of CD3 and CD7 monoclonal antibodies, we further classified the patients' lymphocytes in 16 patients, who have the leukemic blasts with $CD3^-$ $CD7^+$ phenotyping, into two different populations: leukemic blast and non-leukemic cells. The cytokines/chemokines producing cells are different between these two different cell populations. Compared with T lymphocytes from normal donors, the $CD3^+$ $CD7^+$ cell populations in these T-ALL patients revealed significantly higher percentages of IL-4, IL-8, IL-12 and MIP-1α cytokines/chemokines positive cells as well as significant lower percentages of IL-2, IL-16, IFN-α, TNF-γ and GM-CSF cytokines/chemokines positive cells. Compared with the $CD3^-$ $CD7^+$ leukemic blasts from these patients, the $CD3^+$ $CD7^+$ cell populations revealed significantly higher percentages of IL-2, IL-4 and IL-12, IL-16 and IFN-α cytokines positive cells. These cytokines involved both the Th1 and Th2 type cytokines that can be produced by different kinds of T cells. The increase of several different cytokines/chemokines producing cells among the non-leukemic cells in T-ALL patients could be the results of stimulation by the leukemic blasts, or the immuno-regulation of the *in vivo* cell-cell, cell-cytokine interactions. Detection of cytokines/chemokines in leukemic blasts may prove useful for predicting and monitoring response to therapies in which cytokines could be used as potential immunomodulators or therapeutic targets.

5 Conclusions

In this study, we demonstrated that:

(1) Intracellular cytokines/chemokines can be detected in the leukemic cells from T-ALL patients by multiparameter flow cytometry analysis after 6-hour PMA stimulation.

(2) T-ALL leukemic blasts have abnormal cytokine/chemokine producing cell patterns, compared with normal T lymphocytes.

(3) Different levels of cytokines/chemokines productions were observed between the non-leukemic ($CD3^+$ $CD7^+$) and leukemic ($CD3^-CD7^+$) cell populations in T-ALL patients with $CD3^-CD7^+$ phenotyping of blasts.

Acknowledgments

The authors would like to thank Dr. Xifeng Yang, and Dr. Zhang Chen for important input on the preliminary study of this paper.

Correspondence to:
Jifeng Yu
BD Biosciences Pharmingen
San Diego, CA 92121, USA
Telephone: 858-812-3773(W)
Email: jfy8168@yahoo.com

References

1. Bennett JM, Catowsky D, Daniel MT, The French-American-British (FAB) Cooperative Group. The morphological classification of acute lymphoblastic leukaemia: concordance among observers and clinical correlation. Br J Haematol 1981;47: 553 – 8.
2. Dibirdik I, Langlie MC, Ledbetter JA, et al. Engagement of interleukin-7 receptor stimulates tyrosine phosphorylation, phosphoinositide turnover, and clonal proliferation of human T-lineage acute lymphoblastic leukemia cells. Blood 1991;78:564 – 70.
3. Foa R, Migone N, Gavosto F. Immunological and molecular classification of acute lymphoblastic leukemia. Haematologica 1986;71:277-85
4. Uckun FM, Sensel MG, Sun L, et al. Biology and treatment of childhood T-lineage acute lymphoblastic leukemia. Blood 1998;91:735-46.
5. Karawajew L, Ruppert V, Wuchter C, et al. Inhibition of *in vitro* spontaneous apoptosis by IL-7 correlates with bcl-2 up-regulation, cortical/mature immunophenotype, and better early cytoreduction of childhood T-cell acute lymphoblastic leukemia. Blood 2000 ;96(1):297 – 306.
6. Masuda M, Takanashi M, Motoji T, et al. Effects of interleukins 1 – 7 on the proliferation of T-lineage acute lymphoblastic leukemia cells. Leuk Res 1991;15:1091 – 6.
7. Rivera GK, Crist WM. Acute lymphoblastic leukemia. In: Handin RI, Stossel TP, Lux SE, editors. Blood: Principles and Practice of Hematology. Philadelphia: JB Lippincott Company. 1995;743 – 59.
8. Scupoli MT, Vinante F, Krampera M, et al. Thymic epithelial cells promote survival of human T-cell acute lymphoblastic leukemia blasts: the role of interleukin-7. Haematologica 2003 ; 88(11): 1229 – 37.
9. Uckun FM, Sensel MG, Sun L, et al. Biology and treatment of childhood T-lineage acute lymphoblastic leukemia. Blood 1998;91:735 – 46.

Received October 16, 2005

Diagnostic Significance of Combined Detection of Serum Tumor Markers in Lung Cancer

Suxia Luo, Xiaobing Chen, Yijun Xiao

Department of Medical Oncology, Henan Provincial Cancer Hospital, Zhengzhou, Henan 450008, China

Abstract: Serum tumor marker (TM) is one of the major research topics of modern oncology, while the serum detection of lung cancer (LC) has become an important target for the diagnosis of malignancy. However, a single TM would not be satisfactory in both sensitivity and specificity for detection, which shows its limitation in diagnosing LC. Thus, for LC patients, we combined the examination of lung tumor-associated antigen (LTA), cytokeratin fragment antigen 21-1 (CYFRA21-1), carcinoembryonic antigen (CEA) and neuron specific enolase (NSE) in the diagnosis of this mortal disease. The aim of this study is to evaluate the role of the combined detection in the diagnosis of lung cancer. In our series, patients were divided into three groups named lung cancer (LC) group, benign lung disease (BLD) group and control group. The LC group was then subdivided into two subgroups named non-small cell lung cancer (NSCLC) subgroup and small cell LC(SCLC) subgroup. The NSCLE patients were further divided into squamous cell carcinoma subjects and conducted adenocarcinoma patients. The latex agglutination (LA) assay was performed to measure the LTA level of all the subjects. Radioimmunoassay (RIMA) was performed to detect CYFRA21-1, CEA and NSE. The significant data of contrasts among various groups were found through variance analysis and χ^2 was used to compare the positive rates. The positive rates of LTA in NSCLC, CYFRA21-1, NSE and CEA in LC patients were much higher than those in BLD patients and normal control with significant difference between them ($P<0.01$). The positive rates of LTA in NSCLC, CYFRA21-1 in squamous carcinoma, CEA in adenocarcinoma and NSE in SCLC were 75.6%, 84.6%, 81.4% and 82.3% respectively, with a significant difference between them ($P<0.01$). Obviously, there was a correlation between their positive rates and the pathological types of LC. The serum levels of LTA, CYFRA21-1, CEA and NSE in stage Ⅲ and stage Ⅳ patients were much higher than those in stage Ⅰ and stage Ⅱ with a significant difference ($P<0.01$). The positive rates of combined detection of LTA, CYFRA21-1, CEA and NSE were higher than detecting one or three of the above four items. We think LTA is sensitive in distinguishing LC from BLD, among which NSCLC is the highest. This may aid the diagnosis of LC. CYFRA21-1, NSE and CEA are valuable for LC diagnosis. Squamous carcinoma has the highest CYFRA21-1 positive rates, whereas pulmonary adenocarcinoma shows the highest CEA positive rates. For SCLC, the highest positive rates are showed in NSE. The united detection of LTA, CYFRA21-1, CEA and NSE is effective in raising LC detection rate. [Life Science Journal. 2006;3(1):35-39] (ISSN: 1097-8135).

Keywords: lung cancer; tumor-associated antigen (LTA); cytokeratin fragment antigen 21-1 (CYFRA21-1); carcinoembryonic antigen (CEA); neuron specific enolase (NSE)

1 Introduction

Lung cancer is one of the leading causes of cancer death throughout the world with more than one million death annually. The poor survival rates are due to the propensity for early spread, lack of effective tools for screening and early diagnosis, and the inability of systemic therapy to cure metastatic focuses. The discovery that many tumor markers were shed into the circulation led to great expectations that a serum tumor markers test could be developed to detect early lung cancer (Ando, 2003). Many studies evaluated tumor markers such as NSE, CEA, CYFRA21-1 and LTA, which were found through detection of NSCLC (non-small cell lung cancer) (Nackaerts, 1997). Unfortunately, none of these tumor markers proved to be useful or cost-effective in lung cancer screening. However, we have conducted combined detection of the LTA, CYFRA21-1, CEA and NSE in the diagnosis of this mortal disease in order to evaluate the clinical significance of combined detection in the diagnosis of lung cancer.

2 Materials and Methods

Subjects (n = 201) were divided into 3 groups: normal group (control, n = 33, male 13, female 20, age between 22 - 78 years); benign

lung disease group (BLD, $n=69$, male 37, female 32, age between 24 – 84 years; including acute bronchitis 9 cases, pneumonia 38 cases, pulmonary tuberculosis 10 cases, bronchial asthma 9 cases, bronchiectasis 3 cases) and lung cancer group ($n=99$, male 62, female 37, age between 36 – 78 years); according to pathology diagnosis: NSCLC 82, squamous carcinoma 39, adenocarcinoma 43, small cell lung cancer (SCLC) 17. The stages were sorted as UICC standard (1997), stage Ⅰ + Ⅱ: 17 cases (NSCLC 13 cases, SCLC 4 cases), stage Ⅲ: 47 cases (NSCLC 39 cases, SCLC 8 cases), stage Ⅳ: 35 cases (NSCLC 30 cases, SCLC 5 cases).

Serum were collected and stored at −20℃. The latex agglutination (LA) assay was performed to measure the LTA level. Radioimmunoassay (RIMA) was performed to detect the CYFRA21-1, CEA and NSE levels. Statistical analysis was carried out by SPSS 10.0 software.

3 Results

3.1 The levels of four tumor markers in lung cancer, BLD and control groups (Table 1)

According to the results of tumor marker levels from the normal control cases ($n=33$), we determined the normal ranges as LTA < 50 units, CEA < 15 μg/L, NSE < 20 μg/L, CYFRA21-1 < 3.3 μg/L.

3.2 The positive rates, specificity and sensitivity of four tumor markers in lung cancer, BLD and control groups (Table 2)

We detected 16 false positive cases in 69 BLD patients, which were consisted of LTA ($n=9$), CEA ($n=4$), NSE ($n=1$), CYFRA21-1 ($n=2$). The difference of LTA levels might be used to distinguish lung cancer from benign lung diseases.

3.3 Positive rates of tumor markers in different lung cancer groups (Table 3)

According to different types of lung cancer, there were different positive rates of tumor markers. The positive rates of LTA, CEA, CYRFA21-1 in NSCLC patients were significantly higher than those of SCLC patients. An even higher CEA positive rate (81.4%) was found in adenocarcinoma than in squamous carcinoma patients ($P<0.05$). The positive rate of CYRFA21-1 was 84.6%, which was much higher than the adenocarcinoma's level ($P<0.05$). The NSE positive level was 82.3%, markedly exceeding the NSCLC patients' level ($P<0.01$).

3.4 The positive rates of tumor markers in different stages of lung cancer (Table 4)

The LTA, CYFRA21-1, CEA and NSE levels in stage Ⅰ, Ⅱ were significant lower than those in stage Ⅲ, Ⅳ ($P<0.01$). Moreover, the tendency was increasing of four detected tumor markers accompanied by the disease development.

3.5 The positive rates in lung cancer that were determined by combinative detection of the four tumor markers can be seen from Table 5.

The positive rate of lung cancer has been up to 94.9%.

Table 1. Tumor marker levels in different groups ($\bar{\chi}\pm S$)

Group (cases)	LTA (units)	CYFRA21-1 (μg/L)	CEA(μg/L)	NSE(μg/L)
Lung cancer(99)	158.4±87.3*	13.9±11.4*	29.5±27.8*	21.0±29.2*
BLD(69)	60.3±12.5△	1.7±1.2△	10.4±2.2△	12.6±6.8△
Control(33)	30.0±12.6	1.3±0.9	11.4±1.8	11.1±4.5

*Comparisons between lung cancer, BLD, control groups, $P<0.05$; △Comparisons between BLD and control groups, $P>0.05$

Table 2. The positive rates, specificity and sensitivity of four tumor markers in different groups (%)

Lung cancer	LTA	CYFRA21-1	CEA	NSE
Positive rates				
NSCLC	75.6(62/82)	73.2(60/82)	74.4(61/82)	32.9(27/82)
SCLC	29.4(5/17)	29.4(5/17)	35.3(6/17)	82.3(14/17)
Specificity	89.2(91/102)	98.0(100/102)	96.1(98/102)	99.0(101/102)
Sensitivity	67.7(67/99)	65.7(65/99)	67.7(67/99)	41.4(41/99)

Specificity = control groups negative cases / BLD + normal groups cases; Sensitivity = Positive rates of cancer groups / cancer groups cases

Table 3. The positive rates of tumor markers in different types of lung cancers (%)

Group (cases)	LTA	CYFRA21-1	CEA	NSE
NSCLC(82)	75.6*(62/82)	73.2*(60/82)	74.4*(61/82)	32.9(27/82)
Squamous carcinomas(39)	79.5(31/39)	84.6#(33/39)	66.7(26/39)	38.5(15/39)
Adenocarcinomas(43)	72.1(31/43)	62.8(27/43)	81.4&(26/43)	27.9(12/43)
SCLC(17)	29.4(5/17)	29.4(5/17)	35.3(6/17)	82.3△(14/17)

*Comparisons between NSCLC、SCLC, $P<0.01$; △Comparisons between SCLC、NSCLC, $P<0.01$; # Comparisons between squamous carcinomas、adenocarcinomas, $P<0.05$; &Comparisons between adenocarcinomas、squamous carcinomas, $P<0.05$

Table 4. The positive rates of tumor markers in different stage of lung cancer (%)

Stage of lung cancer	Cases	LTA	CYFRA21-1	CEA	NSE
Ⅰ Ⅱ	17	41.2* (7/17)	35.3* (5/17)	35.3* (6/17)	17.6* (3/17)
NSCLC	13	46.2(6/13)	38.5(5/13)	46.2(6/13)	7.7(1/13)
SCLC	4	25.0(1/4)	0(0/4)	0(0/4)	50.0(2/4)
Ⅲ	47	68.1(32/47)	70.2 (33/47)	70.2 (32/47)	44.7(21/47)
NSCLC	39	76.9(30/39)	76.9(30/39)	76.9(30/39)	35.9(14/39)
SCLC	8	25.0(2/8)	37.5(3/8)	25.0(2/8)	87.5(7/8)
Ⅳ	35	80.0(28/35)	74.3(26/35)	77.1(27/35)	48.6(17/35)
NSCLC	30	86.7(26/30)	80.0(24/30)	83.3(25/30)	40.0(12/30)
SCLC	5	40.0(2/5)	40.0(2/5)	40.0(2/5)	100.0(5/5)

*Comparisons between Ⅰ, Ⅱ, Ⅲ, Ⅳ: $P<0.01$

Table 5. The comparison of positive rates by combinative detection of four tumor markers (%)

Combinative tumor makers	Positive rates
LTA + CEA + NSE	80.8 (80/99)
CEA + CYFRA21-1 + NSE	86.9 (86/99)
LTA + CYFRA21-1 + NSE	84.8 (84/99)
LTA + CYFRA21-1 + CEA	87.9 (87/99)
LTA + CYFRA21-1 + CEA + NSE	94.9* (94/99)

The positive rate of combinative detection: Two positive cases/cancer groups cases
*Comparisons between combined three detections, $P<0.05$

4 Discussion

Cancer of lung and bronchus indeed ranked top of all cancer death in both genders. The survival of patients with lung cancer is poor, primarily due to its early and widespread nature of metastases. By the time of diagnosis, lung cancer usually has already been disseminated, with only 20% – 30% patients having limited-stage disease (Nackaerts, 1997). Hence, developing new strategies of screening and early detection is critical. Serum tumor markers in lung cancer have long been studied in the hope of allowing early detection of the disease in asymptomatic individuals, improving diagnosis, as well as monitoring recurrence after treatments. Nonetheless, current serum biomarkers have turned out to be a non-effective clinical tool in screening and in early diagnosis.

Tumor markers of lung cancer, in general, can be classified into serum markers, tissue markers and sputum markers. Serum markers stand out as most attractive due to their easy accessibility over time. A number of serum tumor biomarkers have been studied in lung cancer in the past. Nonetheless, no practical serum tumor biomarkers exist for lung cancer. Here, we developed a method of combined detection of four tumor biomarkers in order to give a new light on screening and early diagnosis of lung cancer.

4.1 LTA and lung cancer diagnosis

Since 1970s, many researches have been focused on proteoglycan and observed that levels of proteoglycan in lung cancer were 1.7 – 3.5 times more than those of normal lung tissue. Such kind of proteoglycan has long fragment of proteoglycan, which is important in tumor's proliferation, metastasis, synthesis collagen. Chondroitin sulfate (CS) and hyaluronic acid (HA) are the basic component of proteoglycan, especially CS, which is related with the differentiation of lung cancer. Hence, detecting the level of CS might be helpful in diagnosing lung cancer (Kulpa, 2002). We have measured LTA levels in 201 cases and found that the positive rates were 6.06%, 13.0%, 75.6%, 29.4% in normal control, benign lung diseases, NSCLC and SCLC groups respectively. The specificity of LTA was 89.2% and the sensitivity was 67.7%.

4.2 Clinical applications values of CYFRA21-1, CEA, NSE in lung cancer

CYFRA21-1 lies in the cytoplasm of monolayer and polylayer tumor cells and is consisted of two monoclonal antibodies of keratin 19. The level of CYFRA21-1 will rise by the release of soluble fragments that were produced by dead tumor cell and the highest positive rate of CYFRA21-1 was found in squamous carcinomas (Brechot, 1997; Pujol, 2004). We have determined the positive rate as well as the specificity of CYFRA21-1 in lung cancer

as 65.7% and 98.0%; the positive rate in squamous carcinomas was 84.6% prior to that of NSE (38.5%) and CEA (27.9%).

CEA is one of the most widely used tumor associated markers in the diagnocancersis of lung cancer, and its diagnostic value in lung has be testified by clinical trials. CEA can been produced by lung cancer cells and it has been considered to be a better tumor marker to evaluate the patient's response to treatment, to monitor disease progression and to predict prognosis. The levels of CEA rose in about two thirds of NSCLC patients and one third of SCLC patients (Buccheri, 2003; Yoshimasu, 2003; Sakao, 2004). In our research the positive rate of CEA was 67.7% in lung cancer and 96.1% in pulmonary adenocarcinomas, in priority to CYFRA21-1 (62.8%) and NSE (27.9%).

NSE is a glycolytic enzyme and the predominant enolase was found in neural tissue (Fizazi, 1998). It has been recognized that SCLC patients frequently had increased levels of NSE at diagnosis compared with control cases (Buccheri, 2003). We observed the positive rate of NSE in lung cancer was 41.4%, specificity was 99.0%, and moreover the positive rate in SCLC patients was 82.3% with significant difference with other types of lung cancer, which was similar to the results of other researches.

Consistent with their locations of tumor markers such as CYFRA21-1 (lies in almost all epidemic cells), CEA (lies in adenoidal cells) and NSE (lies in normal neurocyte and neurosecretory cells), they are sensitive to pulmonary squamous carcinomas, pulmonary adenocarcinomas and SCLC, respectively. Our results were identical to the conclusions with the positive rate of 84.6%, 81.4%, and 82.3%.

4.3 Evaluation of combined determination of LTA, CYFRA21-1, CEA and NSE in lung cancer

In recent years tumor markers have been considered to be more and more important in diagnosis of malign diseases, but the applications of single tumor markers were limited by their low detective rates (Takamoch, 2004; Imura, 2003; Okada, 2003; Sawabata, 2002). As in lung cancer, current serum biomarkers have not been an effective clinical tool in screening or early diagnosing (Buccheri, 2003; Schneide, 2003; Pujol, 2003) Furthermore, there are different treatments for different types of lung cancer, such as pulmonary squamous carcinomas, pulmonary adenocarcinomas and SCLC. Here, we measured the combination of four tumor markers, LTA, CEA, NSE and CYFRA21-1 in order to evaluate the combined diagnostic value in lung cancer. We got the positive rates of LTA, CYFRA21-1, CEA and NSE in lung cancer that were 67.7%, 65.7%, 67.7%, and 41.4%; the specificities were 89.2%, 98.0%, 96.0%, and 99.0% respectively. The positive rates of combined detection of LTA, CYFRA21-1, CEA and NSE were higher than that detecting just one or three of the above four items. The combined detection increased the detection rates of lung cancer to 94.9%.

In conclusion, LTA, CEA, NSE and CYFRA21-1 are useful tumor markers in lung cancer diagnosis, and the united detection of LTA, CYFRA21-1, CEA and NSE is a valuable method in raising lung cancer detection rate and is especially advisable for the early diagnosis of LC and for its effective treatment.

Correspondence to:
Suxia Luo
Department of Medical Oncology
Henan Provincial Cancer Hospital
Zhengzhou, Henan 450008, China
Telephone: 86-371-6558-7739
Fax: 86-371-6596-1505
Email: Luosux@sohu.com

References

1. Ando S, Kimura H, Iwai N, et al. The significance of tumour markers as an indication for mediastinoscopy in non-small cell lung cancer. Respirology 2003; 8:163 – 7.
2. Brechot JM, Chevret S, Nataf, et al. Diagnostic and prognostic value of CYFRA 21-1 compared with other tumour markers in patients with NSCLS: a propective study of 116 patients. Eur J Cancer 1997, 33(3): 385 – 91.
3. Buccheri G, Ferrigno D. Identifying patients at risk of early postoperative recurrence of lung cancer: a new use of the old CEA test. Annals of Thoracic Surgery 2003; 75: 973 – 80.
4. Buccheri G, Torchio P, Ferrigno D. Clinical equivalence of two cytokeratin markers in non- small cell lung cancer: a study of tissue poly peptide antigen and cytokeratin 19 fragments. Chest 2003; 124: 622 – 32.
5. Fizazi K. Normal serum neuron specific enolase (NSE) value after the first cycle of chemotherapy: an early predictor of complete response and survival in patients with small cell lung carcinoma. Cancer 1998; 82 (6): 1049 – 55.
6. Imura H, Iwai N, Ando S, et al. A prospective study of indications for mediastinoscopy in lung cancer with CT findings, tumor size, and tumor markers. Annals of Thoracic Surgery 2003; 75: 1734 – 1739.
7. Kulpa J, Wojcik E, Reinfuss M, et al. Carcinoembryonic antigen, squamous cell carcinoma antigen, CYFRA21-1, and neuron specific enolase in squamous cell lung cancer patients. Clin Chem 2002; 48(11): 1931 – 1937.
8. Nackaerts K, Verbeken E, Deneffe G, et al. Heparan sulfate proteoglycan expression in human lung-cancer

cells. Int J Cancer (Pred . Oncol.) 1997;74:335 – 45.
9. Okada M, Sakamoto T, Nishio W, et al. Characteristics and prognosis of patients after resection of non small cell lung carcinoma measuring 2 cm or less in greatest dimension. Cancer 2003;98:535 – 41.
10. Pujol JL, Quantin X, Jacot W, et al. Neuroendocrine and cytokeratin serum markers as prognostic determinants of small cell lung cancer. Lung Cancer 2003;39: 131 – 8.
11. Pujol JL, Molinier O, Ebert W, et al. CYFRA21-1 is a prognostic determinant in non small cell lung cancer: results of a meta analysis in 2063 patients. British Journal of Cancer 2004, 90:2097 – 105.
12. Yoshimasu T, Kokawa Y, Oura S, et al. Time course of carcinoembryonic antigenafter resection of lung cancer: a predictor of recurrence. Cancer Science 2003, 94:741 – 4.
13. Sakao Y, Tomimitsu S, Takeda Y, et al. Carcinoembryonic antigen as a predictive factor for postoperative tumor relapse in early stage lung adenocarcinoma. European Journal of Cardio Thoracic Surgery 2004;25:520 – 2.
14. Sawabata N, Ohta M, Takeda S, et al. Serum carcinoembryonic antigen level in surgically resected clinical stage I patients with non small cell lung cancer. Annals of Thoracic Surgery 2002;74:174 – 9.
15. Schneider J, Philipp M, Salewski L, et al. Progastrin releasing peptide (ProGRP) and neuron specific enolase (NSE) in therapy control of patients with small cell lung cancer. Clinical Laboratory 2003;49(12):35 – 42.
16. Takamochi K, Yoshida J, Nishimura M, et al. Prognosis and histologic features of small pulmonary adenocarcinoma based on serum carcinoembryonic antigen level and computed tomographic findings. European Journal of Cardio Thoracic Surgery 2004;25:877 – 83.

Received September 30, 2005

Demethylation of the Estrogen Receptor Gene in Estrogen Receptor-negative Breast Cancer Cells Treated with 5-aza-2′-deoxycytidine Can Reactivate Functional Estrogen Receptor Gene Expression

Rui Wang[1], Linwei Li[1], Liuxing Wang[1], Qingxia Fan[1], Peirong Zhao[1], Ruilin Wang[1], Shihhsin Lu[1,2]

1. Department of Oncology, the First Affiliated Hospital of Zhengzhou University, Zhengzhou, Henan 450052, China

2. Cancer Institute, Chinese Academy of Medical Sciences, Beijing 100021, China

Abstract: To study demethylation action of 5-aza-2′-deoxycytidine and its effect on the expression of functional estrogen receptor (ER) genes in the human ER-negative breast cancer cell. The methylation status of ER gene in the ER-negative breast cancer cell was evaluated by methylation specific PCR(MSP) and genomic sequencing. The expression of ER and progesterone receptor (PR) mRNA and production of ER protein were detected by RT-PCR and Western-blot method, respectively. MTT assay was used to examine the function of re-expressed ER protein. The ER gene promoter was highly methylated in the ER negative breast cell line MDA-MB-231 and ER mRNA and ER protein were not expressed in the ER-negative breast cancer cell. The ER-negative breast cells treated with demethylating agent 5-aza-2′-deoxycytidine(5-aza-2′-deoxyC) were restored the expression of ER mRNA and PR mRNA and ER protein. The methylation of ER gene was simultaneously decreased and cytosine demethylated in 17/18 CpG island . The growth of cells treated with tamoxifen was inhibited significantly after MDA-MB-231 was treated with 5-aza-2′-deoxyC ($P<0.05$). The abnormal methylation of ER gene promoter plays an important role in the inactivation of ER gene. 5-aza-2′-deoxyC may lead to demethylation and reactivate functional ER expression silenced by aberrant hypermethylation. [Life Science Journal. 2006;3(1):40-44] (ISSN: 1097-8135).

Keywords: estrogen; receptor; methylation; breast cancer

1 Introduction

Breast cancer has been threatening women's health these years. It has been demonstrated that estrogen plays an important role in the initiation and progression of breast cancer. Its mechanism is that estrogen can combine with estrogen receptor and stimulate the occurrence of breast cancer. Approximately two thirds of breast cancers express estrogen receptor(ER) and their growth is stimulated by estrogen (Ferguson, 1995). For these patients, hormonal therapies target ER pathway are taken via a variety of mechanism including depletion of endogenous estrogen, interference with ligand-receptor interactions, or destruction of ER (Keen, 2003). Compared with combination chemotherapy, endocrine therapy is cheaper and less toxic, which becomes advantageous and promising. However, the remaining fraction of primary breast cancers lack of detectable ER protein and are rarely responsive to hormonal therapy (Ferguson, 1995). ER negative phenotype is associated with increased tumor grade and proliferation.

Many previous study proved that methylation plays an important role in loss of ER expression. In this report we provide evidence that 5-aza-2′-deoxycytidine(5-aza-2′-deoxyC) can lead to demethylation and re-expression of ER mRNA and functional ER protein.

2 Materials and Methods

2.1 Cell culture and reagents

Human ER negative breast cancer cell MDA-MB-231 and ER positive breast cancer cell MCF-7 were maintained in DMEM with 10% FCS, and the cell dense was 5×10^5/ml ~ 1×10^6/ml. The first day, MDA-MB-231 cell was treated with 0.75μmol 5-aza-2′-deoxycytidine. The second day the medium was changed. The third and fifth day, cells were treated repeatedly as the first day. On the sixth

day, cells were harvested. 5-aza-2′-deoxyC (Sigma) was freshly prepared in DMEM.

2.2 Extraction of DNA and RNA

Total RNA was prepared from cells by the method of TRIZOL and quantified by measuring absorbance at 260 nm. The integrity of the RNA and the accuracy of the spectrophotometric determinations were assessed by visual inspection of the ethidium bromide stained 28S and 18S ribosomal RNA bands after agarose gel electrophoresis. DNA was extracted with standard method as described previously (Blin, 1976).

2.3 RT-PCR

RT-PCR was performed as described previously (Issa, 1994). 11.5 μl total cellular RNA were used for each reverse transcription reaction. Primers were designed as follows: ER (5′-ATG-GAGT CTGGTCCTGTG-3′ sense; 5′-TTCG-TATCCCACCTTTCA TC-3′ anti-sense) and PR (5′-CCAGTGCCTCAGTCTCGT-3′ sense; 5′-CCTTCCATTGCCCTCTTA-3′ anti-sense). The length for ER and PR PCR amplification product was 181 bp and 460 bp respectively. β-actin (5′-ACCATGGATGATGAT ATCGC-3′ sense 5′-A-CATGGCTGGGGTGTTGAAG-3′ anti-sense). The length for β-actin PCR amplification product was 400 bp. The PCR sample was subjected to electrophoresis in 1% agarose gel, stained with ethidium bromide and visualized by UV light. The PCR reaction (50 μl) contained 10 × PCR buffer 5 μl, dNTP 4 μl, CDNA 5 μl, ER sense and anti-sense primer 1 μl respectively, β-actin primer sense and anti-sense primer 1 μl respectively, Taq polymerase 0.5 μl, H_2O 33.5 μl. PCR reaction was performed in UNOⅡ Biometra PCR.

2.4 Western blot analysis

Total cellular proteins extracted from breast cancer cells were resolved by electropheresis in a 12% denaturing polyacrylamide gel and proteins were electrotransferred to nitrocellulose membranes. The ER protein was then identified by using rabbit polyclonal antibody, which was specific for the ER protein, and the standard ABC Kit. Diaminobenzidine in a buffer was used in the coloration step indicate the presence of the ER protein.

2.5 Methylation specific polymerase reaction (MSP) and genomic sequencing

DNA was bisulfite modified as described previously (Herman, 1996). According to CpGenome™ DNA Modification Kit (Catalog # S7820), both genomic sequencing and MSP rely on chemical modification of DNA samples. The first step of genomic sequencing was bisulfite modification of the DNA sample followed by PCR. The PCR products amplified with primers specific either for the methylated or for the unmethylated DNA were purified and cloned on an ABI PRISM 377 DNA Sequencer-D Sangon by using M13 primers. Specific primers were designed to distinguish methylated from unmethylated DNA (Blin, 1976). The specific methylated primer ER(m): (5′-CGAGTT GGAGTTTT TGAA TCGTTC-3′; 5′-CTACGCGTTAACGACG ACCG -3′) The length for PCR product was 151 bp; ER (u): (5′-ATGAGTTGG AGTTTTTGAA TTGTTT -3′; 5′-ATAAACCTACACAT TAACA A CAACCA -3′). The length for PCR product was 158 bp. The PCR reaction (50 μl) contained 2 × GC buffer 25μl, 8 μl dNTP Mixture (each 2.5 Mm), sense and anti-sense primer were 1μl respectively, modified DNA 5 μl, LA Taq polymerase 0.5 μl, ddH_2O 9.5 μl, mix briefly and centrifuge. The PCR sample was subjected to electrophoresis in 1% agarose gel.

2.6 MTT

MDA-MB-231 cells treated with 5-aza-2′-deoxyC were detached by 0.25% trypsinization and seeded into 96-well plates (Costar, Cambridge, Mass.) at $10^4 - 10^5$/well in 100 μl of medium contained with estrogen and incubated for 24 h at 37℃. After 24 h, the medium was changed. 10^{-6} mol/L tamoxifen (TAM) or 10^{-8} mol /L E_2 in 200 μl medium were added and cells were incubated for an additional 48 h before quantification of cell growth. The inhibitory effect on cell growth was examined using the MTT (3-(4,5-dimethythiazol-2-yl)-2,5-diphenyl tetrazolium) assay according to the previously described method (Scudiero, 1988).

3 Results

3.1 The methylation status of ER gene CpG Island Region

By MSP, PCR primers were designed to amplify a 158 bp fragment containing 18 CpG sites. Extensively methylation exited within ER gene CpG island and PCR products were observed (M group: 151 bp) in breast cancer cell MDA-MB-231, after treated with demethylating agent 5-aza-2′-deoxyC ER gene promoter demethylated and products were observed (U group: 158 bp); DNA from ER-positive breast cancer cell line MCF-7 was unmethylated within ER gene promoter. The result was shown in Figure1.1.

The PCR products amplified with primers specific either for the methylated or for the unmethylated DNA were purified and cloned by using M13 primers. Cytosine residues outside of the CpG sites were converted to thymine after bisulfite treatment. In untreated breast cancer cell MDA-MB-

231 cytosine residues at CpG sites remained unchanged. In 18 CpG island, cytosine residues at 17 CpG sites cytosines were deaminated and converted to thymine after bisulfite treatment. The result was shown in Figure 1.2.

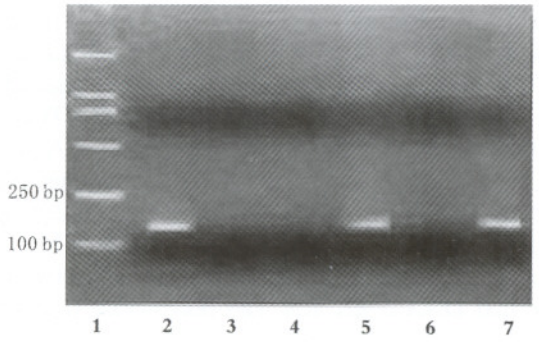

Figure 1.1 The methylation status of ER 5′CpG island by MSP method
From left to right 1: 100 bp marker; 2: MDA-MB-231 breast cancer cell: M group; 3: MDA-MB-231 breast cancer cell : U group; 4: MDA-MB-231 breast cancer cell treated with demethylating agent MDA-MB-231 breast cancer cell: M group; 5: MDA-MB-231 breast cancer cell treated with demethylating agent MDA-MB-231 breast cancer cell: U group; 6: Positive control MCF-7 cell: M group; 7: Positive control MCF-7 cell: U group.

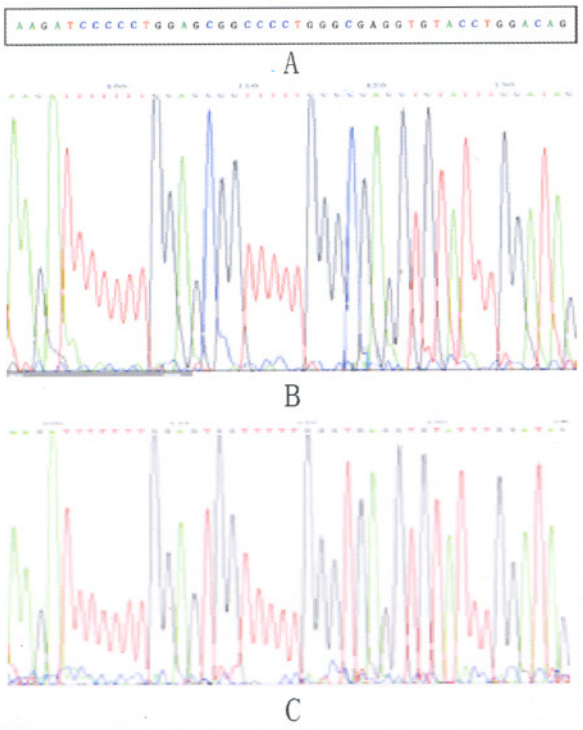

Figure 1.2 (A) Original sequence: before bisulfite treatment. (B) untreated MDA-MB-231 breast cancer cytosine residues at CpG sites remained unchanged although other cytosines were converted to thymine.
(C) MDA-MB-231 breast cancer cell treated with 5-aza-2′-deoxyC: cell cytosines were deaminated and converted to thymine.

3.2 Expression of the ER gene

As shown in Figures 2 and 3, ER gene expression was undetectable by RT-PCR using RNA from MDA-MB-231. After treatment with 5-aza-2′-deoxyC, the cells began to express the gene at levels detectable by RT-PCR. In addition, ER protein re-expressed and was detected by Western blot methods. These data were consistent with the previous findings and affirm that DNA methylation was one participant in the regulation of ER gene expression (Herman, 1996). The β-actin transcripts in each sample were also amplified as internal controls to normalize the amount of ER specific products.

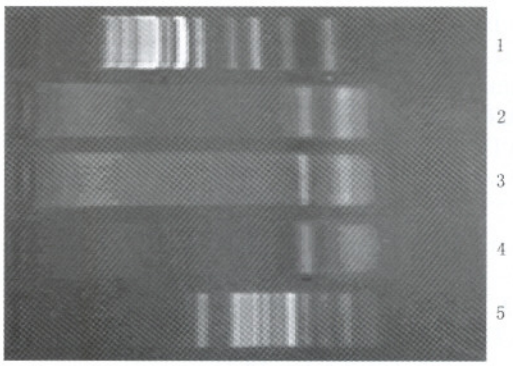

Figure 2. The expression of ER mRNA by RT-PCR method
From top to bottom 1: 200 bp marker; 2: positive control ER(+) MCF-7 cells; 3: MDA-MB-231 cells treated with 5-aza-2′-deoxyC; 4: untreated ER(-)MDA-MB-231 cells; 5: 100 bp marker

ER protein production was detected by Western blot analysis. The result is consistent with ER mRNA expression.

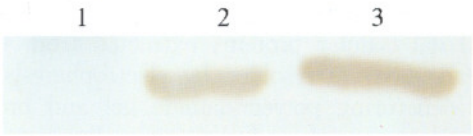

Figure 3. The ER protein by Western blot analysis
Lane 1: untreated ER(−)MDA-MB-231 cells;
Lane 2: MDA-MB-231 cells treated with 5-aza-2′-deoxyC
Lane 3: positive control ER(+) MCF-7 cells

3.3 Functional analysis of ER induced by 5-aza-2′-deoxyC

As shown in Figure 4, PR gene was unexpressed at mRNA level. After treatment, PR gene was re-expressed. Re-expression of an estrogen responsive gene-PR (460 bp) indicated induced ER was functional.

The growth and sensitivity to estrogen and tomoxifen were investigated by MTT, as shown in Table 1. There was statistical significance between

5-aza-2′-deoxyC (control) group and TAM + 5-aza-2′-deoxyC group ($P < 0.05$). After ER protein was re-expressed, TAM could inhibit the growth of MDA-MB-23 cells.

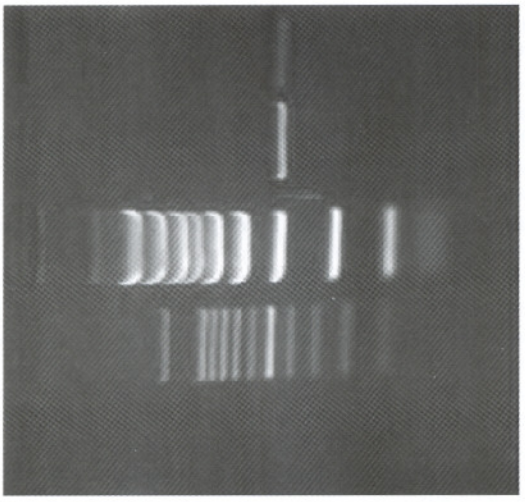

Figure 4. The expression of PR mRNA by PT-PCR method. Lane 1: deoxyC treated MDA-MB-231 cells; Lane 2: positive control: ER(+) MCF-7 cells; Lane 4: 100bp marker; Lane 5: untreate ER(−) MDA-MB-231 cells

Table 1. The inhibition rate of MDA-MB-231 cells in dillorent treated mert groups by MTT

	N	OD(x+/−s)	The rate of inhibition	*P*
5-aza-2′-deoxyC (control)	16	0.1672+/−0.0091	—	
TAM+5-aza-2′-deoxyC	16	0.1530+/−0.0168	8.49%	$P<0.05$
E2+5-aza-2′-deoxyC	16	0.1677+/−0.0121	−0.30%	$P>0.05$

As MTT was shown, there was statistical significance between 5-aza -2′-deoxyC (control) group and TAM + 5-aza-2′-deoxyC group($P<0.05$).

3.4 Statistical analysis

All results were expressed as mean ± SD. $P<0.05$ was considered statistically significant. All statistical analysis was performed by using SPSS 11.0 for Windows. Un-paired T test was adopted.

4 Discussion

The mechanisms involved in suppression of transcription of genes via hypermethylation at CpG islands is an area of active research (Jenuwein, 2001). Abnormal DNA methylation of CpG island is an early event in the progression of some human cancers (Baylin, 1991). Many previous work has demonstrated that ER expression is associated with rearrangement and re-modeling of the chromatin structure surrounding the ER gene (Yang, 2001; Iwase, 2003). Epigenetic modification including DNA methylation is tightly linked with expression of ER in human breast cancer cells, suggesting that chromatin conformation is an essential component of ER expression (Asch, 2001; Jones, 2002; Yang, 2001). CpG island hypermethylation may inhibit transcription by interfering with the recruitment and function of basal transcription factors or transcriptional coactivators. Also, hypermethylation of CpG dinucleotides near the transcriptional regulatory region may initiate the recruitment of the methyl-CpG binding domain (MBD) family proteins that mediate silencing of genes via facilitation of a repressive chromatin environment(Bird, 1999; Wade, 2001). With respect to breast cancer, ER (−) human breast cancer cells have up to a 40-fold higher level of DMT mRNA and up to a 9-fold higher level of DMT activity than ER(+) cells (Ottaviano, 1994). CpG methylation of the ER promoter results in transcriptional silencing (Lapidus, 1998) and inhibition of DNMT activity reactivates ER (Yang, 2001; Yang, 2000). Absence of estrogen receptor expression characterizes 25% of invasive breast cancer. 25% of cancers absent of estrogen receptor have hypermethylation in their promoter (Juttermann, 1994). 5-aza-2′-deoxyC is widely used as DNA methylation inhibitor to induce gene expression and cellular differentiation (Keen, 2003), but fewer reports are on the function of re-expressed ER protein.

To test whether ER induced in 5-aza-2′-deoxyC treated cells was functional, cells grown in the presence of E2 were treated with 0.75 μM 5-aza-2′-deoxyC for the indicated number of days . As is shown by MTT, after MDA-MB-231 cell was treated with demethylating agent 5-aza-2′-deoxyC, OD value in 5-aza-2′-deoxyC control group was 0.1672 +/− 0.0091, OD value in 5-aza-2′-deoxyC + TAM group was 0.1530 +/− 0.0168($P<0.05$) and the rate of inhibition was 8.49%; OD value in E2 + 5-aza-2′-deoxyC group was 0.1677 +/−0.0119($P>0.05$). In MTT experiment, (Table 1) MDA-MB-231 cells were maintained in medium contained with phenol red and phenol red possess estrogen-like function. TAM as anti-estrogen agent can block estrogen to exert the function of stimulating growth and be used as endocrine therapy for ER (+) breast cancers. MTT demonstrated that TAM could inhibit the growth of MDA-MB-231 cell with re-expressed ER protein and reached significant difference($P<0.05$). E2 could stimulate slightly the growth of MDA-MB-231 cell with re-expressed ER protein and reached no significant difference($P>0.05$). The main reason may be as follows. First, cells adapt to medium contained with estrogen-like

substances and are not sensitive to exogenous estrogen. Alternatively, estrogen receptor can be partially re-expressed and reach saturation in endogenous estrogen. The function of stimulating cell growth has exerted the maximum. All the results demonstrated that ER was functional. In addition, we further investigated the ability of the drug-induced ER to activate expression of the endogenous ER-responsive PR gene (Figure 4).

In our experiment, MSP method is a most sensitive method to detect methylation. The result demonstrated that there was extensively methylation in breast cancer cell MDA-MB-231 ER gene 5′ CpG island. Treatment of the cells with demethylating agents led to demethylation and re-expression of ER mRNA and subsequent production of the functional protein (Figures 2,3).

Chao et al (Hongxia, 2000) demonstrated that 5-aza-2′-deoxyC could inhibit tumor growth by reactivating regulatory-genes silenced by hypermethylation on endometrial carcinoma xenografted nude mice. Our further study is being under investigation on xenograft nude breast cancer mice. Therefore, it is conceivable that the demethylating agents can render ER(−) breast cancers responsive to hormonal therapies.

Correspondence to:
Liuxing Wang, Ruilin Wang
Department of Oncology,
The First Affiliated Hospital
Zhengzhou University
Zhengzhou, Henan 450052, China
Email: wlx2246@sohu.com

References

1. Asch BB, Barcellos-Hoff MH. Epigenetics and breast cancer. J Mammary Gland Biol Neoplasia 2001; 6 (2): 151−2.
2. Baylin SB, Makos M, Wu JJ, et al. Abnormal patterns of DNA methylation in human neoplasia: potential consequences for tumor progression. Cancer Cells 1991; 3 (10): 383−90
3. Bird AP, Wolffe AP. Methylation-induced repression-belts, braces, and chromatin. Cell 1999 ;99 (5): 451−4.
4. Blin N, Stafford DW. A general method for isolation of high molecular weight DNA from eukaryotes. Nucleic Acid Res 1976; 3 (9): 2303−8.
5. Chao HX, Sun JH, Lu SH, et al. Growth inhibition effect of 5-aza-CdR on endometrial carcinoma xenografted in nude mice by P16 gene demethylaton. Chin J Obstet Gynecol 2000; 35(4): 229−32.
6. Ferguson AT, Lapidus RG, Baylin SB, et al. Demethylation of the estrogen receptor gene in estrogen receptor-negative breast cancer cells can reactivate estrogen receptor gene expression. Cancer Res 1995; 55 (11): 2279−83.
7. Herman JG, Graff JR, Myohanen S, et al. MSP: A novel PCR assay for methylation status of CpG islands. Proc Natl Acad Sci 1996; 93 (18): 9821−6.
8. Issa JP, Ottaviano YL, Celano P, et al. Methylation of the oesotrogen receptor CpG island links ageing and neoplasia in human colon. Nat Genet 1994; 7 (4): 536−40.
9. Iwase H. Molecular action of the estrogen receptor and hormone dependency in breast cancer. Breast Cancer 2003; 10 (2): 89−96.
10. Jenuwein T, Allis CD. Translating the histone code. Science 2001; 293 (5532): 1074−80.
11. Jones PA, Baylin SB. The fundamental role of epigenetic events in cancer. Nat Rev Genet 2002; 3 (6): 415−28.
12. Juttermann R, Li E, Jaenisch R. Toxicity of 5-aza-2′-deoxycytidine to mammalian cells is mediated primarily by covalent trapping of DNA methyltransferase rather than DNA demethylation. Proc Natl Acad Sci USA 1994; 91: 11797−801.
13. Keen JC, Davidson NE. The biology of breast carcinoma. Cancer 2003; 97 (3 Suppl): 825−33.
14. Keen JC, Yan L, Mack KM, et al. A novel histone deacetylase inhibitor, scriptaid , enhances expression of functional estrogen receptor α(ER) in ER negative human breast cancer cells in combination with 5-aza-2′-deoxycytidine. Breast Cancer Research and Treatment 2003; 81 (3): 177−86.
15. Lapidus RG, Nass SJ, Butash KA, et al. Mapping of ER gene CpG island methylation specific polymerase chain reaction. Cancer Res 1998; 58 (12): 2515−9.
16. Ottaviano YL, Issa JP , Parl FF, et al. Davidson NE methylation of the estrogen receptor gene CpG island marks loss of estrogen receptor expression in human breast cancer cells. Cancer Res 1994; 54 (10): 2552−5.
17. Scudiero DA, Shoemaker RH, Paul KD, et al. Evaluation of a soluble tetrazolium/formazan assay for cell growth and drug sensitivity in culture using human and other tumor cell lines. Cancer Res 1988; 48 (17): 4827−33.
18. Wade PA. Methyl CpG-binding proteins and transcriptional repression. Bioessays 2001; 23 (12): 1131−7.
19. Yang X, Ferguson AT, Nass SJ, et al. Transcriptional activation of estrogen receptor alpha in human breast cancer cells by histone deacetylase inhibition. Cancer Res 2000; 60 (24): 6890−94.
20. Yang X, Phillips D, Ferguson AT, et al. Synergistic activation of functional estrogen receptor (ER)-alpha by DNA methyltransferase and histone deacetylase inhibition in human ER-alpha-negative breast cancer cells. Cancer Res 2001; 61 (19): 7025−9.

Received September 29, 2005

Effects of Residues of Organochlorine Pesticides on Reproductive Endocrinology in Pregnant Women at Delivery

Guohong Liu[1], Kedi Yang[1], Xipin Liu[2], Qifa Qin[3], Shihai Liu[1], Li Chen[4]

1. Department of Environmental Health, School of Public Health, Tongji Medical College, Huazhong University of Science and Technology, Wuhan, Hubei 430030, China

2. Hubei Tianmeng Hospital for Maternal and Child Care, Hubei, China

3. Xiaogan Center for Disease Control and Prevention, China

4. Hubei Family Planning Institute, China

Abstract: Some pesticides and synthetic chemicals are known to act as hormonal modulators, often possessing endocrine-disrupting effects. They are persistent and accumulative in environment, wildlife, animals and humans. The aim of our study was to explore effects of residues of organochlorine pesticides (OCPs) on reproductive endocrinology in human. We determined accumulative levels of DDT and BHC and their metabolites (isomers) in the 71 lying-in women's venous blood and documented associations among levels of total OCPs (T-OCPs), concentrations of follicle stimulating hormone (FSH), luteinizing hormone (LH), estradiol and progesterone in blood, and the expression of alpha-estrogen receptor (α-ER), beta-endorphin (β-EP) and gonadotropin releasing hormone (GnRH) mRNA in placental and umbilical cord tissues. The results showed that, a) with the increase of blood burden of T-OCPs, levels of FSH, estradiol and progesterone in the women's sera and FSH, LH and estradiol in the umbilical cord sera increased in a dose-effect manner, respectively. However, LH in the women's sera and progesterone in the cord sera presented a dose-related significant decrease ($P<0.05$); b) the abundant expression of α-ER and β-EP mRNA in the placental and cord tissues also increased in a dose-dependent manner, respectively, following the rising pesticides' burdens in maternal sera. While expression of GnRH mRNA in placental tissues presented no significant difference among the groups, moreover, its expression was not found in umbilical cord tissues; c) number of previous adverse pregnancy outcomes (PAPO) went up with the increase of the residues' burdens in maternal sera. But the number of PAPO in the high-residue group was smaller than that in the mid-residue. The average weights of newborns in the low and intermediate residue groups, but not the high residue group, were heavier than that in the control group ($P<0.05$). These findings provide evidence that the residues of OCPs in maternal blood possess endocrine-disrupting effects. It seems that estrogenic activity was dominant when concentration of T-BHC was markedly higher than that of T-DDT in blood. [Life Science Journal. 2006; 3(1): 45 - 51] (ISSN: 1097 - 8135).

Keywords: endocrine-disrupting effect; hormone; gene; organochlorine pesticides; reproductive endocrinology

1 Introduction

1, 1, 1-trichloro-2, 2-bis (p-chlorophenyl) ethane (DDT) and benzenehexachloride (BHC) of OCPs were initially introduced as an insecticide into agriculture production activities and used to control some vector-borne diseases, such as malaria and typhus (Edward, 2003). They have been officially banned in the world for two decades because of their potential harmful effects on humans, wildlife, and the environment. Their persistence, biomagnification via the food chain, reproductive toxicity, and endocrine disrupting function have been of great concerns (Matthew, 2001). Although the production and application of BHC and DDT have been officially forbidden in China since 1983, some of OCPs, for example γ-BHC, are still being produced and used in our partial regions (Yang, 2004; Bao, 1988). Numerous investigations (Yang, 2004; Bao, 1988; Yu, 2001) have reported the residues of BHC and DDT in maternal milk and their harmfulness on human health in recent decades. Their disruptive effects on reproductive endocrinology include decreased sperm counts, decreased motor ability, rising malformation ratio and

infertility, and increase of cancer incidence in testis and prostate in men and prematurity, menstrual dysfunction, hyperplasia of endometrium, habitual abortion and increase of cancer in uterus, ovary and mammary gland in women, causing great concerns in scientific community. However, the studies on the association between accumulative levels of pesticides in maternal sera and concentrations of the related hormones and expression of genes remain scarce. Tainmeng District, a residential area where the residues of DDT in the female adipose tissue samples were up to top in China in 1985 (Bao, 1988), was selected as our sampling point. In this report, we further explored effects of DDT and BHC and their metabolites on concentrations of the related hormones in maternal and cord sera and expression of genes in placental and umbilical cord tissues.

2 Materials and Methods

2.1 Subjects selection and samples collection

The pregnant women who delivered their babies at term in Tianmeng Hospital For Maternal and Child Care in Hubei province during Jan 1st to Apr 30th in 2004 were recruited for the present study, based on a) their history of potential exposure to pesticides; b) their inhabitation duration in the locality for at least five years without any known occupational exposure to DDT and BHC, and c) no hormone use for three months before their blood samples were collected.

Venous blood samples (10 ml) from the studied individuals by venipuncture at delivery as well as from the umbilical cords were collected into clear glass tubes, respectively, precipitated for 30 minutes at room temperature, and followed by centrifugation at 2 000 rpm for 5 – 10 min. Sera were then collected and stored at −20° C until analyzed. Placental tissues (10 – 15g) and umbilical cord tissue samples (10 cm) from the same subjects were also obtained, rinsed with RNase-free water, and quickly frozen in liquid nitrogen, and stored at −80° C until used for testing.

Every participant provided written informed consent and completed a questionnaire on pregnancy health. We have collected totally 71 maternal and cord blood samples and 71 placental and cord tissue samples and questionnaires, respectively. These blood and tissue samples were handled in accordance with the ethic standards established by the Committee of Ethics and Scientific Research of Tongji Medical College.

2.2 Determination of residue of OCPs in the blood from pregnant women at delivery

According to the standard method (GB/T5009.19-1996) with minimal modification, concentrations of the eight major metabolites of DDT and BHC were determined by capillary gas chromatography with electron capture detector (GC-ECD, GC 3800 chromatograph, Varian Co., USA.) using a 30 m × 0.25 mm i.d. WCOT Fused Silica CP-sil 5 CB (Varian Co., USA.) with 0.25 μm film and nitrogen carrier gas flow (99.99% purity) at 1.1 ml/min. The injector was operated in split mode, with a split ratio of 20 : 1 and injector temperature of 275℃. The oven temperature was held at 75℃ for 1 min and programmed at 20℃/min to 210℃ and held for 10 min and then programmed at 10℃/min to 260℃ and held for 10 min. Detection was by electron capture within 800 mV signal range and temperature of 300℃. Added sample volume per time was 1 μl and the minimum detectable level was 0.005 μg/L. Quantification was facilitated by comparison of peak areas with those derived from a calibration curve for each analyte. According to the concentrations of the T-OCPs in the maternal sera, the 71 studied individuals were divided into four groups, 9 of whom with non-detected level (<0.005 μg/L) were grouped as the control, other subjects whose levels of the T-OCPs were within the range of 0.005～10 μg/L, 10～40 μg/L and 40 μg/L or greater included 26, 17 and 19 individuals, respectively, of corresponding to the low, intermediate and high residue groups.

2.3 Determination of levels of the hormones in maternal and umbilical cord sera

Concentrations of FSH, LH, estradiol and progesterone in maternal and umbilical cords sera were determined using the Serozyme kits (Bio-Ekon biotechnology Co., Beijing, China), following the procedures described by the manufacturer. Concentrations of FSH and LH were determined by the technology incorporating two high affinity monoclonal antibodies into immunoenzymetric system to form a sandwich, while a high affinity monoclonal antibody was used in a competitive enzyme immunoassay system to detect levels of estradiol and progesterone. All detected values of samples, standards and controls fell within the range of quality control standard required by the kits.

2.4 Expression of α-ER, β-EP and GnRH mRNA in placental and umbilical cord tissues

According to the protocols described by Liu Hongkai and Grigorakisl SI with modification (Liu, 2004; Grigorakise, 2000), the total RNA was extracted as follows. 1 ml Trizol reagent was added into the 2 ml glass tube to homogenate tissue (50 – 100 mg). Then the lysate was moved into

1.5 ml EP tube without RNase and incubated for 5 min on ice to permit their complete dissociation. Then, 0.2 ml chloroform was added to each of the tubes, shaken for 15 sec, kept on for 2 – 3 min, and then centrifuged at 12, 000g for 15 min at 4 ℃. The colorless upper aqueous phase containing the RNA was transferred to a new tube without RNase. About 0.5 ml isopropanol was added to the tube, incubated for 2 hr at – 20 ℃, and then the RNA was precipitated by centrifugation (4℃, 10 min, 14,000 g). The RNA pellet was washed with 75% ethanol and recovered in 10 – 20 μl water treated with diethylene pyrocarbonate (DEPC). The RNA purity was checked by both gel electrophoresis and optical density ratio, which was between 1.8 and 2.0. The RNA solution was preserved at – 70℃ for further analysis.

3.0 μg of total RNA from each sample was reverse transcribed into cDNA using a reverse transcription kit (Fermentas Life Sciences Co., USA) in 12 μl of reaction mixture containing oligo dT primer and MMLV reverse transcriptase at 42℃ for 1 hour. This reaction was stopped by incubation at 94 ℃ for 5 min. Aliquot of 1 μl of the reverse transcription reaction was amplified with Taq polymerase (Fermentas Life Sciences Co., USA) in a final volume of 50 μl containing 25 mM $MgCl_2$, 20 pmol of sequence-specific primers for α-ER, β-EP and GnRH (all primers were synthesized by Bioasia corporation in Shanghai, China) and 2mM dNTP Mix. The mixture was amplified by PCR for 35 cycles for α-ER (1 cycle = 94 ℃ for 50 sec, 57 ℃ for 45 sec, and 72 ℃ for 1 min), or 35 cycles for β-EP (1 cycle = 94 ℃ for 45 sec, 55 ℃ for 45 sec, and 72 ℃ for 2 min), or 35 cycles for GnRH (1 cycle = 94 ℃ for 50 sec, 60°C for 45 sec, and 72 ℃ for 2 min). Primer sequences were designed as follows. α-ER: 5′-GGC TAC ATC ATC TCG GTT CC-3′ and 5′-GTG ATC TTG GCC AGG ACT CG-3′ (product length was 369 bps). β-EP: 5′-CCT ACA GGA TGG AGC ACT TC-3′ and 5′-GTA GGC GTT CTT GAT GAT GG-3′ (product length was 130 bps). GnRH: 5′-AGC CAG CAA GTG TCT CTG AG-3′ and 5′-TTC CAC GCA CGA AGT CAG TA-3′ (product length was 224 bps). Products of the PCR reaction (5 – 10 μl) were analyzed on 2% agarose gels in 0.5 × TBE, stained with ethidium bromide (EB), and photographed. To correct the amount of RNA analyzed and to evaluate the relative levels of α-ER, β-EP, and GnRH expression, a ubiquitin gene (β-actin) was also used as the internal control. The relative expression was determined by using the ratio of intensity of target genes to that of β-actin.

2.5 Statistical analysis

The analysis of variance (ANOVA) with SNK test was used to compare the data. If their distribution deviated from normality or presented heterogeneous variances, nonparametric methods (Wilcoxon test) were used instead, and the statistics were expressed as median/inter quartile range. A difference at $P<0.05$ was considered statistically significant.

3 Results

3.1 Comparison of major characteristics for the studied mothers and their babies and families in various groups

The studied pregnant women's age range was from 21 to 35 yr and there was no significant difference among the four groups. The indexes such as average pregnant times, average laboring times, average pregnant duration, percent of vaginal delivery (VD) and elective cesarian section (CS), percent of single-fetus term delivery and average monthly family income among the groups presented also no significance ($P > 0.05$). However, the number of PAPO (i.e., spontaneous abortion, induced abortion, ectopic pregnancy, premature delivery, post-term delivery, et al.) in the low, intermediate, high residue groups were greater than that in the control group and significant differences were found. Average weights of newborns in low and intermediate groups were markedly heavier than that in the control group, and the differences among groups were statistically significant ($P < 0.01$). Nevertheless, no difference was observed between high residue group and the control group ($P > 0.05$). It was interesting that rank of the weight from high to low was the low > intermediate > high residue > the control groups (Table 1).

3.2 Levels of major metabolites of DDT and BHC in blood from pregnant women at delivery

The eight isomers, α-, β-, γ-, δ-BHC and p, p′-DDE, o, p-DDT, p, p′-DDD, p, p′-DDT, were found in the 62 individuals but not the 9 samples in the control group, where concentrations of residues in maternal sera were lower than the minimum detectable level (MDL). In the low, intermediate and high residue groups, the percentages of α-BHC (50.00%, 52.94% and 63.16%) and o, p-DDT (11.54%, 41.18% and 78.95%) determined in the blood were relatively higher in comparison with those of β-BHC (23.08%, 47.06% and 36.84%) and p, p′-DDE (19.23%, 35.29% and 42.11%). In the low, intermediate and high residue groups means of the total BHC, the sum of α-, β-, γ- and δ-BHC, were 4.65 μg/L, 15.09 μg/L and

56.49 μg/L, and means of the total DDT which equaled to the sum of p,p′-DDE, o,p-DDT, p,p′-DDD and p,p′-DDT were 0.72 μg/L, 9.12 μg/L and 54.56 μg/L, respectively. The former were significantly higher than the latter. In the control, low, intermediate and high residue groups the means of T-OCPs, sum of the eight isomers, were < 0.005 μg/L, 5.37 μg/L, 24.21 μg/L and 111.05 μg/L, respectively. Significant differences were found ($P<0.05$) (Table 2).

Table 1. Comparison of major characteristics for the studied mothers and their babies and families in various groups

Parameter	Groups			
	Control($n=9$)	Low($n=26$)	Intermediate($n=17$)	High($n=19$)
Mother's age (years)	26.56±3.61	25.88±3.18	26.82±3.88	25.79±3.49
Average pregnancy number	1.67±1.12	1.73±1.08	2.18±1.01	2.32±1.57
Average delivery number	1.22±0.44	1.19±0.40	1.24±0.44	1.42±0.84
Average pregnancy weeks	38.7±4.12	38.5±3.66	38.2±4.51	38.1±4.22
Average number of PAPO	0.33±0.50	0.42±0.50[a]	0.59±0.51[ab]	0.53±0.51[abc]
Percent of VD(%)	33.33	11.54	11.76	21.05
Percent of CS(%)	66.67	88.46	88.24	78.95
Percent of single-fetus term delivery(%)	100	96.15	100	100
Average weight of newborn(g)	3228±404.75	3408±319.28[a]	3353±379.75[ab]	3250±463.98[bc]
Average monthly family income(yuan)	1844.4±127.5	1830.8±201.3	1788.2±154.3	1705.3±142.5

Note. Data in the table are mean±SD except percentage. [a]Values compared to the control, $P<0.05$. [b]Values compared to the low-residue group, $P<0.05$. [c]Values compared to the intermediate, $P<0.05$.

Table 2. Levels of metabolites of DDT and BHC in maternal blood

Parameter	Groups			
	Control($n=9$)	Low($n=26$)	Intermediate($n=17$)	High($n=19$)
Percent of detected α-BHC (%)	<MDL	50.00	52.94	63.16
Percent of detected β-BHC (%)	<MDL	23.08	47.06	36.84
Percent of detected γ-BHC (%)	<MDL	3.85	29.41	68.42
Percent of detected δ-BHC (%)	<MDL	42.31	35.29	5.26
Percent of detected p,p'-DDE (%)	<MDL	19.23	35.29	42.11
Percent of detected o,p'-DDT (%)	<MDL	11.54	41.18	78.95
Percent of detected p,p'-DDD (%)	<MDL	0.00	11.76	31.58
Percent of detected p,p'-DDT (%)	<MDL	3.85	0.00	21.05
Total BHC(μg/L) ($\bar{\chi}\pm S$)	<MDL	4.65±2.42[a]	15.09±9.25[ab]	56.49±38.74[abc]
Total DDT(μg/L)($\bar{\chi}\pm S$)	<MDL	0.72±1.65[a]	9.12±8.56[ab]	54.56±55.43[abc]
T-OCPs (μg/L)($\bar{\chi}\pm S$)	<MDL	5.37±2.22[a]	24.21±9.75[ab]	111.05±45.26[abc]

Note. All targeted components were not determined in the samples of the control group. MDL: minimum detectable level. [a]Values compared to the control, $P<0.01$. [b]Values compared to the low-residue group, $P<0.01$. [c]Values compared to the intermediate, $P<0.05$.

3.3 Concentrations of FSH, LH, estradiol and progesterone in maternal and cord sera

As shown in Table 3, with the increase of blood burden of T-OCPs, levels of FSH, estradiol and progesterone in the maternal sera and FSH, LH, and estradiol in the umbilical cord sera increased, respectively. There was an obvious dose-effect relationship. However, LH in the women and progesterone in the cord sera decreased in a dose-dependent manner, respectively, as accompaniment with the rising pesticides' levels. Significance was found between groups ($P<0.05$).

3.4 Expression of α-ER, β-EP and GnRH mRNA in placental and cord tissues

Table 4 indicates that abundant expression of α-ER and β-EP in the placental and cord tissues went up respectively following the rising pesticides' burdens in maternal sera. Their dose-effect relationship existed steadily ($P<0.01$). Expression of GnRH mRNA in placental tissues did not show statistically significant difference ($P>0.05$), although levels of various residue groups were higher as compared to the control group. It was noticed that transcription of GnRH gene in cords was not detected in the present study.

Table 3. Comparison of levels of FSH, LH, estrodial and progesterone in sera of women and cord($\bar{\chi} \pm S$)

Parameter		Groups			
		Control($n=9$)	Low($n=26$)	Intermediate($n=17$)	High($n=19$)
Maternal sera	FSH (mIU/ml)	0.83 ± 0.29	1.08 ± 0.48	1.63 ± 0.31^{ab}	2.27 ± 0.61^{abc}
	LH (mIU/ml)	1.47 ± 0.45	1.08 ± 0.53	0.80 ± 0.36^{a}	0.63 ± 0.21^{ab}
	estrodial (ng/ml)	41.80 ± 7.72	52.82 ± 7.52^{a}	54.99 ± 8.30^{a}	43.15 ± 8.25^{bc}
	progesterone (ng/ml)	$264:04 \pm 29.21$	294.59 ± 16.50^{a}	306.94 ± 22.61^{ab}	327.22 ± 31.38^{abc}
Cord sera	FSH (mIU/ml)	1.41 ± 0.41	1.54 ± 0.50	1.62 ± 0.56	2.91 ± 0.91^{abc}
	LH (mIU/ml)	0.60 ± 0.28	0.64 ± 0.38	0.79 ± 0.29	2.07 ± 0.81^{abc}
	estrodial (ng/ml)	12.53 ± 3.28	18.01 ± 7.01^{a}	24.03 ± 3.92^{ab}	23.83 ± 9.98^{ab}
	progesterone (ng/ml)	804.47 ± 73.76	767.04 ± 62.32	654.74 ± 24.45^{ab}	604.70 ± 26.82^{abc}

Note. [a]Values compared to the control, $P<0.01$. [b]Values compared to the low-residue group, $P<0.01$. [c]Values compared to the intermediate, $P<0.05$.

Table 4. Comparison of abundant expression of α-ER, β-EP and GnRH mRNA in placental and cord tissues($\bar{\chi} \pm S$)

Gene mRNA		Groups			
		Control($n=9$)	Low($n=26$)	Intermediate($n=17$)	High($n=19$)
Placental tissues	α-ER	1.62 ± 0.41	1.93 ± 0.76	2.13 ± 1.00	2.42 ± 0.92^{a}
	β-EP	0.36 ± 0.17	0.50 ± 0.17^{a}	0.62 ± 0.22^{a}	0.68 ± 0.25^{ab}
	GnRH	1.61 ± 0.68	1.80 ± 0.54	2.09 ± 0.63	1.68 ± 0.56
Umbilical cord tissues	α-ER	1.49 ± 0.45	1.72 ± 0.68	1.90 ± 0.91	2.14 ± 0.82^{a}
	β-EP	0.24 ± 0.17	0.31 ± 0.14	0.43 ± 0.19^{ab}	0.46 ± 0.18^{ab}

Note. [a]Values compared to the control, $P<0.01$. [b]Values compared to the low-residue group, $P<0.01$. [c]Values compared to the intermediate, $P<0.05$.

Data in the table were the ratio of densitometric units of targeted genes to β-actin.

3.5 Rank correlation between the expressional abundance of the genes in placental and umbilical cord tissues and levels of the hormones in maternal and cord sera

As shown in Table 5, significant correlations were found among the following indexes such as, a) between expressional abundance of β-EP in placental and cord tissues and concentrations of FSH in maternal and cord sera ($r=0.2963, P=0.0121$; $r=0.3053, P=0.0096$; $r=0.2793, P=0.0183$; $r=0.2354, P=0.0482$), respectively. b) between expression of β-EP in cord tissues and level of progesterone in maternal blood ($r=0.2744, P=0.0206$). c) between concentration of estradiol in cord sera and expression of α-ER and β-EP in placental and cord tissues ($r=0.4732, P\leqslant 0.0001$; $r=0.4700, P\leqslant 0.0001$; $r=0.5633, P\leqslant 0.0001$; $r=0.5243, P\leqslant 0.0001$), respectively. d) between level of progesterone in cord sera and expression of α-ER and β-EP in placental and cord tissues ($r=-0.2584, P=0.0296$; $r=-0.2425, P=0.0416$; $r=-0.4303, P=0.0002$; $r=-0.4016, P=0.0005$), respectively.

Table 5. Rank correlation between the expressional abundance of α-ER, β-EP and GnRH in placental and cord tissues and the levels of FSH, LH, estradiol and progesterone in maternal and cord sera

Parameter		Placental tissues			Umbilical cord tissues	
		α-ER	β-EP	GnRH	α-ER	β-EP
Maternal sera	FSH	$r=0.2329$ $P=0.0506$	$r=0.2963$ $P=0.0121$	$r=0.1295$ $P=0.2818$	$r=0.2162$ $P=0.0702$	$r=0.3053$ $P=0.0096$
	LH	$r=0.0874$ $P=0.4688$	$r=-0.1474$ $P=0.2201$	$r=-0.1660$ $P=0.1666$	$r=0.0756$ $P=0.5308$	$r=-0.0923$ $P=0.4439$
	estradiol	$r=0.0069$ $P=0.9545$	$r=-0.0528$ $P=0.6617$	$r=0.0432$ $P=0.7208$	$r=0.0310$ $P=0.7976$	$r=-0.0233$ $P=0.8469$
	progesterone	$r=0.1772$ $P=0.1392$	$r=0.2251$ $P=0.0591$	$r=-0.0419$ $P=0.7286$	$r=0.1604$ $P=0.1815$	$r=0.2744$ $P=0.0206$
Umbilical cord sera	FSH	$r=0.1927$ $P=0.1073$	$r=0.2793$ $P=0.0183$	$r=0.0048$ $P=0.9683$	$r=0.1812$ $P=0.1305$	$r=0.2354$ $P=0.0482$
	LH	$r=-0.0044$ $P=0.9708$	$r=0.2142$ $P=0.0729$	$r=0.1396$ $P=0.2457$	$r=-0.0195$ $P=0.8715$	$r=0.1663$ $P=0.1658$
	estradiol	$r=0.4732$ $P=<0.0001$	$r=0.5633$ $P=<0.0001$	$r=-0.0844$ $P=0.4841$	$r=0.4700$ $P=<0.0001$	$r=0.5243$ $P=<0.0001$
	progesterone	$r=-0.2584$ $P=0.0296$	$r=-0.4303$ $P=0.0002$	$r=-0.0767$ $P=0.5250$	$r=-0.2425$ $P=0.0416$	$r=-0.4016$ $P=0.0005$

4 Discussion

Although OCPs (i.e., DDT and BHC) have been officially banned for decades in the world, their chemical characteristics predict that once into the food chain these pesticides are difficult to eliminate. Moreover, as a consequence of their global distillation effect, high lipophilicity and long persistence, they may have multi harmful effects on humans, animal, wildlife and environment. These ubiquitous organochlorine pollutants have shown toxicity, mutagenesis, carcinogenesis, and especially endocrine disrupting function, which have aroused increasing concerns (Yu, 2001; Fernando, 2001; Chou, 2004). However, some of OCPs are still produced and used due to a type of cheap and broad-spectrum insecticide in some regions in China (Chou, 2004). Therefore, high level of residues of BHC and DDT are still found in part of food, milk and blood, etc. The studies on their harmful effects on human and animals, especially endocrine-disrupting effects, are necessary and significant. In present study Tianmeng district, as a cotton-planting region where DDT and BHC were used extensively and massively during the last century, was selected as our sampling point. Its aim is to understand effects of residues of OCPs on reproductive endocrine function in the population who have inhabited such a heavily polluted area by DDT and BHC for five years or more.

71 lying-in women were recruited to participate in this study. Our results indicated that high levels of residues of OCPs were still capable to be found in part of the subjects. The 19 individuals of high residue group possessed means of the T-BHC, T-DDT and T-OCPs of 56.49, 54.56, 111.05 μg/L, corresponding to medians of 50.00, 41.80, 98.70 μg/L, respectively. This was markedly higher than that in its adjacent district-Xiaogan where means of T-DDT and T-BHC of the sampled people were 3.61 ± 0.22 μg/L, 5.96 ± 0.41 μg/L, respectively (Liu, 2004).

The hypothalamic-pituitary-ovarian axis is an integrated and coordinated neuroendocrine system which regulates female reproductive endocrine activity. GnRH secreted in pulse by hypothalamic stimulates release of FSH and LH synthesized by pituitary, which regulates synthesis and secretion of estradiol and progesterone. At the same time, estradiol and progesterone regulate in feedback synthesis and secretion of GnRH, FSH, and LH. Beta-endorphin, as a neuropeptide, mostly suppresses activity of GnRH. Estradiol binding to its receptor regulates transcription and translation of the target genes. Therefore, to some extent, changes of quantity and activity of estradiol and ER indicate estrogenic and anti-estrogenic activity for xenobiotics (Antonin, 2003; Graeme, 2002). Changes of concentrations of hormones in blood and expressional abundance of some genes in placental and umbilical cord tissues are probably a sensitive biomarker, which indicates that some xeno-compounds are able to disrupt endocrine function. The present study revealed that not only concentrations of FSH, LH, estradiol and progesterone but also abundant expression of α-ER, β-EP and GnRH mRNA could be changed, which corresponded to blood burden of metabolites of DDT and BHC in maternal sera. Moreover, number of PAPO increased due to residues of OCPs. All these show that residues of DDT and BHC possess endocrine-disrupting effects. It seems that estrogenic activity was dominant when concentration of T-BHC was markedly higher than that of T-DDT in maternal blood (Deborah, 2002).

In conclusion, concentrations of residues of OCPs are still relatively high in some people of China. They are capable to disrupt endocrine function so as to induce reproductive dysfunction and developmental malformation. However, many problems have been not still solved. Therefore, further studies are needed to address effects of exposure to xenoestrogens during a specific period of development, probable roles of other substances with proven or suspected hormonal activity, potential synergism of such compounds, and differences in individual susceptibility.

Acknowledgments

We are grateful to the staff members at the Tianmeng Hospital for Maternal and Child Care for their assistance during samples collection. The authors would like to express their sincere thanks to Dr. Wei Qingyi for his critical review of the manuscript.

Correspondence to:
Kedi Yang
Hubei Tianmeng Hospital for Maternal and Child Care
Wuhan, Hubei 430030, China

References

1. Antonin Bukovsky, Michael R. Caudle, Maria Cekanova, et al. Placental expression of estrogen receptor beta and its hormone binding variant-comparison with estrogen receptor alpha and a role for estrogen receptors in asym-

metric division and differentiation of estrogen-dependent cells. Reprod Biol Endocrinol 2003;1(1):36－46.
2. Bao Keguang, Xia Shijun, Yin Binzhi, et al. The harmful effects of environmental pesticides on human health. China Environmental Science 1988;8(2): 53－7.
3. Chou CS, Beristain AG, MacCalman CD, et al. Cellular localization of gonadotropin-releasing hormone (GnRH) I and GnRH II in first-trimester human placenta and decidua. Clin Endocrinol Metab 2004; 89(3):1459－66.
4. Deborah L, Swope J, Chuck Harrell, et al. Genomic structure and identification of a truncated variant message of the mouse estrogen receptor-alpha gene. Gene 2002;294: 239－47.
5. Edward J Calabress, Linda A Baldwin. Toxicology rethinks its central belief. Nature 2003;421;691－92.
6. Fernando M Reis, Pasquale Florio, Luigi Cobellis, et al. Human placenta as a source of neuroendocrine factors. Biology of the Neonate 2001;79;150－56.
7. Graeme A Scobie, Sheila Macpherson, Michael R Millar, et al. Human oestrogen receptors: differential expression of ERalpha and beta and the identification of ERbeta variants. Steroids 2002;67(12):985－92.
8. Grigorakis SI, E Anastasiou, Dai K, et al. Three mRNA transcripts of the proopiomelanocortin gene in human placenta at term. European Journal of Endocrinology 2000; 142: 533－6.
9. Liu Hongkai, Wang Chong, Liu Shihais, et al. The effects of p, p′-DDE on transferrin in sertoli cells of rat testis *in vitro*. J Environ Health 2004; 21(4): 207－9.
10. Liu Shouliang, Qin Qifa, Li Qiquan. Analysis of the accumulative levels of organochlorine pesticides in human body fat and blood in Xiaogan. J Environ Health 2004; 21(4): 238－40.
11. Matthew P Longnecker, Mark A Klebanoff, Zhou Haibo, et al. Association between maternal serum concentration of the DDT metabolite DDE and preterm and small-for-gestation-age babies at birth. Lancet 2001;358:110－14.
12. Yang Kedi. Present status of environmental health study and its developmental trend in China. J Environ Health 2004; 21(1): 10－2.
13. Yu Huifang, Zhao Xudong, Zhang Xiaoming, et al. Dynamic study on the accumulative levels of organochlorine pesticides in the mother's milk in Beijing. J Environ Health 2001;18(60): 352－54.

Received November 5, 2005

Inactivation of Hemoglobin by Hydrogen Peroxide and Protection by a Reductant Substrate

Dejia Li[1], Xu Zhang[1], Yue Long[2], Ximeng Sun[2]

1. Department of Biochemistry, Basic Medical School, Zhengzhou University, Zhengzhou, Henan 450052, China

2. Department of Chemistry, Zhengzhou University, Zhengzhou, Henan 450052, China

Abstract: Inactivation and degradation of hemoglobin were examined in the presence of hydrogen peroxide and guaiacol. Hemoglobin is inactivated upon exposure to hydrogen peroxide. The inactivation and degradation of hemoglobin are two correlated processes. The presence of reducing substrate in addition to hydrogen peroxide partly or completely protected the hemoglobin from inactivation. A reaction mechanism is proposed, in which two competitive routes exist for Compound Ⅱ of hemoglobin; one catalytic and one inactivating. [Life Science Journal. 2006; 3(1):52-58] (ISSN: 1097-8135).

Keywords: hemoglobin; hydrogen peroxide; guaiacol; inactivation

1 Theory

Hemoglobin (Hb) is the major heme protein of red blood cells and is responsible for the transport of oxygen to the tissues. The function of Hb depends upon the ability of ferrous iron in the heme group to bind and release oxygen. Despite its principle role as an oxygen-carrier, the Hb molecular possesses different enzymatic activities (Giardina, 1995).

Hb has been reported as able to oxide aniline (Mieyal, 1976), lipids (Yoshida, 1994), dibenzothiophene (Wu, 1994), N-heterocycles (Ortiz, 1992), styrene (Ortiz, 1985) and o-phenylenediamine (OPDA) (Zhang, 2000; Liu, 2000). Zhang et al (2000) had reported that the catalytic effectiveness of methemoglobin (metHb) with OPDA as a substrate was the highest comparing with the other mimic of peroxidase such as hemin, βCD-hemin and MnTCPP. Moreover, metHb had a higher catalytic activity than the horseradish peroxidase (HRP) if their catalytic effectiveness is expressed on a molar basis rather than in terms of unit weight (Zhang, 2000). As with HRP (Maria, 2002), lignin peroxidase (Mylrajan, 1990), manganese peroxidase (Timofeevski, 1998), lactoperoxidase (Huwiler, 1986), and other peroxidases, hemin is inactivated by an excess of hydrogen peroxide (H_2O_2) or organic hydroperoxides in the absence of reducing substrate (Zheng, 2001). The substrate inactivation of peroxidases leads to the modification of the heme prosthetic group and probably to the formation of a verdohemoprotein as a final product (Rodriguez-López, 1997). The inactivation mechanism of peroxidases, however, has not yet been clearly elucidated.

The knowledge and understanding of Hb inactivation and reactivation kinetics and its related mechanisms would offer new possibilities in improving the potential and effective use of this pseudoenzyme in such diverse and broad areas. As the oxidant substrate of peroxidase, H_2O_2 is also an inactivation agent of this enzyme (Kathy, 1994). The reaction of H_2O_2 with Fe(Ⅱ) Hb (oxyHb and deoxyHb) and Fe(Ⅲ) Hb results in the formation of ferrylhemoglobin (ferrylHb) and oxoferrylhemoglobin (oxoferrylHb), respectively (Kathy, 1994; Giuliv, 1994). Both are strong oxidizing agents. The formation of heme-derived products that are covalently cross-linked to the globin molecule has been reported during the reaction of hemeproteins with H_2O_2 and trichlorobromomethane (Osawa, 1996; Osawa, 1994). The reaction of Hb with a molar excess of H_2O_2 will lead to the degradation of heme, the release of iron (Gutteridge, 1986), and the formation of two fluorescent products (Enika, 1998). As a mimetic enzyme of HRP, hemin can also be inactivated during the catalytic process for the oxidation degradation of it (Zheng, 2001; Lissi, 1994). But the inactivation of Hb during its catalytic reaction process

has not been reported.

The main objective of this work was to give a kinetic and mechanistic study of Hb inactivation during the reaction of Hb with the guaiacol/H_2O_2 system.

2 Materials and Methods

2.1 Materials

MetHb (bovine) from Shanghai Institute of Biochemistry (Shanghai, China) was used without further purification. Guaiacol was purchased from Sigma. The stock solution of guaiacol was prepared by dissolved 116 mg guaiacol in 400 μL dioxane and 500 μL double distilled deionized water, the working solution was prepared by dissolve the stock solution to appropriate concentration. Hydrogen peroxide solutions were prepared by appropriate dilution of the 30% solution with double distilled deionized water (standardized by titration with $KMnO_4$). All other reagents were of the highest available grade and all solutions were prepared in 0.1 M citric-Na_2HPO_4 buffer (pH 5.0) and all experiments were carried out at room temperature (25 ±1°C) unless stated otherwise.

2.2 Apparatus

UV-Vis measurements were performed on a UV-1601 rapid scan spectrophotometer (Shimdzu, Japan) using 1 cm light path quartz cuvette. A 420A pH meter (Orion Research Inc. USA) was used.

2.3 Determination of the heme bleaching of Hb

The reaction was carried out in 3 mL 0.1 mM citric-Na_2HPO_4 buffer (pH 5.0) at 25°C, containing 1 mM Hb and different concentration of H_2O_2 (~1 mM), in the presence or absence of 0.4 mM benzidine. After 30 min of reaction, the absorbance at 410 nm was recorded.

2.4 Rate of inactivation of Hb

The inactivation of Hb was carried out at 25°C in 1-ml incubations of 0.1 M citric-Na_2HPO_4 buffer containing the enzyme (37 μM). Two types of incubation were performed: (a) incubation in the presence of 10 mM H_2O_2 and (b) incubation in the presence of 5 mM guaiacol. At specified time intervals, 30 μL aliquots of the incubation mixtures were transfer to cuvetts containing 3 mL of an assay mixture composed of 5 mM guaiacol and 1.0 mM H_2O_2 in 0.1 M citric-Na_2HPO_4 buffer (pH 5.0). the peroxidase activity was measured by the increase in the absorbance at 470 nm, which is characteristic for the guaiacol oxidation product tetra-guaiacol ($\varepsilon_{470} = 5570\ M^{-1}cm^{-1}$) (Alexander, 2000).

2.5 Determination of the product accumulated at the end of the reaction

The reactions were realized in 0.1 mM citric-Na_2HPO_4 buffer (pH 5.0). The media, with a final volume of 3 mL, were incubated at 25°C, Hb, guaiacol and H_2O_2 were added, the concentration of each in turn being varied while the remaining two were kept constant. Thus, because the final values of $A_{470\ nm}$ showed a good stability, it was possible to estimate maximum values for the product accumulated at the end of each reaction. The experiments were run a minimum of three times.

2.6 Iron release from Hb during the inactivation reaction

Hb (10 μM) was incubated with the different concentrations of H_2O_2 in the presence and absence of guaiacol in 0.1 mM citric-Na_2HPO_4 buffer (pH 5.0) at 25°C for 30 min. Free iron was measured by the Ferrozine method (Cater, 1971). Briefly, a 0.45-ml sample taken from the reaction mixture was mixed with 50 ml of 100% (W/V) trichloroacetic acid. Then, 0.5 ml of 0.02% ascorbic acid in 0.1 N HCl was added, the system was incubated for 5 min at room temperature, and 0.4 ml of ammonium acetate (10%) and 0.1 ml of Ferrozine solution (75 mg of Ferrozine and 75 mg of neocuproine in 25 ml water) were added. After an additional incubation for 5 min at room temperature, the color developed was measured at 562 nm. The iron concentration was calculated using a millimolar extinction coefficient of 27.9 $mM^{-1}cm^{-1}$.

3 Results

3.1 Heme degradation of Hb mediated by H_2O_2

H_2O_2 can mediated the heme degradation of various hemoproteins (Gutteridge, 1986; Jose, 2000). Mixing of Hb with H_2O_2 results in a red shift in the maximal absorbance of Hb from 405 nm to 409 nm as observed previously (Hai-cheng, 2002), probably due to the formation compound I, and a rapid decline in peak absorbance in the Soret region indicating the degradation of the heme prosthetic group (Figure 1). The rate constants for heme destruction and the loss of catalytic activity differed (Figure 2). After five minutes of incubation with H_2O_2, the Hb lost 78% of its activity (Figure 2), 83% of the heme has been destroyed, according to the Soret band (Figure 2). The heme destruction process therefore appeared to precede the inactivation process.

The residual enzymatic activity was checked after incubation of Hb in media containing: (a) H_2O_2 or (b) guaiacol. Figure 2 showed a different behavior for both kinds of incubation. After 10 min

of incubation of Hb and H_2O_2, the activity loss of Hb was 93.5%, but for guaiacol, the activity loss of Hb was only 4.8%. Therefore, the loss in Hb activity did not depend on the guaiacol; instead, H_2O_2 was the inactivation agent.

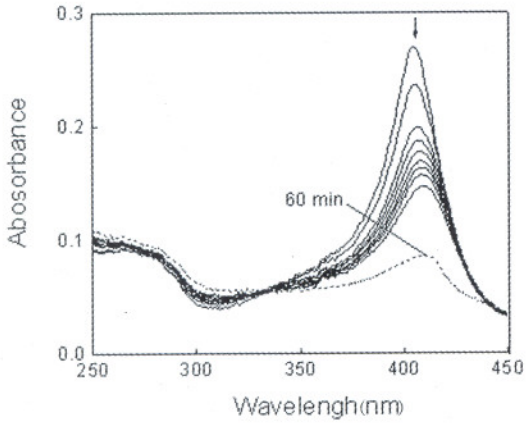

Figure 1. Hb degradation by H_2O_2. Hb (0.5 μM) was mixed with 10 mM H_2O_2 in citric-Na_2HPO_4 buffer (pH 5.0), and incubated at 25°C. Absorption spectra (250 – 450 nm) were taken at 1.0 min intervals starting immediately after mixing (9 upper continuous traces) and then after 60 min (dotted trace) at 250 – 450 nm. Heme prosthetic group destruction as indicated by disappearance of the Soret band, and the arrow indicates the direction of change.

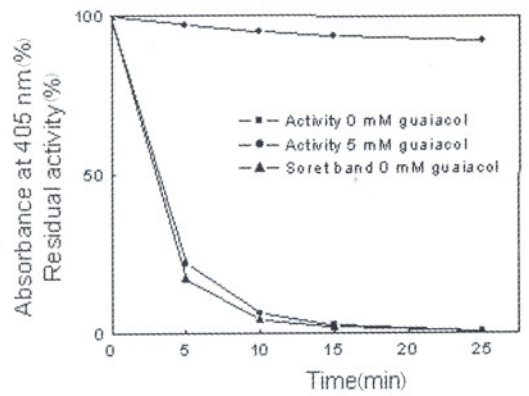

Figure 2. Time-dependent inactivation and heme degradation of Hb. 37 μM Hb was incubated with 10 mM H_2O_2 or 5 mM guaiacol. At specified time intervals, 30 μL aliquots of the incubation mixtures were transfer to cuvetts containing 3 ml of an assay mixture composed of 5 mM guaiacol and 1.0 mM H_2O_2 in 0.1 M citric-Na_2HPO_4 buffer (pH 5.0). The peroxidase activity was measured by the increase in the absorbance at 470 nm. As for the heme degradation, at specified time intervals, the absorbance of Hb at 405 nm was determined using the completely degraded Hb solution (with the same concentration of Hb incubated with large excess of H_2O_2 at 25°C for 2 h) as control.

To corroborate the heme destruction results, the iron release was measured using Ferrozine method (Figure 3). Incubation of Hb with various concentrations of H_2O_2 for 30 min resulted in the release of iron detected in the reaction mixture in a dose dependent manner (Figure 3). After 30 min incubation in the presence of 100 mM H_2O_2, 47% of iron present in the protein was released and could be detected as protein-free iron in the supernatant solution, after protein precipitation. No soluble iron was detected in control samples incubated without H_2O_2 and extracted in the same manner as the experimental samples. In contrast, negligible iron was released from Hb in the presence of 5 mM guaiacol.

Figure 4 showed the Hb degradation mediated by H_2O_2 and the protection role of benzidine. 0.17 mM H_2O_2 caused about 87% of the Soret band loss of Hb. Addition of 0.4 mM benzidine strongly inhibited this process.

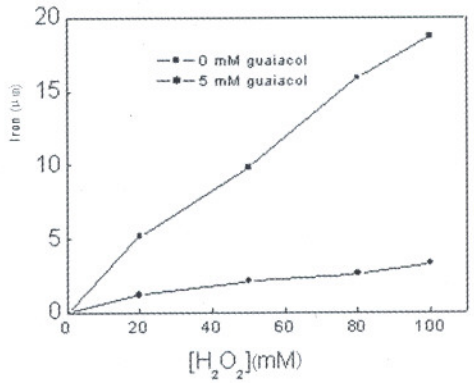

Figure 3. Iron release from Hb mediated by H_2O_2 in the presence and absence of guaiacol. Hb (10 μM) was incubated with the indicated concentrations of H_2O_2 in the presence and absence of guaiacol in 0.1 mM citric-Na_2HPO_4 buffer (pH 5.0) at 25°C for 30 min in a total volume of 1.0 mL. The concentration iron was determined by the Ferrozine method.

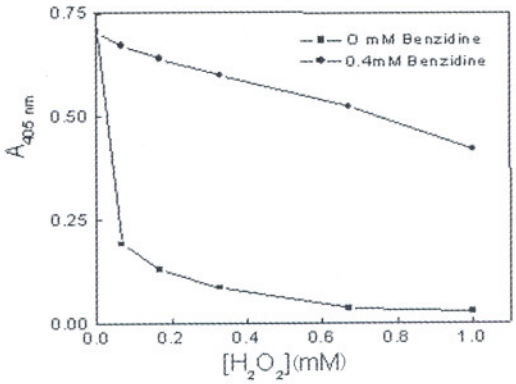

Figure 4. Heme bleaching of Hb by excess H_2O_2 in the presence and absence of benzidine, 1.0 μM Hb was incubated with different concentration of H_2O_2 in the presence and absence of 0.4 mM benzidine for 30 min, then the absorbance at 405 nm was determined.

3.2 Effect of H_2O_2 on the product accumulated in the end of the reaction

The Hb inactivation may also be demonstrated by measuring the product accumulated at the end of reaction. Figure 5A showed the time courses of guaiacol oxidation for a range of variable H_2O_2 concentrations. The product accumulated at the end of the reaction was obtained in a shorter reaction time when the H_2O_2 concentration was higher. Figure 5B showed that as the concentration of H_2O_2 was increased, the values of the absorbance of the product decreased. This confirmed the inactivating nature of the H_2O_2.

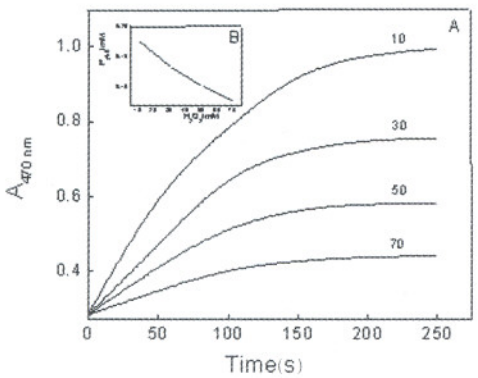

Figure 5. Relationship between the product accumulated at the end of the reaction and H_2O_2 concentration. (A) Time-courses of guaiacol oxidation for a range of variable H_2O_2 concentrations. The reaction mixture contained 0.25 μM Hb, 10 mM, guaiacol; 10, 30, 50, 70 mM H_2O_2 respectively. The reaction was followed as $\triangle A_{470}$ nm vs. time. (B) The values of product accumulated at the end of the reaction (Pyield), obtained from (A), were plotted vs. H_2O_2 concentration.

3.3 Effect of guaiacol on the product accumulated in the end of the reaction

Figure 6 showed a plot of the absorption of product vs. the concentration of guaiacol. Keeping the Hb concentration constant, it could be observed that lower H_2O_2 concentrations produce higher yield of the product for each H_2O_2 concentration. When the guaiacol concentration was increase, the yield of the product also increaseed.

These results confirm the inactivating nature of the H_2O_2 and also showed the protective behavior of guaiacol towards Hb: this protective behavior increaseed as its concentration was increased.

3.4 Effect of Hb on the product accumulated in the end of the reaction

The plot of concentration of product vs. concentration of Hb when both guaiacol and H_2O_2 concentrations are kept constant. Figure 7 showed a linear trace, indicating that Hb inactivation did not depend on any product of the reaction. The slope of this straight line was related to the partition ratio ($r = [P_{yield}]/[Hb]$), which was the number of turnover carried out by one active site of the enzyme before its inactivation. This parameter remained constant for the total range of Hb concentrations used (Figure 7). It should be pointed out that the value of r depended on the [guaiacol]/[H_2O_2] ratio used (Figure 6).

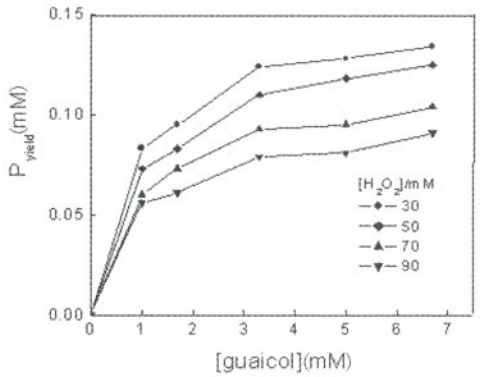

Figure 6. Concentration of reaction product accumulated at the end of the reaction as a function of the initial guaiacol concentration. Different concentrations of H_2O_2 were also assayed. The media contained 0.25 μM Hb in 0.1 mM citric-Na_2HPO_4 buffer (pH 5.0). Each product absorption value was estimated as in Figure 5.

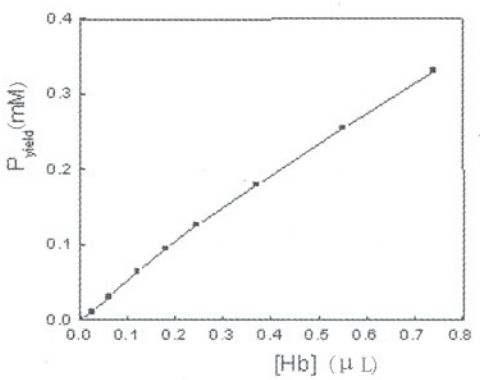

Figure 7. Concentration of product accumulated at the end of the reaction as a function of Hb concentration. The media contained 5 mM guaiacol and 30 mM H_2O_2 in 0.1 mM citric-Na_2HPO_4 buffer (pH 5.0). The product concentration was estimated as Figure 5.

4 Discussion

It is well established fact, and it has been known since the 1950s, that Hb possesses various pseudoenzymatic activities and is able to catalyze the oxidation of a variety of compounds (Mieyal, 1985; Grisham, 1991). It has considerable peroxidase activity (Everse, 1994), thus, Hb is able to mimic the enzymatic activities of a variety of other heme enzymes. Particular attention has been paid to ability of this protein to catalyze the oxidation of

aromatic substrates, including polycyclic aromatic hydrocarbons (Ortiz-Leon, 1995).

Over 20 years ago, Brown (1976) analyzed the biliverdin isomers produced by the H_2O_2 oxidation of various hemoproteins and suggested that the amino acid residues adjacent to the methylene bridges of the porphyrin ring might protect these sites against H_2O_2 oxidation. As shown in Figure 1 and Figure 2, Hb is inactivated by treatment with H_2O_2, and the heme prosthetic group is degraded. In the case of peroxidases, H_2O_2 inactivation leads to the modification of the heme prosthetic group to form a verdohaemoprotein as a final product (Mylrajan, 1990). Two principal mechanisms have been proposed for the inactivation of peroxidases by H_2O_2. One mechanism involves the reaction of Compound Ⅱ with H_2O_2 in the absence of a reducing substrate to form Compound Ⅲ. If Compound Ⅲ is a peroxyiron(Ⅲ) porphyrin free radical, it should be considered a highly reactive intermediate. Because of the proximity of the uncoupled electron to the porphyrin ring, any electron transfer from the ferrous state to an extra H_2O_2 moiety would generate a hydroxyl radical, which could in turn react with the heme group to produce irreversible inactivation. An alternative mechanism involves a reaction of Compound I with an excess of H_2O_2 in the absence of reducing substrate to form an irreversibly inactivated verdohaemoprotein. In this mechanism, Compound Ⅲ is proposed to be a superoxide-anion-generating system that has a protective effect against inactivation. The inactivation mechanism for peroxidases, however, has not been clearly elucidated at present (Cai, 1992; Hiner, 1995; Rodriguez-López, 1997).

In this work, we have shown that turnover-induced inactivation of Hb and peroxide-induced heme destruction are two correlated processes. Heme destruction appears to precede inactivation process (Figure 2). In the absence of reducing substrates and at high H_2O_2 concentrations, Hb is inactivated in a time- and H_2O_2- concentration dependent process. The reducing substrate has a protective effect on the H_2O_2 mediated Hb degradation. This protective effect of reducing substrate has also been described for types of peroxidase other than Hb, such as HRP (Arnao, 1990) and the lignin-degrading peroxidase (Wariishi, 1989).

It has been reported that ferrylHb, corresponds to peroxidase Compound Ⅱ, can withdraw one electron from the reducing sbustrate. In the absence of reducing substrate, ferrylHb would oxidize H_2O_2 to produce superoxide and metHb, and the superoxide generated in the heme pocket can oxidize the tetrapyrole rings, leading to the degradation of heme, the release of iron (Enika, 2000). But oxoferrylHb, corresponds to peroxidase Compound Ⅰ, can react with H_2O_2 in the absence of reducing substrates to produce metHb and oxygen (Arnao, 1990), which cannot mediated heme degradation. Our experimental results showed that the heme degradation and inactivation of Hb are two correlated process, so we can conclude that the H_2O_2 mediated the inactivation of Hb through the reaction of H_2O_2 with Compound Ⅱ, not with Compound Ⅰ.

Arnao (1990) has reported that H_2O_2 mediated the peroxidase inactivation by reaction with Compound Ⅰ base on the founding that the number of catalytic cycles given by the enzyme before its inactivation is a function of a constant set and the [ABTS]/[H_2O_2] ratio, in which the number of turnover is linearly with the [ABTS]/[H_2O_2] ratio. Our results show that the number of catalytic cycles given by Hb before its inactivation is a function of the [guaiacol]/[H_2O_2] ratio, but not linearly with it (Figure 4), so the mechanism of Hb inactivation mediated by H_2O_2 is different from that of peroxidase.

The results presented in this paper suggest the need to include a Hb inactivation step (Hbi) in the usual schemes for reactions catalyzed by Hb. In consequence, and according to Arnao (Arnao, 1990) a mimimum scheme for the Hb/H_2O_2/guaiacol system could be:

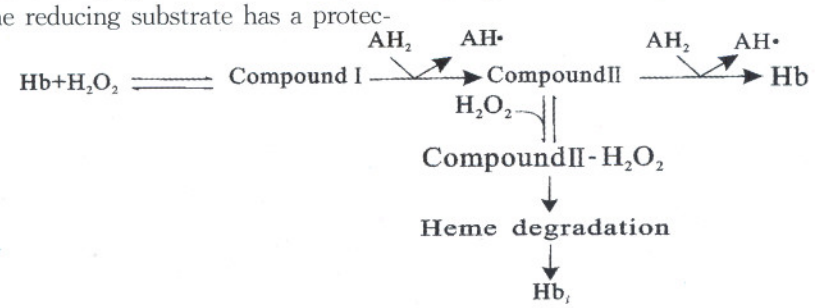

Scheme 1. Possible catalytic and inactivation pathways of Hb. AH_2 is the reducing substrate such as guaiacol, ABTS, benzidine and so on.

The expression (Compound Ⅱ-H_2O_2) represents an intermediate complex in the pathway, which leads to the heme degradation of Hb and thus the inactivation of it. As can be seen in Scheme 1, a competition for Compound Ⅱ between guaiacol and H_2O_2 is established, which protects Hb as long as [guaiacol]/[H_2O_2] ratio is high.

We show in this paper that H_2O_2 itself is the inactivating agent, and that the heme degradation and inactivation of Hb are two correlated process. We also show that the reducing substrates are necessary for the catalytic turnover of the Hb and to protect the Hb from inactivation.

Acknowledgments

The authors gratefully acknowledge the support of this research by grant (No. 38770200) from National Natural Science Foundation of China.

Correspondence to:
Dejia Li
Department of Biochemistry, Basic Medical School
Zhengzhou University
Zhengzhou, Henan 450052, China
Telephone: 86-371-6665-8172

References

1. Arnao MB, Acosta M, del Rio JA, et al. Inactivation of peroxidase by hydrogen peroxide and its protection by a reductant agent. Biochim Biophys Acta 1990; 1038: 85 - 9.
2. Arnao MB, Acosta M, del Rio JA, et al. A kinetic study on the suicide inactivation of peroxidase by hydrogen peroxide. Biochim Biophys Acta 1990; 1041: 43 - 7.
3. Baynton KJ, Bewtra JK, Biswas N, et al. Inactivation of horseradish peroxidase by phenol and hydrogen peroxide: a kinetic investigation. Bioehim Biophys Acta 1994; 1206: 272 - 8.
4. Brown SB. Stereospecific haem cleavage. Biochem J 1976; 159: 23 - 7.
5. Carter P. Spectrophotometric determination of serum iron at the submicrogram level with a new reagent (ferrozine). Anal Biochem 1971; 40: 450 - 8.
6. Everse J, Johnson MC, Marini MA. Peroxidative activities of hemoglobin and hemoglobin derivatives. Methods Enzymol 1994; 231: 547 - 61.
7. Messana I, Scatena R, Castagnola M. The multiple functions of hemoglobin. Critical Rev Biochem Mol Biol 1995; 30:165 - 96.
8. Giulivi C, Davies KJA. Hydrogen peroxide-mediated ferrylhemoglobin generation *in vitro* and in red blood cells. Methods Enzymol 1994; 231:490 - 6.
9. Grisham MB, Everse J. Pro-oxidant activity of hemoglobin and myoglobin. In: Everse J, Everse KE, Grisham MB, (eds.), Peroxidases in chemistry and biology, Boca Raton, FL:CRC Press I 1991,335 - 344.
10. Gutteridge JM. Iron promoters of the Fenton reaction and lipid peroxidation can be released from haemoglobin by peroxides. FEBS Lett 1986; 201: 291 - 5.
11. Hiner ANP, Rodriguez-lopez JN, Arnao MB, et al. Kinetic study of the inactivation of ascorbate peroxidase by hydrogen peroxide. Biochem J 2000; 348: 321 - 8.
12. Huwiler M, Jenzer H, Kohler H. The role of compound Ⅲ in reversible and irreversible inactivation of lactoperoxidase. Eur J Biochem 1986; 158: 609 - 14.
13. Li HC, Li DJ, Zou GL. The influence on the Compound Ⅱ of hemoglobin with hydrogen peroxide by various pH buffer. J Wuhan Univ (Nat Sci Ed) 2002; 48(2): 213 - 6.
14. Liu ZH, Wang QL, Mao LY, et al. Highly sensitive spectrofluorimetric determination of ascorbic acid based on its enhancement effect on a mimetic enzyme-catalyzed reaction. Anal Chim Acta 2000; 413: 167 - 73.
15. Maria F, Machado JS. Inactivation and reactivation kinetics of horseradish peroxidase in phosphate buffer and buffer-dimethylformamide solutions. J Mol Catal B: Enzymatic 2002; 19-20: 451 - 7.
16. Mieyal JJ, Acherman RS, Blumer JL, et al. Characterization of enzyme-like activity of human hemoglobin: Properties of the hemoglobin-P-450 reductase-coupled aniline hydroxylase system. J Biol Chem 1976; 251: 3436 - 41.
17. Montellano PR, Catalano CE. Epoxidation of styrene by hemoglobin and myoglobin: Transfer of oxygen equivalents to the protein surface. J Biol Chem 1985; 260: 9265 - 71.
18. Mylrajan M, Valli K, Wariishi H, et al. Resonance Raman spectroscopic characterization of compound Ⅲ of lignin peroxidase. Biochemistry 1990; 29: 9617 - 23.
19. Nagababu E, Rifkind JM, Formation of fluorescent heme degradation products during the oxidation of hemoglobin by hydrogen peroxide. Biochem Biophys Res Com 1998; 247: 592 - 6.
20. Nagababu E, Rifkind JM. Reaction of hydrogen peroxide with ferrylhemglobin: superoxide production and heme degradation. Biochemistry 2000;39: 12503 - 11.
21. Ortiz JC, Montellano PR. Thianthrene 5-oxide as a probe of the electrophilicity of hemoprotein oxidizing species. Biochemistry 1992;31: 8315 - 22.
22. Ortiz-Leon M, Velasco L, Vazquez-Duhalt R. Biocatalytic oxidation of polycyclic aromatic hydrocarbons by hemoglobin and hydrogen peroxide. Biochemical and Biophysical Research Communication 1995;215(3): 968 - 73.
23. Osawa Y, Fellows CS, Meyer CA, et al. Structure of the novel heme adduct formed during the reaction of human hemoglobin with BrCCl3 in red cell lysates. J Biol Chem 1994; 269:15481 - 7.
24. Osawa Y, Williams MS. Covalent crosslinking of the heme prosthetic group to myoglobin by H_2O_2: toxicological implications. Free Rad Biol Med 1996; 21:35 - 41.
25. Rodriguez-López JN, Hernández-Ruiz J, García-Cánovas F, et al. The inactivation and catalytic pathways of horseradish peroxidase with mchloroperoxybenzoic acid: a spectrophotometric and transient kinetic study. J Biol Chem 1997; 272: 5469 - 76.
26. Timofeevski SL, Reading NS, Aust SD. Mechanisms for protection against inactivation of manganese peroxidase by hydrogen peroxide. Arch Biochem Biophys 1998; 356: 287 - 295.

27. Villegas JA. Mauk AG, Vazquez-Duhalt R. A cytochrome c variant resistant to heme degradation by hydrogen peroxide. Chem Biol 2000; 7:237－244.
28. Wariishi H, Gold MH. Lignin peroxidase compound Ⅲ: formation, inactivation and conversion to the native enzyme. FEBS Lett 1989; 243: 165－8.
29. Winterbourn CC. Oxidative reactions of hemoglobin. Methods Enzymol 1990; 186:265－272.
30. Wu S, Lin J, Chan SI. Oxidation of dibenzothiophene catalyzed by heme-containing enzymes encapsulated in sol-gel glass: a new form of biocatalysts. Biochem Biotechnol 1994; 47: 11－20.
31. Yoshida Y, Kashiba K, Niki E. Free radical-mediated oxidation of lipid induced by hemoglobin in aqueous dispersion. Biochim Biophys Acta 1994; 201: 165－172.
32. Zhang K, Cai RX, Chen DH, et al. Determination of hemoglobin based on its enzymatic activity for the oxidation of o-phenylenediamine with hydrogen peroxide. Anal Chim Acta 2000; 413: 109－113.
33. Zhang K, Mao LY, Cai RX. Stopped-flow spectrophotometric determination of hydrogen peroxide with hemoglobin as catalyst. Talanta 2000; 51:179－186.
34. Zheng N, Ge CH, Guo ZX, et al. Comparative studies on hemin as a mimic of peroxidase with horseradish peroxidase. J Anal Sci 2001; 17(4):265－269.

Received September 28, 2005

Synthesis and Antimicrobial Activity of Nano-fumed Silica Derivative with N, N-dimethyl-n-hexadecylamine

Xia Xu, Shurong Li, Fayun Jia, Pu Liu

Laboratory Center of Medical Science, Zhengzhou University, Zhengzhou, Henan 450052, China

Abstract: Nano-fumed silica derivative with N, N-dimethyl-n-hexadecylamine was synthesized with γ-Chloropropyltrimethoxysilane as the roupling agent, and subsequently treated with N, N-dimethyl-n-hexadecylamine. The nano-fumed silica derivative was confirmed by Fourier-transform infrared spectroscopy (FTIR). The zeta potentials of nano-fumed silica and nano-fumed silica derivative were measured as a function of pH in suspensions and showed the isoelectric point of modified nano-fumed silica has increased in the direction of pH rising compared with nano-fumed silica. Antimicrobial properties of the nano-fumed silica derivative against selected microorganisms were tested by the quantitative suspension method. The results showed that the obtained polymer inhibited the growth of *E. coil*, *S. aureus* and *C. albicans*. It was found that the growth inhibiting effect of polymer varied with the time exposed to the microorganism. When the time exposed to the microorganism was 15 min, each of their inhibitory rates was 99.99%, 99.99% and 95.23%, respectively. [Life Science Journal. 2006;3(1):59-62] (ISSN: 1097-8135).

Keywords: nano-fumed silica; silane coupling agents; quaternary ammonium group; antimicrobial

1 Introduction

Quaternary ammonium compounds (QAC) belong to the group of compounds, which exhibit high antimicrobial activity. They are widely used in many of domains such as environmental disinfection, equipment surfaces and disinfection in hospitals. These compounds seem to be safer than chemically active disinfectants such as chlorine and glutaraldehyde. However, since the irritant and cytotoxic effects of these compounds on human cells/tissues such as keratinocytes, fibroblasts, cornea and respiratory mucosa have been shown previously (Augustin, 1995; Damour, 1992; Steinsvag, 1996; Tripathi, 1989), the improvement of QACs is necessary, not only for their antimicrobial activity but also for human cells' safety. To overcome these problems, anchoring the QAC to a polymer backbone by a covalent might be promising in developing materials which would have antimicrobial activity by themselves.

Nano-fumed silica (NFS) is utilized in industry, e.g. as fillers for elastomer reinforcement, additives in fluids, free-flow agents in powders, medicinal and industrial adsorbents, etc. And it is a kind of extremely important superfine inorganic material. There are many hydroxyl groups at the surface of nano-fumed silica that are allowed to react with silane coupling agents, and the resulting composites connected with many organic functional groups show expectable characteristics, such as biological activity (Demir, 2005), heat resistance (Fu, 2004), mechanical (Agnihotry, 2004) electrical properties (Paik, 2005), and other properties.

In our study, the nanometer antimicrobial material that contained organic antimicrobial agent was reported and the preparation of the nano-fumed silica derivative with quaternary ammonium group using the γ-Chloropropyltrimethoxysilane as silane coupling agent was investigated (It can avoid the small molecular antimicrobial losing). Furthermore, the antimicrobial activity was also studied.

2 Materials and Methods

2.1 Materials

Nano-fumed silica (mean particle size 40 nm) was purchased from Jibishi Chem. Lin (Guangzhou, China); N, N-dimethyl-n-hexadecylamine was kindly donated by the Feixiang Chem. Lin (Jiangsu, China). γ-chloropropyltrimethoxysilane was bought from Yingcheng Debang Chemical Industrial New Materials Co., Ltd. Toluene, acetonitrile are of reagent grades.

2.2 Tested microorganism

Tested microorganism included the Gram negative bacteria *Escherichia coli* (8099), Gram positive bacteria *Staphylococcus aureus* (ATCC 6538). Bacteria and fungi were maintained on Subourond agar slopes. LB medium was sterilized by autoclaving for 30 min at 121℃.

2.3 Reaction

The procedure was schematically shown in

Figure 1(Ⅰ). After a mixture of nano-fumed silica, the toluene and a little water was added to the three-necked with stirring for a period of time, and amount of γ-Chloropropyltrimethoxysilane was added and refluxed at 80℃ for 6 h. The resulting nano-fumed silica (MNFS-1) was washed with toluene to remove excess γ-Chloropropyltrimethoxysilane and then dried at 110℃ for 16 h in vacuo. The subsequent reaction with N, N-dimethyl-n-hexadecylamine is schematically shown in Figure 1(Ⅱ). A mixture of MNFS-1 and N,N-dimethyl-n-hexadecylamine and acetonitrile was refluxed with stirring at 80℃ for 8 h. The product containing the quaternary ammonium group (MNFS-2) was washed to remove excess N, N--dimethyl-n-tetradecylamine and dried in vacuo.

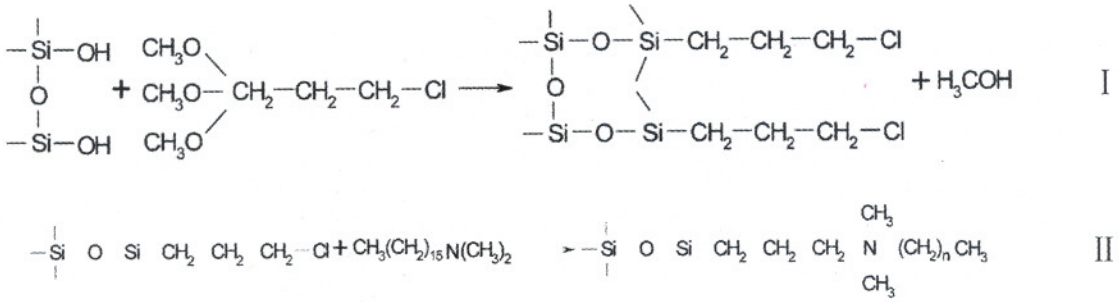

Figure 1. Scheme of reaction

2.4 Measurement

FT-IR spectra were recorded on a Fourier-transform infrared spectroscopy (MAGNA. 506 Nicolet USA). The mean size and the zeta potential of the NFS and MNFS-2 were measured with Zetarsizer Nano series (MALVERN).

2.5 Antimicrobial activity

In order to assess antimicrobial functions of MNFS-2, the suspension quantitative test was employed. The bacteria used were *E. coli* (8099), *S. aureus* (ATCC6538) and *Candida albicans* (ATCC 10231). They were characterized as the bacteria of Gram negative bacteria and Gram positive bacteria as well as the fungus, respectively. The control was the bacterial of the solution of N. S. The suspension quantitative test determining the antibacterial activity was as follows: 0.5 g MNFS −2 was added to 150 ml Erlenmeyer flask containing 5 ml 108 cfu/ml of *Escherichia coli* and 45 ml N. S. The resulted solution was shaken at 37℃ by a Burrell wrist action shaker for 5 min, 15 min and 30 min, respectively, and kept station for 30 min to obtain a mixture. 1 ml supernatant of the mixture was diluted gradiently, and then 1 ml dilution solution was added to agar plate and incubated at 37℃ for 24 h. After incubation, the colonies of bacteria were counted to indicate bactericidal activity.

3 Results and Discussion

3.1 FTIR Analysis 1

Figures 2(a), (b) and (c) showed the IR of NFS, MNFS-1 and MNFS-2, respectively. The absorption peaks of active hydroxyl group at the surface of NFS were observed at 3438 cm^{-1} and 1640 cm^{-1}. The absorption peaks of the Si-O-Si asymmetric stretching vibration, symmetric stretching vibration, and bending vibration were observed at 1110 cm^{-1} and 805 cm^{-1} and 475 cm^{-1}. As seen from Figure 2(b), the absorption peaks of the methyl and methylene stretching vibration were in the range of 2850 ~ 3000 cm^{-1}; The peak of the C-H symmetric deformation vibration was at 1460 cm^{-1}. The intensities of these absorption peaks increased with chain length of the alkyl group. As seen from Figure 2(c), the absorption peaks of the methyl and methylene stretching vibration were observed in the range of 2850 ~ 3000 cm^{-1}, and they were stronger than Figure 2(b) for the number of $-CH_2$ increasing.

3.2 Zeta potential analysis

0.05% (wt) of NFS and MNFS-2 were titrated with 0.25 mol/L HCl and 0.25 mol/L NaOH at 25℃, while zeta-potential changes with pH were tested, respectively. The results were as follows (Figure 3).

Figure 3 showed the zeta potential of NFS and MNFS-2. The isoelectric point of the NFS is usually known to exist at pH of 2 − 3. The isoelectric point of the NFS in this work has a pH value about 4.5 from Figure 3(a). The Si-OH at the surface of NFS (pH < 4.5) showed a positive charge for an added proton:

$$—Si—PH + H^* \rightarrow SiOH_2^+$$

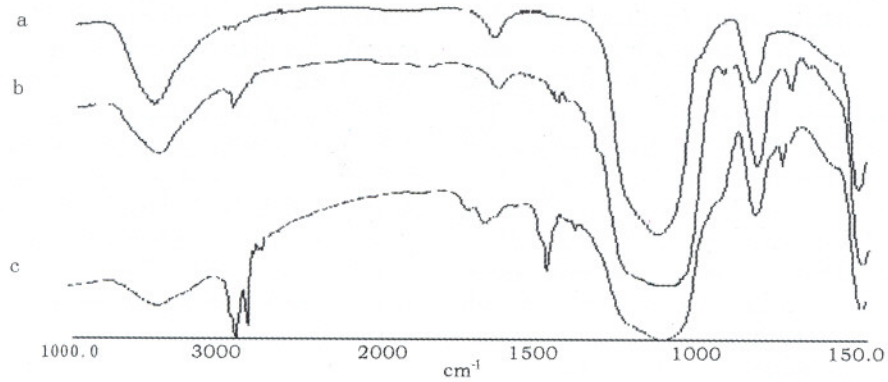

Figure 2. FTIR spectra of nano-fumed silica (a)NFS (b) MNFS-1 (c)MNFS-2

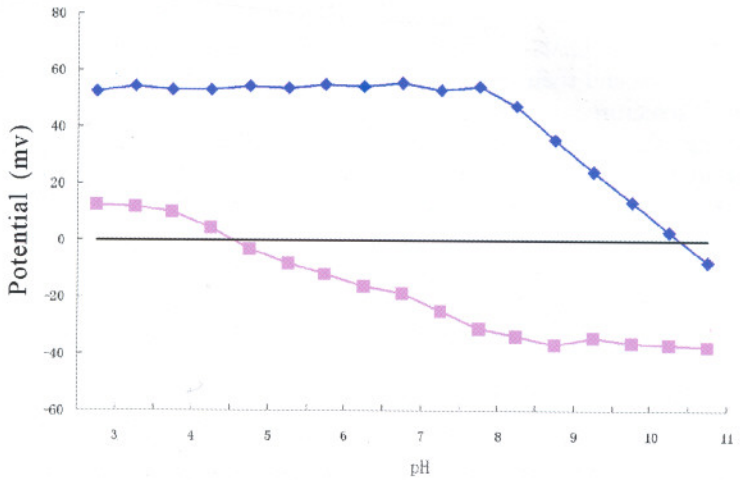

Figure 3. PH titration graph of NFS and MNFS: (a) NFS; (b) MNFS

The Si-OH at the surface of NFS ($pH > 4.5$) showed a negative charge for a liberated proton:

$$—Si—PH + H^* \rightarrow SiO^- + H^+$$

When pH of solution was more than 4.5, surface of NFS showed negative electric charge; as pH increases, absolute value of zeta potential increased.

In contrast, the zeta potential of MNFS-2 constantly showed a positive charge in the range of pH 3-10.5. The zeta potential rapidly decreased when $pH > 10.5$. Suhara (1995) measured the zeta potential of fine silica power modified with the quaternary ammonium group. In the pH range of 2-10, the zeta potential of fine silica power modified with the quaternary ammonium group showed the positive charge range was wider than that of the original fine silica powder and its value of the zeta potential ($pH < 10$) was almost constant. And the decrease in the zeta potentials of the quaternary ammonium group was considered to be due to the quaternary ammonium group being neutralized by the base in the range of $pH > 10$; the zeta potentials of fine silica powder may change the negative charge owing to adsorption of an anion or ionic bond. As described in previous papers; the decrease in the zeta potential of MNFS-2 was considered to be due to the N,N-dimethyl-n-hexadecylamine being neutralized by the base in the range of $pH > 10.5$. The mechanism of the change of the zeta potential is similar to the paper of Huhara.

3.3 Antimicrobial activity

Table 1. Bacteriostatic efficacy of MNFS-2 after exposure for different periods of time

Microorganism	Average bacterial count of control group($\times 10^6$)	Average bacteriostatic rate (%) after exposure for different period of time (min)		
		5	15	30
Escherichia coli	19.8	97.01	99.99	99.99
S. aureus	28.2	99.12	99.99	99.99
C. albicans	15.9	94.92	95.23	95.99

Note: The temperature was 19~22℃. The results are means of triplicate tests.

The antimicrobial activity of nano-fumed silica modified quaternary ammonium salts was investigated and shown in Table 1. The results obtained showed that as the exposure time increased, the antimicrobial activity increased. And it was found that bacteriostatic rates of inhibiting the growth of *E. coli* and *S. aureus* were higher than that of *C. albicans*. The polymer inhibited the growth of *E. coli* (8099), *Staphylococcus aureu* (ATCC6538) and *Candida albicans* increased with the exposed time. The inhibition became stronger as the sequence, *Candida albicans* < *Escherichia coli* < *Staphylococcus aureu*.

Quaternary ammonium salts possessing at least one alkyl substituted are able to kill microorganisms such as bacteria and fungi. So QAS belong to the membrane active compounds and their biological activity depends on their structure and physicochemical properties affecting the interaction with the phospholipid bilayer in the cytoplasmic membrane of bacteria and influencing cell metabolism.

The antimicrobial activity of the nano-fumed silica derivative with quaternary ammonium group is considered to be one of the important properties linked directly to the possible applications. Its mechanism was proposed for the antimicrobial activity exerted by antimicrobial polymeric derivative with quaternary ammonium salts. It is that the polycationic nature of nano-fumed silica derivative with quaternary ammonium group interferes with bacterial metabolism by electrostatic stacking at the cell surface of bacteria. This mechanism is evaluated in term of the value of the zeta potential of nano-fumed silica derivative with quaternary ammonium group. Because MNFS-2 shows positive charge in aqueous solution (pH=7), its antimicrobial activity is stronger.

4 Conclusions

1. Hydroxyl groups on surface of nano-fumed silica and tertiary amine can be connected with γ- chloropropyltrimethoxysilane, and powder antimicrobial material was prepared by quaternization.

2. From FTIR spectra, γ-chloropropyltrimethoxysilane bonding on the surface of nano-fumed silica by acting with hydroxyl groups on surface of nano-fumed silica can be seen. From alkyl radical peak on NFS modified with quaternary ammonium salts, we can see NFS carried alkyl groups.

3. After researches on change of isoelectric points of NFS and modified NFS, we can see that owing to isoelectric points of modified NFS increasing in the direction of pH enhancing by 4, ions of modified NFS in aqueous solution showed positive charge, and it can kill microbial.

4. By the quantitative suspension method, the bacteriostatic efficacy of powder antimicrobial material modified with N, N-dimethyl-n-hexadecylamine to *Escherichia coli* (8099), *Staphylococcus aureus* (ATCC6538) and *Candida albicans* (ATCC 10231) was 99.99%, 99.99% and 95.23%, respectively.

Correspondence to:
Xia Xu
Laboratory Center of Medical Science
Zhengzhou University
Zhengzhou, Henan 450052, China

References

1. Agnihotry SA, Ahmad S, Gupta D. Composite gel electrolytes based on poly (methylmethacrylate) and hydrophilic fumed silica. Electrochimica Acta 2004; 49: 2343-9.
2. Augustin C, Damour O. Pharmacotoxicological applications of an equivalent dermis: three measurements of cytotoxicity. Cell Biology and Toxicology 1995; 11: 167-71.
3. Damour O, Hua SZ, Lasne F, et al. Cytotoxicity evaluation of anti-septics and antibiotics on cultured human fibroblasts and keratinocytes. Burns 1992; 18: 479-85.
4. Demir MM, Menceloglu YZ, Erman B. Effect of filler amount on thermoelastic properties of poly(dimethylsiloxane) networks. Polymer 2005; 46: 4127-34.
5. Fu M, Qu B. Synergistic flame retardant mechanism of fumed silica in ethylene-vinyl acetate/magnesium hydroxide blends. Polymer Degradation and Stability 2004; 85: 633-9.
6. Paik U, Kim JY, Hackley VA. Rheological and electrokinetic behavior associated with concentrated nanosize silica hydrosols. Materials Chemistry and Physics 2005; 91: 205-11.
7. Steinsvag SK, Bjerknes R, Berg OH. Effects of topical nasal steroids on human respiratory mucosa and human granulocytes *in vitro*. Acta Otolaryngologica, 1996; 116: 868-75.
8. Suhara T, Fukui H, Yamaguchi M. Fine silica powder modified with quaternary ammonium groups 2. The influence of electrolyte and pH Colloids and Surfaces A: Physicochemical and Engineering Aspects 1995; 101: 29-37.
9. Tripathi BJ, Tripathi RC. Cytotoxic effects of benzalkonium chloride and chlorobutanol on human corneal epithelial cells *in vitro*. Lens and Eye Toxicity Research 1989; 6: 395-403.

Received September 29, 2005

Construction of Prokaryotic Expression Vectors Bearing S Gene of Isolate TH-98 from Transmissible Gastroenteritis Virus

Jiechao Yin, Guangxing Li, Yijing Li, Xiaofeng Ren

Department of Veterinary, College of Veterinary Medicine, Northeast Agricultural University, 59 Mucai Street, Harbin, Heilongjiang 150030, China

Abstract: Sa fragment containing major antigenic sites A, B, C and D of S gene from transmissible gastroenteritis virus (TGEV) Chinese isolate TH-98 was purified with *Eco*RI and *Kpn*I from recombinant pUC-S and cloned into prokaryotic expression vector pProExHTb. The recombinant SaPRO was identified with restriction enzyme (RE). Sa derived from recombinant SaPCI was inserted into *Eco*RI and *Not*I sites of expression vector pET30c with the similar DNA recombination technique. The construct designated SaPET was transformed into *Escherichia coli* (*E. coli*) BL21. Then, SaPET was digested with *Xho*I and ligated in order to gain the recombinant SasPET carrying B, C and D sites of S gene, which was also transformed into BL21. The acquisition was subcloned into corresponding sites of another prokaryotic expression vector pGEX-6P-1 after digestion with *Eco*RI and *Xho*I. The verified recombinant Sas6P-1 was re-transformed into BL21. [Life Science Journal. 2006;3(1):63 - 66] (ISSN: 1097 - 8135).

Keywords: TGEV; S gene; prokaryotic expression vector; construction

1 Introduction

Transmissible gastroenteritis virus (TGEV) is one of the important pathogens for virus diarrhea of swine (Yin, 2005). Spike(S) protein is the major immunogen among four major structural proteins (S, M, N and sM) of TGEV (Krempl, 1997). Particularly the 5′ end half of S gene encoding the major antigenic sites are critical for inducing neutralizing antibodies (Gebauer, 1991; Tuboly, 1994). To gain the S protein is a prerequisite for the diagnosis, prevention and treatment of transmissible gastroenteritis (TGE). The prokaryotic expression system shows some significant advantages over other systems in production cost, technology and cycle etc. However, the limited expression capacity for foreign genes and the different expression efficiency of different vectors used in this system are the disadvantages.

For these reasons, we constructed several recombinant plasmids encoding the 5′ end half of S gene or major antigenic site fragment using different prokaryotic expression vectors. These plasmids have been transformed into *Escherichia coli* (*E. coli*). This study provided the important materials for S protein expression and comparison of vector expression efficiency.

2 Materials and Methods

2.1 Vector, host cells, tool enzymes and primers

Recombinant plasmids pUS-C and SaPCI respectively containing full-length and 5′ end half of S gene of TGEV have been constructed in our laboratory (Ren, 2003). Prokaryotic expression vectors, pProExHTb (GIBCO), pET30c (Novagen) and pGEX-6P-1 (Amersham Biosciences) were commercially purchased. TG1, DH5α and BL21 competent cells were also commercially obtained. Tool enzymes were purchased from Takara Biotechnology Company (Dalian, China). Primers, PS3: 5′-TACAGTGAGTGACTCGAGCT-3′ (1242) and PR3:5′-GGTGTTGTTGTCCAATGTG-3′ (2408) were used for nested PCR (The figures in brackets are the corresponding or complementary position of S gene).

2.2 Construction of expression plasmids containing S gene of TGEV

Recombinant pUC-S was digested with *Eco*RI and *Kpn*I to obtain the 5′ end half of S gene named Sa. Sa was ligated with vector pProExHTb digested with the same enzymes and transformed into DH5α cells. A positive recombinant named SaPRO

was selected in LB agar plate containing appropriate antibiotic and identified with restriction enzyme (RE). Recombinant SaPCI was digested with *Eco*RI and *Not*I, and a linearized fragment encoding the Sa region was cloned into pET30c vector using the similar method described above. A positive recombinant was named SaPET after the identification with RE and by nested PCR. To facilitate further inducible expression, SaPET was transformed into BL21 cells. A strain of plasmid-containing cells was selected.

DNASIS software analysis indicated there were two *Xho*I sites located in near nucleotide 1120 of S gene and in the multiple cloning sites after Sa fragment in SaPET. Therefore we digested SaPET with *Xho*I and a resulting fragment containing vector and 5′ end S gene about 1100 base pair (bp) in length was ligated and transformed into DH5α cells. A recombinant named SasPET was identified with RE and re-transformed into BL21 cells. SasPET was digested with *Eco*RI and *Xho*I, and the foreign fragment was cloned into vector pGEX-6P-1. A positive recombinant identified with RE was named Sas6P-1. All the recombinants were sequenced to confirm the authenticity of the sequence.

3 Results

3.1 Identification of SaPRO with RE

SaPRO was digested with RE according to the physical map of the vector pProExHTb and Sa sequence. The digested fragments were visualized by 0.8% agarose gel electrophoresis. This result was identical to theoretical calculation (Figure 1).

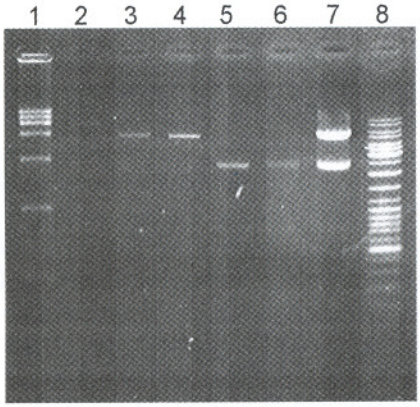

Figure 1. Identification of SaPRO with RE
Lane 1: DL 15, 000 DNA marker (TaKaRa, China).
Lane 2: SaPRO digested with *Xho*I, of about 7.1 kb.
Lanes 3 and 4: Vector pProExHTb linearized with *Eco*RI and *Kpn*I, of about 4.8 kb.
Lanes 5 and 6: Fragment Sa digested with *Eco*RI and *Kpn*I, of about 2.3 kb.
Lane 7: SaPRO digested with *EcoR* I and *Kpn*I, of about 2.3 kb and 4.8 kb respectively.
Lane 8: DNA Ladder (MBI Fermentas).

3.2 Identification of SaPET

Recombinant SaPET was identified with RE and primer-specific PCR. The agarose gel electrophoresis showed that Sa has been inserted pET30c vector (Figure 2).

Figure 2. Identification of recombinant SaPET
Lane 1: Identification of SaPET by nested PCR, of about 1.2 kb.
Lane 2: DL 15,000 DNA marker.
Lane 3: SaPET digested with *Eco*RI, of about 7.7 kb.
Lane 4: SaPET digested with *Xho*I, of about 7.7 kb.

3.3 Identification of SasPET

SasPET was analyzed with RE, and the result indicated that 5′ end fragment of S gene about 1100 bp in length has been cloned into pET30c (Figure 3).

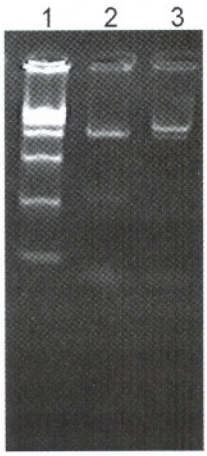

Figure 3. Identification of recombinant SasPET
Lane 1: DL 15,000 DNA marker.
Lane 2: SasPET digested with *Eco*RI and *Xho*I, of 1.1 kb and 5.4 kb respectively.
Lane 3: SasPET digested with *Eco*RI, of 6.6 kb.

3.4 Identification of Sas6P-1

Sas6P-1 was digested with RE, and the analysis result of agarose gel indicated the correct insertion of fragment of interest (Figure 4).

3.5 Sequencing analysis

The sequencing report verified there was no nucleotide insertion and deletion in the S gene used in this study and it was identical to the published sequence (GenBank™ accession number AF494337).

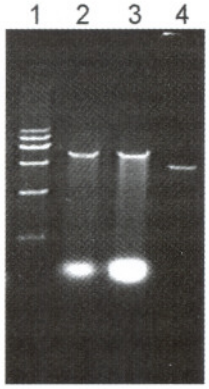

Figure 4. Identification of recombinant Sas6P-1
Lane 1: DL 15,000 DNA marker.
Lane 2: Sas6P-1 digested with *Bam*HI, of about 6.1 kb.
Lane 3: Sas6P-1 digested with c*Eco*RI, of about 6.1 kb.
Lane 4: Vector pEGX-6P-1 linearized with *Eco*RI and *Xho*I, of about 4.9 kb.

4 Discussion

Gene expression system(GES) is very useful in genetic engineering field. Currently, prokaryotic, yeast and eukaryotic expression systems are frequently used GES. In which reformed *E. coli* is very popular for protein production in large scale due to their rapid growth rate, facilitation for continuous fermentation and relatively low cost. However, the genome of *E. coli* is well characterized and a lot of cloning vectors are available (Grisshammer, 1995).

The initial purpose of this study is to express 5′ end half of S gene using *E. coli*. However the expression level of foreign gene in *E. coli* might be influenced by the type of prokaryotic expression vector and length of gene of interest (Francisco, 1993; Wels, 1995; Jahn, 1995).

Therefore, we took full advantage of different vectors and different fragments of S gene to construct various recombinant plasmids. At the same time, we tried to decrease the length of S gene under the circumstance of retaining the major antigen sites in order to increase the probability of successful expression of S gene. The usage of different vectors enables us to make multiple choices for future protein purification.

In the process of construction, the sequenced recombinants were utilized to give gene of interest, which enhanced the positive recombination ratio and decreased possible mutation might derived from PCR amplification. However, it should be noted that open reading frame (ORF) of S gene must be correct after inserting into suitable vectors to prevent the shift of ORF. Most vector we used here are high efficient vectors that can express gene of interest in the form of fusion protein, decrease the toxicity to host cells and facilitate the downstream purification.

To sum up, we constructed four recombinant plasmids encoding the major antigenic sites of TGEV. These positive *E. coli* strains might be induced to express the gene of interest, which provided the useful materials for further related research.

Acknowledgments

This work was partially supported by funds from China Scholarship Council(CSC) and by grant from "Project of the Tenth-five" of Heilongjiang Province Scientific and Technique Committee, China.

Correspondence to:
Yijing Li, Xiaofeng Ren
Department of Veterinary
College of Veterinary Medicine
Northeast Agricultural University
59 Mucai Street, Harbin
Heilongjiang 150030, China
Email: rxfemail@yahoo.com.cn
yijingli@yahoo.com

References

1. Francisco JA, Campbell R, Iverson BL, et al. Production and fluorescence-activated cell sorting of *Escherichia coli* expressing a functional antibody fragment on the external surface. Proc Natl Acad Sci USA 1993;90:10444－8.
2. Gebauer F, Posthumus WP, Correa I, et al. Residues involved in the antigenic sites of transmissible gastroenteritis coronavirus S glycoprotein. Virology 1991;183:225－38.
3. Grisshammer R, Tate CG. Overexpression of integral membrane proteins for structural studies. Q Rev Biophys 1995;28:315－422.
4. Jahn S, Roggenbuck D, Niemann B, et al. Expression of monovalent fragments derived from a human IgM autoantibody in *E. coli*: The input of the somatically mutated CDR1/CDR2 and of the CDR3 into antigen binding specificity. Immunobiology 1995;193:400－19.
5. Krempl C, Schultze B, Laude H, et al. Point mutations in the S protein connect the sialic acid binding activity

with the enteropathogenicity of transmissible gastroenteritis coronavirus. J Virol 1997;71:3285－7.
6. Ren XF, Liu BQ, Li YJ. Cloning and homology comparison of S gene for isolate TH-98 of porcine transmissible gastroenteritis virus. Agric Sci China 2003;2:314－20.
7. Tuboly T, Nagy E, Dennis JR, et al. Immunogenicity of the S protein of transmissible gastroenteritis virus expressed in baculovirus. Arch Virol 1994;137:55－67.
8. Wels W, Beerli R, Hellmann P, et al. EGF receptor and p185erbB-2-specific single-chain antibody toxins differ in their cell-killing activity on tumor cells expressing both receptor proteins. Int J Cancer 1995;60:137－44.
9. Yin JC, Ren XF, Li YJ. Molecular cloning and phylogenetic analysis of ORF7 region of Chinese isolate TH-98 from transmissible gastroenteritis virus. Virus Genes 2005;30:395－401.

Received September 3, 2005

High GC Amplification: A Comparative Study of Betaine, DMSO, Formamide and Glycerol as Additives

Zhaoshu Zeng[1,2], Hongtao Yan[1], Xudong Zheng[1], Gangzheng Hu[3], Ying Chen[4], Mei Ding[2]

1. Department of Legal Medicine, School of Basic Medicine, Zhengzhou University, Zhengzhou, Henan 450052, China

2. Department of Serology, School of Forensic Medicine, China Medical University, Shenyang, Liaoning 110001, China

3. Department of Internal Medicine, the Second Affiliated Clinical College, China Medical University, Shenyang, Liaoning 110001, China

4. Division of Pneumoconiosis, School of Public Health, China Medical University, Shenyang, Liaoning 110001, China

Abstract: High GC content is proved to be an obstacle for successful PCR when following standard protocols recommended by Mullis KB. To avoid this false negative, additives are often used. However, among those easily accessible additives such as betaine, dimethylsulfoxide (DMSO), formamide and glycerol, their concentrations used in the PCR mixture were reported to be in a wide range, and no systematic researches exist either about the most optimal concentration of each additive or about which additive is the most powerful. Using human leucocyte antigen-B (HLA-B) PCR amplification as a model, we evaluated the effects of these 4 additives with a KCl-contained or KCl-free reaction buffer, and with different additive concentrations. We found that 0.6 M for betaine, 10% for DMSO, 5% for formamide and 10% for glycerol were their optimal concentrations, respectively, and the 0.6 M betaine had the highest successful rate. We also found that KCl will greatly improve the amplification yields when the template GC content was moderate, while zero KCl could improve the yields when the template GC content was high. We thus recommended a 0.6 M betaine and KCl-free buffer as the first choice in high GC amplifications. [Life Science Journal. 2006;3(1):67-71] (ISSN: 1097-8135).

Keywords: human leucocyte antigen-B (HLA-B); polymerase chain reaction (PCR); GC rich sequence; betaine; dimethylsulfoxide (DMSO); formamide; glycerol

1 Theory

The polymerase chain reaction (PCR) method invented by Mullis, et al (Mullis, 1987) greatly enhanced the biologists' capacity to isolate, characterize, and produce large quantities of DNA *in vitro*. Since its emergence, no one has ever doubted the effectiveness of the procedures recommended by Mullis, especially when the GC content of amplified DNA sequence is between 40% - 60%. While a fact continues to bother labs and researchers having PCR needs: the standard procedures are very hard to produce products when the template is rich with GC. The high GC content of human leucocyte antigen-B (HLA-B) (Robinson, 2003), ApoE (Jacobsen, 2002), p16 (Jung, 2002), prostate-specific membrane antigen (PSM) gene (Henke, 1997), even including HLA-A, C, etc., which is among 65% - 70% or higher, often leads to low yields of the target DNA sequence and the accompanying amplification of undesired nonspecific bands, and keeps to be a problem in PCR amplifications.

As GC base pair has 3 hydrogen bonds while AT pair has only 2 bonds, so GC pair exhibits stronger base-base interactions, leading to stable self-complementary superstructures such as hairpin-loop and dimer, producing regions with higher melting temperatures, and making the DNA strand harder to be opened and amplified (Benita, 2003; Weissensteiner, 1996). To tackle such problems, additives such as dimethylsulfoxide (DMSO), formamide, glycerol and betaine are often reported to be used in such amplifications due to their ability of reducing the effect of hydrogen bonding, destabilizing the secondary structure, and enhancing the specificity of the amplification reaction (Weissensteiner, 1996; Chakrabarti, 2002; Chakrabarti, 2001). However, until recently, no systematic

comparison study exists about the effect of each additive. Therefore, we performed an evaluation of the effect of these additives with HLA-B gene as a model and we were aimed at finding clues about which additive is more powerful than others.

Weissensteiner et al showed that there are two key factors in influencing the amplification outcomes when additives are used (Weissensteiner, 1996): one is the concentration of monovalent cations in the reaction mixture, such as K^+, NH_4^+, which will increase the stability of double-stranded DNA (dsDNA), thus make the GC-rich region more stable; the other is the concentration of additives like betaine, which will lower the stability of dsDNA and thus make the GC-rich region less stable, easier to be opened and more ready for the primers to bind and extend. So in our study we lowered the concentration of KCl to 0 mM to observe the full potential of each additive and to avoid any counteractions from the cations.

2 Materials and Methods

2.1 Materials

2.1.1 Blood samples

2 ml peripheral vein blood (from each of 20 paternity testing personnel, who belong to the Han nationality in the northeast China).

2.1.2 Reagents

dNTP (Takara Co., Shiga, Japan); rTaq DNA polymerase (Sino-American Biotechnology Company, Luoyang, China); betaine (Weifang Sunwin Chemicals, Shandong, China); DMSO (Sigma, USA); formamide (Sigma); glycerol (Shenyang Chemicals, Shenyang, China); primers pairs for HLA-B gene (Cao, 1999): forward 5′-GGG AGG AGC GAG GGG ACC G/CCA G-3′, reverse 5′-GGA GGC CAT CCC CGG CGA CCT AT-3′ (Sangon Company, Shanghai, China); primers pairs for CCR5 (chemokine C-C motif receptor 5) gene (Balotta, 1997): forward 5′-GAA GGT CTT CAT TAC ACC TG-3′, reverse 5′-AGA ATT CCT GGA AGG TGT TC-3′; φX174-*Hae* Ⅲ Digest DNA Marker (Takara).

2.1.3 Apparatus

UV-310 Ultraviolet Spectrophotometer (Pye-Unicam/Spectronic, UK); UNO Ⅱ thermocycler (Biometra, Germany); Mini-PROTEAN 3 Electrophoresis System (Bio-Rad, CA, USA); 377 ABI PRISM™ DNA Sequencer (Applied Biosystems, CA, USA).

2.2 Methods

2.2.1 DNA preparation

Genomic DNA was prepared by Phenol/Chloroform extraction and dissolved in 120 μl Tris/EDTA solution. The OD260:OD280 ratio was adjusted to near 1.8.

2.2.2 PCR reaction

Both the commercial 10× reaction buffer and a self-made KCl-free 10× reaction buffer were being used, while the latter contains all the ingredients except KCl, e. g., including 100 mM Tris-HCl, 1.0% Triton X-100 and 15 mM $MgCl_2$. The PCR was carried out in a total volume of 20 μl on the UNO Ⅱ thermocycler. All PCR mixtures contained the following at a final concentration: 0.2 mM of each dNTP, 1 unit rTaq polymerase, 0.25 μM each of HLA-B-specific forward and reverse primers, approximately 1μg DNA template, and with or without additives. The forward primer was located in HLA-B intron 1 and the reverse primer was located in intron 3. Amplification parameters consisted of denaturation for 5 minutes at 96℃, followed by 35 cycles of 22 seconds at 94℃, 50 seconds at 65℃, 30 seconds at 72℃ and then a final extension of 10 minutes at 72℃ (Cao, 1999).

Additives and KCl were used with four combinations: KCl-contained, no additives; KCl-free, no additives; KCl-contained, with additives; and KCl-free, with additives. Each sample was amplified without additive and with each one of the 4 following additives: betaine, DMSO, formamide, glycerol. Glycerol was diluted to 50% to decrease the viscosity and facilitate the transfer. A concentration titration was used to determine which concentration is the optimal. The titration for betaine was 0.3 M, 0.6 M, 0.9 M, 1.5 M, while the gradient for DMSO, formamide and glycerol was 0%, 5%, 10% and 15%. Positive control was set up in a separate amplification with CCR5 gene, using the same dNTP, rTaq polymerase and DNA except two CCR5-specific primers. The cycling conditions were as follows: a 3-minute 94℃ pre-denaturation; 35 cycles of 30-second denaturation at 94℃, 30-second annealing at 56℃, 30-second extension at 72℃; and a final extension at 72℃ for 10 minutes (Balotta, 1997). Both KCl-contained buffer and KCl-free buffer were separately used. Negative control was set up with no template DNA added.

2.2.3 Polyacrylamide gel electrophoresis (PAGE) and silver staining

PCR products were analyzed by PAGE. Polyacrylamide gels ($C = 6\%$, $T = 5\%$) were prepared. After gel pre-run, the products as well as a lane of φX174-*Hae* Ⅲ Digest DNA Marker were loaded and a constant current was set to separate the PCR products. After electrophoresis, the gel was fixed with 10% acetic acid for 20 minutes, and then was put into 0.1% $AgNO_3$ solution (formaldehyde contained) for 30 minutes with gen-

tle shaking, and then the gel was developed in a 4% Na_2CO_3 solution (formaldehyde contained).

2.2.4 Products sequencing

Successful amplified products were sent to Takara Biotech Company and were sequenced with a 377 ABI PRISM™ DNA Sequencer.

2.2.5 Statistical analysis

A chi-square test was performed with SAS (Version 6.12) to find out whether there is a difference between these additives.

3 Results

3.1 Confirmation of successful amplification

Successful amplification of HLA-B gene will have a band at the 943 bp position. Successful amplification of the positive control, CCR5 gene, will produce a band at 276 bp. No PCR products were generated in our negative controls.

3.2 Amplification effects of KCl and additives

In all the 20 samples, CCR5 gene was amplified successfully with the KCl-contained or KCl-free PCR buffer, while the KCl-contained buffer generated more yields at 276 bp position as expected. Either with KCl-contained or KCl-free buffer, fewer yields were found when additives were used.

To the HLA-B amplifications, KCl-contained buffer produced only non-specific bands, KCl-free buffer with additives generated band at 943 bp position as expected. Either with or without additives, a KCl-contained buffer was able to produce more bands than a KCl-free buffer. But all the bands generated by the KCl-contained buffer were non-specific, not at the 943 bp position and usually smaller than 943 bp, while with the KCl-free buffer combining one of the additives, a single band of the expected size at 943 bp position was obtained. Different concentrations of each additive had different successful amplification rates (Figure 1). For details, see Table 1.

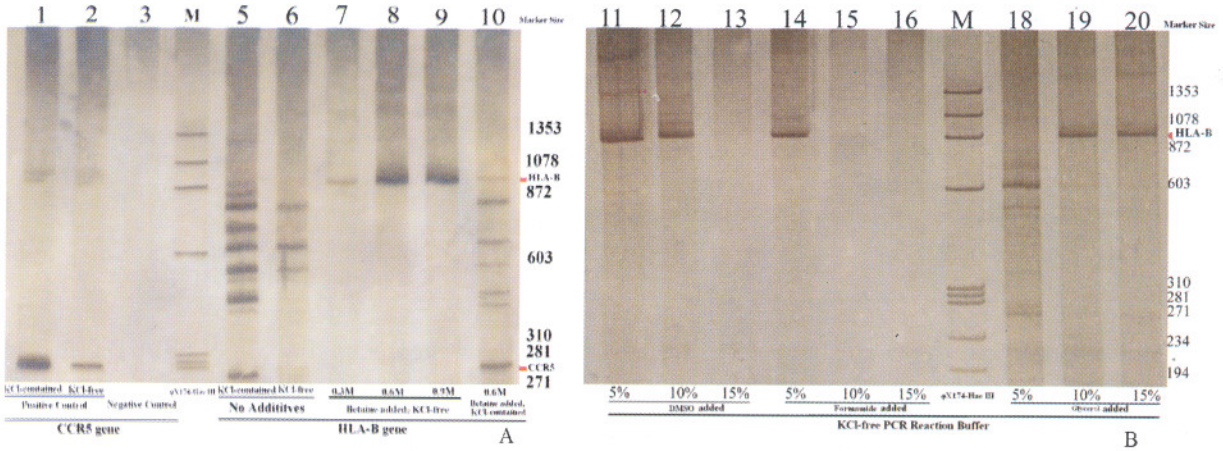

Figure 1. Amplification effects of KCl and the 4 additives on Sample 3. Lane 2 showed that without KCl in the PCR buffer, the amount of the CCR5 decreased greatly. Lanes 8, 9, 11, 12, 14, 19 and 20 showed that with a KCl-free buffer and a proper additive, HLA-B was amplified successfully.

3.3 Sequencing results

The products of successful amplification were reported to have HLA-B intron 1, exon 2, intron 2, exon 3 and partial intron 3 sequences, and were in accordance with the HLA-B sequences of GenBank (Takara sequencing No: SYS587).

3.4 Statistical analysis

Significant difference was observed among these 4 additives. When 5%, 10% and 15% concentrations were used, the overall successful rate of formamide was lower than that of DMSO or formanide or betaine.

4 Discussion

HLA typing is one of the most widely involved techniques in clinical applications such as liver transplantation, the diagnosis of axial spondyloarthritis (AS) (Rudwaleit, 2004) or insulin-dependent diabetes mellitus (IDDM) (Gillespie, 2004). Reliable HLA gene typing depends on the effective amplification of HLA genes. But the HLA-B gene sequence is rich with GC, which easily forms secondary structures such as hairpins, dimers. These will make the Taq polymerases (especially sequenases) falling off from the templates, causing premature termination of PCR or sequencing reactions (Baskaran, 1996) and leading to low yields insufficient for further analysis. So GC content is very critical in determining the amplification outcomes. Even more recently, Benita Y et al

found that the regionalized GC content is a good predictor of PCR success across multiple templates (Benita, 2003). However, this GC-content-caused problem is often overlooked when compared with those efforts put into primer design.

High GC content sequences widely exist among the whole genome. A common approach to the optimization of such GC-rich amplification reactions is the addition of small quantities of certain organic chemicals, such as DMSO, betaine, glycerol and formamide, etc., to the reaction mixture (Jung, 2002; Henke, 1997; Weissensteiner, 1996; Chakrabarti, 2002; Chakrabarti, 2001; Papp, 1996). These additives are minim but so effective that they break the GC hydrogen bonds, destabilize the GC-rich region, open the hairpin-loops, lower the melting temperature and greatly enhance the amplification yields and fidelity.

Table 1. HLA-B amplification results of applying different PCR reaction buffer and different additives

PCR Buffer Types	Additives	Total Sample	Successful Amplifications	Rate
Standard buffer (KCl contained)	No	20	0 (except many non-specific bands)	0%
KCl-free buffer	No	20	0 (except few non-specific bands)	0%
KCl-free buffer	0.3 M Betaine	20	15	75%
	0.6 M Betaine	20	20	100%
	0.9 M Betaine	20	16	80%
	1.2 M Betaine	20	10	80%
KCl-free buffer	5% DMSO	20	17	85%
	10% DMSO	20	18	90%
	15% DMSO	20	0	0%
KCl-free buffer	5% Formamide	20	16	80%
	10% Formamide	20	7	35%
	15% Formamide	20	0	0%
KCl-free buffer	5% Glycerol	20	9	45%
	10% Glycerol	20	18	90%
	15% Glycerol	20	17	85%
	20% Glycerol	20	10	50%
KCl-contained buffer	Each additives	5	Non-specific: high amount; Specific: trace amount	0

But among those easy available ones as mentioned above, the optimal concentrations were reported to be in a wide range. For example, most researchers reported the effective concentration of formamide is between 5% – 15%, and that of glycerol is between 5% – 20%, while the wide range has made it very hard to choose a concrete concentration to begin. Moreover, so far, there has not been a systematic comparison once performed to demonstrate which additive has the most effective and consistent amplification-enhancing effect. So in our study, we used 4 easily accessible reagents to find out which concentration was optimal and which additive had the best enhancing effect. We collected 20 DNA samples and amplified them with four combinations: with or without KCl, combining with or without additives. Our results showed that 0.6 M for betaine, 10% for DMSO, 5% for formamide and 10% for glycerol were their optimal concentration, respectively. Our results demonstrated that formamide was less powerful than the other 3 additives. Our results also indicated that the use of 0.6 M betaine as a destabilizing additive yielded consistent amplification of HLA-B gene. In fact, betaine has more advantages over other additives: it is not as viscid as glycerol, which is hard to be transferred; it is not as inhibitive to Taq polymerase as formamide, which will require more enzymes when a higher concentration of formamide is applied. Furthermore, betaine is compatible with various downstream procedures such as product-purification, sequencing, etc. Other researchers demonstrated that betaine was able to amplify 84% GC sequences while other additives were not (Papp, 1996). Henke W et al also reported that betaine was able to amplify prostate-specific membrane antigen (PSM) mRNA (66% GC) while both DMSO and glycerol not (Henke, 1997).

Another feature of our research was the comparison of applying a KCl-contained and a KCl-free PCR reaction mixture except the addition of additives. We found that a KCl-contained buffer was able to improve the yields greatly when we were amplifying a medium GC content gene, CCR5. Even when KCl-contained buffer was used to amplify the high GC sequences, it still was able to

produce discernible bands. However, in the latter case, all the bands were non-specific, and there were no presence of the specific bands at 943 bp as expected, as shown in Figure 1. Only when the GC content was medium, the KCl-contained buffer was specific and effective. In contrast, the KCl-free buffer showed a synergistic effect with additives. As Weissensteiner T et al pointed out, without KCl, the dsDNA in the solution was much more unstable (Weissensteiner, 1996). A KCl-free buffer helped the additives destabilize the superstructure, strengthened the effects of additives, and thus enhanced specificity and improved yields. While there are many other attempts of combining two of the many enhancers to get better results, we suggest the combining use of betaine and the KCl-free reaction buffer should be more effective. The sequencing result demonstrated that such a strategy could be quite helpful in cases of difficult PCR amplification. We used HLA-B gene to demonstrate a series of conditions that may be used to optimize the amplification of other high-GC templates.

5 Conclusion

To find out the most optimal amplification conditions for high GC DNA template, we evaluated the effects of 4 additives Betaine, DMSO, formamide and glycerol on HLA-B amplification at different additive concentrations under the settings of KCl-contained or KCl-free reaction buffer. We found that 0.6 M for betaine, 10% for DMSO, 5% for formamide and 10% for glycerol were their optimal concentrations, respectively, and the 0.6 M Betaine had the highest successful rate. We also found that KCll greatly improved the amplification yields when the template GC content was moderate, while zero KCl could improve the yields when the template GC content was high. We thus recommended a 0.6 M Betaine and KCl-free buffer as the first choice in high GC amplifications.

Acknowledgments

We thank Dr. Thomas Weissensteiner for his valuable suggestions; we thank Dr. Guangfei Dong for his academic help on statistics analysis.

Correspondence to:
Zhaoshu Zeng
Department of Legal Medicine
School of Basic Medicine
Zhengzhou University
Zhengzhou, Henan 450052, China
Telephone: 86-371-6665-8173 (Office)
Email: zengzhaos@yahoo.com.cn
or zs_zeng@yahoo.com

References

1. Balotta C, Bagnarelli P, Violin M, et al. Homozygous delta 32 deletion of the CCR-5 chemokine receptor gene in an HIV-1-infected patient. AIDS 1997; 11(10): F67-71.
2. Baskaran N, Kandpal RP, Bhargava AK, et al. Uniform amplification of a mixture of deoxyribonucleic acids with varying GC content. Genome Res 1996; 6: 633-8.
3. Benita Y, Oosting RS, Lok MC, et al. Regionalized GC content of template DNA as a predictor of PCR success. Nucleic Acids Res 2003; 31(16): e99.
4. Cao K, Chopek M, Fernandez-Vina MA. High and intermediate resolution DNA typing systems for class I HLA-A, B, C genes by hybridization with sequence-specific oligonucleotide probes (SSOP). Rev Immunogenet 1999; 1(2): 177-208.
5. Chakrabarti R, Schutt CE. The enhancement of PCR amplification by low molecular weight amides. Nucleic Acids Res 2001; 29(11): 2377-81.
6. Gillespie KM, Bain SC, Barnett AH, et al. The rising incidence of childhood type 1 diabetes and reduced contribution of high-risk HLA haplotypes. Lancet 2004; 364 (9446): 1699-700.
7. Henke W, Herdel K, Jung K, et al. Betaine improves the PCR amplification of GC-rich DNA sequences. Nucleic Acids Res 1997; 25(19): 3957-8.
8. Jacobsen N, Bentzen J, Meldgaard M, et al. LNA-enhanced detection of single nucleotide polymorphisms in the apolipoprotein E. Nucleic Acids Res 2002; 30(19): e100.
9. Jung A, Ruckert S, Frank P, et al. 7-Deaza-2′-deoxyguanosine allows PCR and sequencing reactions from CpG islands. Mol Pathol 2002; 55(1): 55-7.
10. Mullis KB, Faloona FA. Specific synthesis of DNA *in vitro* via a polymerase-catalyzed chain reaction. Methods Enzymol 1987; 155: 335-50.
11. Papp AC, Snyder PJ, Sedra M, et al. Strategies for amplification of trinucleotide repeats: optimization of fragile X and androgen receptor PCR. Mol Diagn 1996; 1(1): 59-64.
12. Robinson J, Waller MJ, Parham P, et al. IMGT/HLA and IMGT/MHC: sequence databases for the study of the major histocompatibility complex. Nucleic Acids Research 2003; 31: 311-4.
13. Rudwaleit M, van der Heijde D, Khan MA, et al. How to diagnose axial spondyloarthritis early. Ann Rheum Dis 2004; 63(5): 535-43.
14. Weissensteiner T, Lanchbury JS. Strategy for controlling preferential amplification and avoiding false negatives in PCR typing. Biotechniques 1996; 21(6): 1102-8.

Received September 5, 2005

Cloning and Sequencing of the Tumor Antigen MAGE-12 Gene

Guojun Zhang[1], Guoqiang Zhao[2], Huaqi Wang[1], Shijie Zhang[2], Xiaohui Xia[1]

1. Department of Respiratory, the First Affiliated Hospital of Zhengzhou University, Zhengzhou University, Zhengzhou, Henan 450052, China

2. Department of Microbiology and Immunology, Basic Medical College, Zhengzhou University, Zhengzhou, Henan 450052, China

Abstract: Objective. To clone the MAGE-12 gene, preparing for researching its biological effects on MAGE-12 positive malignant tumors. **Methods.** mRNA was extracted from human lung cancer specimen. MAGE-12 gene was amplified by reverse transcriptase polymerase chain reaction(RT-PCR) and was identified by enzyme cutting with Pvu Ⅱ. The PCR fragment was inserted into pGEM-T easy plasmid, and then was transformed into JM109. After the selection of blue/white screening, the primers designed with T7/SP6 sequence of pGEM-T easy plasmid were applied to identify the recombinant. Further more, DNA sequence of the recombinant was analyzed. **Results.** The length of the DNA fragment RT-PCR amplified by mRNA was 944 base pairs. which was conformed by enzyme Pvu Ⅱ cutting identification. The correctness of linking between MAGE-12 and pGEM-T easy was verified through selection of blue/white screening and identified by T7/SP6 primers, and the sequences of DNA fragment were homology with corresponding sequences published in GenBank, which indicated that the target gene had been inserted into pGEM-T easy successfully. **Conclusion.** The MAGE-12 gene was cloned successfully, which made the foundation of biological treatment by using MAGE-12 gene. [Life Science Journal. 2006;3(1):72-74] (ISSN: 1097-8135).

Keywords: MAGE-12; tumor antigen; gene

1 Introduction

Melanoma antigen-1(MAGE-1) gene, expressed by malignant melanoma, was first found by van der Bruggen et al with cloning technique in 1991. And it's encoding antigen MZ2-E, expressed in variant degree not only in melanoma but also in other tumors, however, never expressed in normal tissue(except testicle and placenta). The finding of tumor specific antigen established a strong base for the active specific immunotherapy of human tumor vaccine. Tumor specific antigen, as a basis for human tumor specific immunotheraphy, should be paid more attention nowadays especially when biotheraphy of tumor developing is so fast. From studying and analyzing, the authors cloned MAGE-12 gene successfully, and which made the foundation of biological effect in malignant tumor and producing tumor gene vaccine by investigating MAGE-12.

2 Materials and Methods

2.1 Materials

All specimen of lung cancer tissue were from the First Affiliated Hospital of Zhengzhou University, plasmid vector pGEM-T easy, restriction enzyme Pvu Ⅱ, AMV-reverse transcriptase, Taq DNA polymerase 6-mers random primer, T4 DAN joinase were Promega products. TRIZOL reagent was Invitrogen product; gelatin of Wharton reclaiming kit was V-Gene product; isopropy-β-D-thiogalactoside (ITPG), 5-bromo-4-chloro-3-indolyl-β-D-galactoside(X-Gal) were Takara products; *E. coli*. JM109 were from our department's preservation.

2.2 Methods

2.2.1 The design and synthesis of primer

According to MAGE-12 gene sequences published in GenBank, designed the primer. Ecto-supra primer M1: 5′-GCACTAGCTCCTGCCCACAC-3′; ecto-infra primer M2: 5′-TGGGCCTCATGTCACACGAC-3′; ento-supra primer M3: 5′-ACTCGAGGCCACCATGCCACTTGAGCAGAGGAG-3′; partake Xho Ⅰ enzyme cutting site and translation initiation codon; ento-infra primer M4: 5′-TGGTA CCCTCTTCCCCCTCTCTAAAAG-3′ partake Kpn Ⅰ enzyme cutting site. According to the T7, SP6 promoter sequence, which are on both sides of multiple clone site in plasmid pGEM-T easy, design the consensus primer T7: 5′-TAATACGACTCACTATAGGGAGA-3′; SP6: 5′-CATACGTATTAGGTGACACTA TAG-3′. All primers we used were synthetized by Shanghai Sangon

Biotechnology Co., Ltd.

2.2.2 Extraction of total RNA

Put lung cancer tissue specimen just sliced into grinder and levigate it, add 1 ml TRIZOL reagent, misce bene and transfer the mixture into 1.5 ml centrifuge tube; standing at room temperature for 5 minutes to make sure ribosome lyzed completely; add chloroform of 0.2 ml, freezing centrifuged with 12000 rpm at 4℃ for 5 minutes; shift the supernatant into another centrifuge tube and add dimethylcarbinol of 0.5 ml; misce bene lightly, freezing centrifuged with 12000 rpm at 4℃ for 10 minutes; dislodge supernanant and add 75% ethyl alocohol of 1 ml; freezing centrifuged with 7,500 rpm at 4℃ for 5 minutes; dislodge supernanant; air drying at room temperature for 10 minutes; add DEPC liquor of 30 μl, put into bain-marie at 55℃ for 10 minutes. Then get total RNA and reverse transcribe target gene fragment immediately.

2.2.3 RT-PCR and amplification of target gene fragment

Preparation of cDNA: reaction system(30 μl): 5 × Buffer 6 μl, 4 × dNTP(2.5 mmol/l dNTP) 2 μl, 6-mers random primer 1 μl, AMV 1 μl, template(the total RNA we extracted) 5 μl, DEPC liquor 15 μl; reaction condition: aqueous bath at 42℃ for 1 hour, aqueous bath at 72℃ for 5 minutes to inactivate enzyme AMV. Amplification of target gene with PCR: reaction system of the first amplication: 10 × Buffer 3 μl, 4 × dNTP 2 μl, M1 0.5 μl, M2 0.5 μl, Taq DNA polymerase 0.5 μl, Mini-H_2O 18.5 μl, cDNA 5 μl; reaction condition: predict apomorphosis at 94℃ is 5 minutes, apomorphosis at 94℃ for 45 seconds, renaturation at 55℃ for 45 seconds, elongation at 72℃ for 60 seconds, 35 reaction circulations, and elongation at 72℃ for 5 minutes the last time. Reaction system of the second amplification: 10 × Buffer 3 μl, 4 × dNTP 2 μl, M3 0.5 μl, M4 0.5 μl, Taq DNA polymerase 0.5 μl, Mini-H_2O 18.5 μl, product of the first amplication 5μl; reaction condition: predict apomorphosis at 94℃ is 5 minutes, apomorphosis at 94℃ for 45 seconds, renaturation at 55℃ for 45 seconds, elongation at 72℃ for 60 seconds, 35 reaction circulations, and elongation at 72℃ for 5 minutes the last time. Take suction of amplified sample for 5 μl and identify with 1.5% agarose gel electrophoresis, preserve the product of the second amplification into frige at −20℃.

2.2.4 Verification of enzyme Pvu Ⅱ cutting target gene and gelatin of Wharton reclaiming target gene

Reaction system: Mini-H_2O 6.5 μl, target gene product of ultimum amplification 1.5 μl, 10 × Buffer 1 μl, Pvu Ⅱ 1 μl; reaction condition: aqueous bath at 37℃ for 2 hours, aqueous bath at 72℃ for 5 minutes to inactivate enzyme Pvu Ⅱ. Product and target gene, from enzyme cutting, which were identified with 1.5% agarose gel electrophoresis. Then reclaiming product of the second PCR amplification with V-Gene gelatin reclaiming kit.

2.2.5 Construction and sequence analysis of human MAGE-12 gene cloning vector

Ligate MAGE-12 gene that gelatin reclaimed with vector Pgem-T easy, The ligation get through the night at 4℃, then have the ligation transfected into *E. coli*. JM109. After the selection of blue/white screening, select the white colony, then amplified by polymerase chain reaction(PCR). After identifing the positive cloning, sent the product for PCR to sequence analysis.

3 Results

3.1 The product of PCR and identification of enzyme cutting

Taking the cDNA as template, M1, M2 as the primer, amplified by RT-PCR. Electrophorese the product with 1.5% agarose gel. The stripe we get is located at about 1000 bp contrasting with DNA marker(Figure. 1), this is close to our anticipation. Electrophorese the product digested by PVU Ⅱ with 1.5% agarose gel, the stripe is at about 500 bp contrasting with DNA marker(Figure 2). In the abstract, PVU Ⅱ enzyme cutting site of the MAGE-12 gene is at 3434 bp, after the enzyme cutting, the lengths of the gene fragment are 474bp and 470 bp. The result is consistent with the abstract. The product amplified by RT-PCR is our anticipating gene.

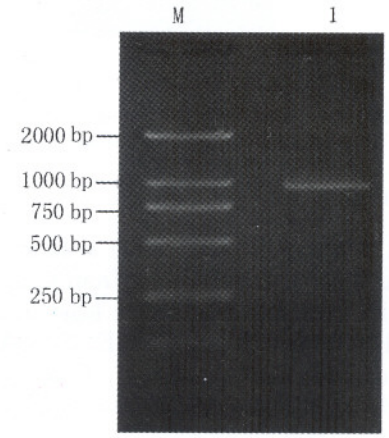

Figure 1. The product of RT-PCR(1.5% agarose gel electrophoresis). Lane M: DNA marker; Lane 1: the product of PCR

3.2 Cloning and analysis of the target gene

After reclaiming target gene with gelatin, link the MAGE-12 gene with the vector pGEM-T easy.

Transfect into E. coli. JM109, select 4 stochastic bacteria *colanys* to identified by PCR. The amplified gene fragments are about 1000 bp contrasting with DNA marker the stripe locating at about 100bp is the empty plasmid colonies (Figure 3). The result is consistent with the abstract. This suggests that we have cloned the MAGE-12 gene successfully.

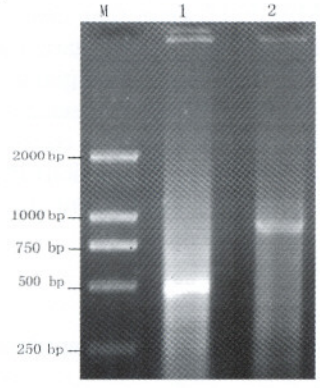

Figure 2. The result of identified by PVU Ⅱ (1.5% agarose gel electrophoresis). Lane M: DNA marker; Lane 1: product digested by PVU Ⅱ; Lane 2: MAGE-12 gene

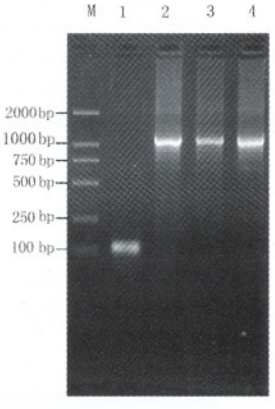

Figure 3. Identification of recombinant vector PGEM-T easy-MAGE-12
Lane M: DNA marker; Lane 1: amplified product of negative clone; Lane 2~4: amplified product of positive clones.

4 Discussion

In 1991, van der Bruggen et al found the first melanoma antigen(MAGE-1). From then on, people found that MAGE family at least included six sub-family: MAGE-A, B, C, D, E, F. MAGE-A is constituted by 12 genes. At first, these genes were named MAGE-1 ~ MAGE-12, and later some people suggested that these genes were called MAGE-A1 ~ MAGE-A12. The MAGE-12 gene was found by Ding M et al in DM150 melanoma cell line, which was homology with MAGE-2, MAGE-3. These genes are all belong to tumor special antigen (TSA), which have MHC-Ⅰ restriction and are mainly expressed in malignancy tumor, and never expressed in normal tissues except testicle and placenta. Therefore, MAGE-12 is a perfect target antigen in anti-tumor immunity. Yanqiu Li and Yuzhang Wu doped out the MAGE-12 epitope identified by CTL, which was restricted by HLA-A2, using the immunology methods. The CTL identified epitod is located at about 271-279 (FLWGPRALV) remnant-radix. In our country, the literature about the MAGE-12 gene in human lung cancer was rare.

The authors cloned the MAGE-12 gene successfully using the reverse transcriptase polymerase chain reaction (RT-PCR), and constructed pGEM-T easy-MAGE-12 cloning vector. After the sequence analysis, the sequences of DNA fragment were homology with corresponding sequences published in GenBank. The authors constructed the pGEM-T easy-MAGE-12 cloning vector, and made the foundation for constructing the eukaryotic expression vector and developing the MAGE-12 gene vaccine.

Correspondence to:
Guojun Zhang
Department of Respiratory
The First Affiliated Hospital
Zhengzhou University, Zhengzhou, Henan 450052, China
Email: zgj@zzu.edu.cn

References

1. DePlaen E, Arden K, Traversari C, et al. Structure, chromosomal localization, and expression of 12 genes of the MAGE family. Immunogenetics 1994;40(5):360-9.
2. Ding M, Beck RJ, Keller CJ, et al. cloning and analysis of MAGE-1 related genes. Biochem Biophys Res Commun 1994;202(1):549-55.
3. Itoh K, Hayashi A, Nakao M, et al. Human tumor rejection antigens MAGE. J Biochem (Tokyo) 1996 Mar;119(3):385-90. Review.
4. Li YQ, Wu YZ, Jia ZC, et al. Predication of Secondary Structures and epitopes of tumor antigen MAGE-12. Immunological Journal 2001;17(4):268-270. (in Chinese).
5. Lucas S, DeSmet C, Arden KC, et al. Identification of a new MAGE gene with tumor-specific expression by representational difference analysis. Cancer Res 1998 Feb 15;58(4):743-52.
6. Lurquin C, DeSmet C, Brasseur F, et al. Genomics, two members of the human MAGEB gene family located in Xp21.3 are expressed in tumors of various histological origins. Genomics 1997 Dec 15;46(3):397-408.
7. Muscatelli F, Walker AP, DePlaen E, et al. Isolation and characterization of a MAGE gene family in the Xp21.3 region. Proc Natl Acad Sci U S A 1995 23;92(11):4987-91.
8. van der Bruggen P, Traversari C, Chomez P, et al. A gene encoding an antigen recognized by cytolytic T lymphocytes on a human melanoma. Science 1991;254(5038):1643-7.

Received October 28, 2005

Recovering Extremely Low Frequency Signal from the Signal-Dependent Noise Background

Hsien Chiao Teng[1], Shen Cherng[2]

1. Department of Electrical Engineering, Chinese Military Academy, Fengshan, Kaohsiung, Taiwan 830, ROC

2. Department of Electrical Engineering, Chengshiu University, Niaosong, Kaohsiung, Taiwan 833, ROC

Abstract: We developed a signal dependent noise tensor, which can be used to describe the fluctuated geomagnetic field coupled with Extremely Low Frequency (ELF) signals for our further biological signal processing study. In order to isolate the coupled ELF signals from the signal dependent noise, we introduced Quantization (QT) decoding method to discrete the noise and recover the coupled signals from the background. The signal to noise ratio of the coupling ELF can be amplified by QT in the power density spectrum (PDS). [Life Science Journal. 2006;3(1):75-77] (ISSN: 1097-8135).

Keywords: Extremely Low Frequency (ELF); noise; power density spectrum (PDS); signal

1 Introduction

The signal dependent noise can be presented as a noise tensor n_{ij} at time t_{ij}, in which index indicates the ith sample at energy level j. The signal can be shown as s_{ij}. Power density spectrum (PDS) analysis for tensor $n_{ij} \oplus s_{ij}$ can be used to identify the coupled signalsin s_{ij} in n_{ij}. The intrinsic coupling oscillation can be captured by probe and converted to electrical voltages shown in oscilloscope.

2 Theory and Methods

Set an AC ELF signal as input to the background, the output can be transformed to electrical voltages shown to oscilloscope. By using HP Benchlink, we collect the output data and transform it to Microsoft Excel as text files. Matlab and Fortran programs were performed to analyze the data and get PDS. Figure 1 illustrates the flow chart of the QT process.

Consider the data output sequence $x_{ij} = s_{ij} \oplus n_{ij}$, where x_{ij} indicate the jth element in ith ensample.

Step 1: Get x_{ij}

Step 2: Set QT value from v_1 to v_6, where $v_1 > v_2 > \cdots > v_6$ for six QT levels

Step 3: Compute x_{ij}, the average value of x_{ij}

Step 4: If $x_{ij} > \bar{x}_{ij}$, set $m_h = x_{ij}$, a high threshold value m_h should be defined.

If $x_{ij} < \bar{x}_{ij}$, set $m_1 = x_{ij}$, a low threshold value m_1 should be defined.

If $x_{ij} > m_h$ set $m_{hh} = x_{ij}$, a second high threshold m_{hh} should be defined.

Step 5: Set $\bar{x}_{ij} = m_{hh}$ if $m < \bar{x}_{ij} < m_h$

$\bar{x}_{ij} = m_{1h}$, if $m_l < \bar{x}_{ij} < m_h$

$\bar{x}_{ij} = m_{11}$, if $\bar{x}_{ij} << m_1$, where

$m_{hh} > m_h > m_{h1} > m > m_{1h} > m_1 > m_{11}$.

Step 6: if $x_{ij} > m_{hh}$, set $\bar{x}_{ij} = v_1$;

if $m_{1h} < x_{ij} < m_{hh}$, set $x_{ij} = v_2$;

if $m_{h1} < x_{ij} < m_h$, set $\bar{x}_{ij} = v_3$;

if $m < x_{ij} < m_{h1}$, set $x_{ij} = v_4$;

if $m_{1h} < x_{ij} < m$, set $x_{ij} = v_5$;

if $m_1 < x_{ij} < m_{1h}$, set $x_{ij} = v_6$;

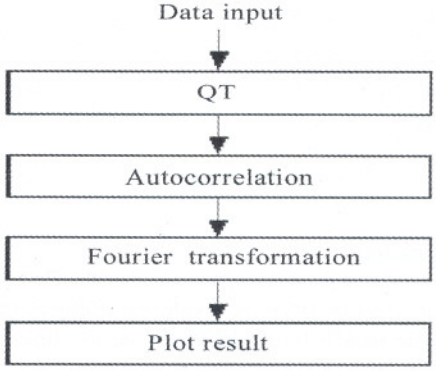

Figure 1. The flow chart of the QT

It is defined amplitude signal to noise ratio as $\mathrm{ASNR}=\frac{A_s}{A_n}$, where A_s is the amplitude of the coupled ELF signal and A_n is the amplitude of the noise. In contrast, $\mathrm{SNR}=\frac{P_s}{P_n}$, where P_s is the power of the output ELF signal calculated from PDS and P_n is the power of the noise. Noise can be defined as all unpredictable signals in PDS. Since both ASNR and SNR can be calculated, the plot of ASNR versus SNR produces a function curve showing the correlation between input amplitude and output power. Even through noise may have its own characteristic, we can calibrate the function curve with the help of adjusting trial signal's amplitude to control the power difference by QT analysis. For instance, using a data sequence to simulate a sample function consisting of 2000 elements including a 15 Hz sinusoid signal, $x_{ij}(t)=s_{ij}(t)+k\times n_{ij}(t)$, label index i is from 1 to 2000 for this sequence. The dimension of the noise tensor is $2000\times j$. For simplicity, take $j=1$, the power spectrum can be simply calculated. Note that the identified ELF signal is supposed being occurred at 15 Hz. The frequency component of power density spectrum of the noise being illustrated will depend upon the characteristic of n_{ij}.

In addition, Figures 2 to 5 can demonstrate the magnetic fluctuation very near the cell layer on the patch substrate.

3 Results

The power density spectrum calculation result is illustrated in Table 1. We are not able to identify ELF 15 Hz without QT if its signal to noise ratio (S/N) is lower than 0.015.

Table 1. The power density spectrum calculation result (−: not able to identify ELF 15Hz, however; +: able to identify ELF 15 Hz)

ASNR	15 Hz	QT	S/N Ratio
1.0	+	+	1.5
0.5	+	+	0.37
0.1	−	+	0.015
0.05	−	+	0.004
0.01	−	+	0.0001

4 Discussion

Our results provide evidence suggesting that QT is able to affect the PDS, which is linked with the energy modulation within the noise and shows the power that the noise could sense. The purpose of this report is to provide a new method to recognize the ELF buried in signal dependent background noise.

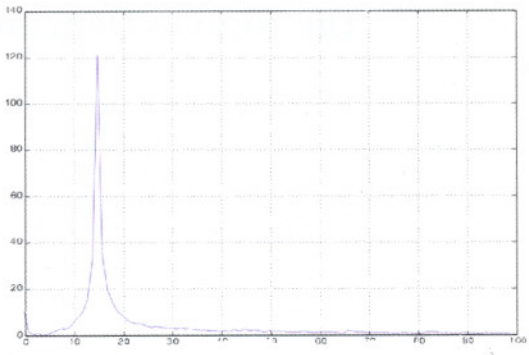

Figure 2. If $S/N=1.5$, the ELF signal component at 15 H_z is shown

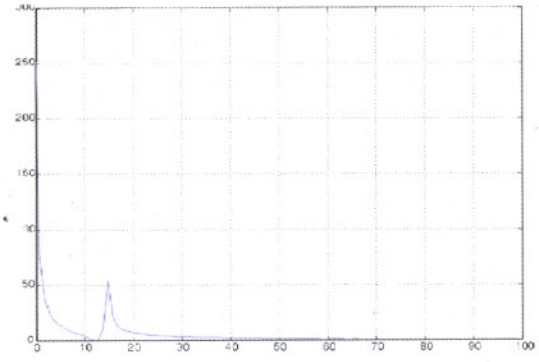

Figure 3. If $S/N=0.37$, the ELF component signal at 15 H_z still can be shown

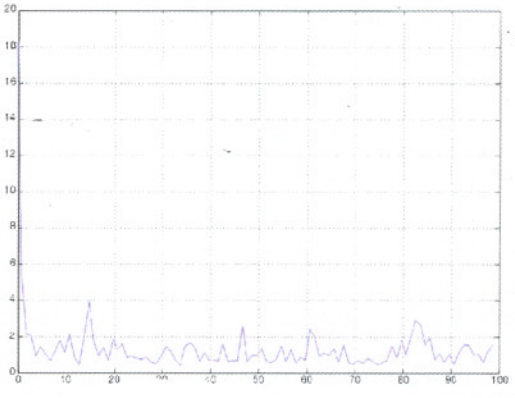

Figure 4. If $S/N<0.37$, we are not able to identify the ELF signal at 15 Hz

5 Conclusion

The noise sensitivity to the ELF signal has been studied for years. QT can help to recognize ELF and increase both ASNR and the SNR providing a function curve to characterize the signal dependent noise. By using this function curve, we

can find the best estimate signal-to-noise ratio of the coupled ELF. The remaining question is how can we find the best combination of the weights of QT in experiments. Fuzzy and neuronet analysis may help for further noise tensor characteristic studies.

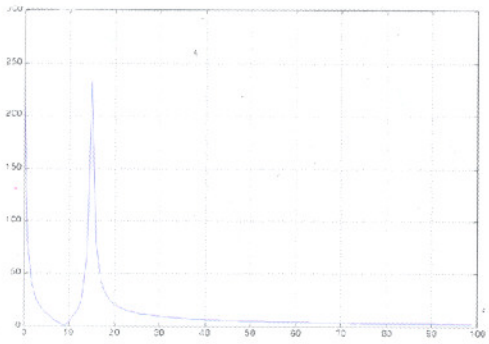

Figure 5. ELF signal at 15 H_z is identified by QT when $0.0001 < S/N < 0.3$

Correspondence to:

Hsien-Chiao Teng
Department of Electrical Engineering
Chinese Military Academy
Fengshan, Kaohsiung
Taiwan 830, Republic of China
Telephone: 886-7747-9510 ext 134
Email: scteng@cc.cma.edu.tw

References

1. Galvanovskis J, Sandblom J. Amplification of electromagnetic signals by ion channels. Biophysical Journal 1997; 73:3056-65.
2. Schatzer L, Weigert S. Solvable three-state model of a driven double-well potential and coherent destruction of tunneling. Physical Review A 1998;57(1):57-78.

Received November 4, 2005

The Genetic Improvement of Rapeseed in China

Baoming Tian

Department of Bioengineering, Zhengzhou University, Zhengzhou, Henan 450001, China

Abstract: Rapeseed is a major edible oilseed and protein crop in China. Its oil is 35% of the total vegetable oil in China, and its meal is 25%. The rapeseed production in China has been increased steadily since 1980s, especially in 1990s. The yearly averagee planting acreage of rapeseed is 6.25 million hectares, from 5.70 – 6.90 million hectares, three times of the 1950s – 1960s'. The total production has been increased 10 times since then. At present, the total vegetable oil production is 8.5 million tons, meanwhile the consumption is about 11 – 12 million tons, so there is still a shortage of 3 – 4 million tons every year. There are about 144 double and single low cultivars registered officially in China during 1985 – 2002, and 67 are OP's cultivars and 77 are hybrids. The potential yield of the double low OP's cultivars is about 5% higher than that of the normal cultivars(check ,double high), and yield of the hybrids are 15% – 20% higher than that of the checks. It is predicated that: the planting acreage can reach 7 – 8 million hectars in 5 – 10 years; double low cultivars will replace double high normal cultivars; hybrids will replace OP's cultivars; cytoplasm male sterility and genic male sterility are still the two important system for heterosis application; the studies on transgenic rapeseed will become important and high yield, high oil content and good resistance to diseases will be more important breeding goals in China. [Life Science Journal. 2006;3(1):78 – 80] (ISSN: 1097 – 8135).

Keywords: rapeseed; genetic improvement; China

1 Brief Introduction of Rapeseed Production

Rapeseed is an important edible oil and protein crop in China. Its oil is 35% of the total vegetable oil in China, and its meal is 25%. The rapeseed production in China has been increased steadily since 1980s. The yearly averagee planting acreage of rapeseed is 6.25 million hectares, from 5.70 – 6.90 million hectares, three times of the 1950s – 1960s'. The total production has been increased 10 times since then(Table 1 and Table 2).

Table 1. Rapeseed production in the World

Nations	Area ($10^6 hm^2$)	Yield (kg/hm^2)	Total Yield ($10^4 t$)
World	25.057	1469.5	3690.1
China	6.807	1434.9	977.7
India	6.560	888.3	579.6
Canada	4.826	1449.3	700.3
Autralia	1.117	1327.4	145.1
Europe	4.387	2628.0	1155.6

Several reasons have been promoting the development of rapeseed production since 1990s. Firstly, with the development of Chinese economy, the national and international market demand for edible oil has been increased greatly. Secondly, the planting acreage of winter wheat in the country was decreased because the demand for wheat was decreased. There is potential land for farmers to plant more rapeseed. Thirdly, the rotation of rice-rapeseed made the changes of rotation systems, as a result that a lot of areas of rice-rapeseed rotation has replaced other crops.

Table 2. The production and consumption in China

Year	Production ($10^4 t$)	Consumption ($10^4 t$)	Shortage ($10^4 t$)
1994 – 1995	615	963	338
1995 – 1996	680	937	257
1996 – 1997	684	1000	316
1997 – 1998	746	1130	384
1999 – 2000	832	1120	288
2001 – 2002	850	1200	350

Finally, more and more rapeseed cultivars with high yield and good quality were registered. These cultivars brought a lot of benefit to farmers.

At present, the production of edible oils in China is about 8.5 millions (rapeseed oils about 3.5 million tons) while market demand is 11 – 12 million tons (9 kg per person). There is a shortage of 3.0 – 4.5 million tons. Comparing to the consumption of 15 – 16 kg oils per person in the Southeast Asia, the demand might be 18 – 20 million tons in the countries. This analysis indicates that there is a great of market potential for edible oils in China.

2 Quality Improvement in Rapeseed

The rapeseed production has been increased

steadily since 1950s and 1960s in China, *Brassica napus replaced Brassica campestris* (the cultivation of *B. campestris* was over 80% before 1960s). In 1970s, *B. napus* became popular (over 80%). In the early 1990s, a lot of single low or double low OP's (open-pollinated) varieties were extended, meantime, some single low or double low hybrids were registered. After 1995, the planting acreage of single low varieties was decreased and the acreage of double low varieties (include OP's varieties and hybrids) were increased.

In 1975, the low erucic acid variety, "Oro", was introduced into China. In 1980, the double low variety, "Tower", was also introduced into China. Both of them are the spring type and are planted only in a spring rapeseed area which are unsuitable for the winter rapeseed area, such as the Yangtze River basin. The winter rapeseed area is over 80% of total rapeseed areas, a short-day photoperiod in China. Due to the varities from Canada and Europe with strong photoperiod sensitiveity, they need a long-time photoperiod to flower, so their maturity time is longer than that of semi-winter and winter types, and their growth are not so good. Some winter type varieties from Europe have also been introduced to China, and their maturity date is also delayed because of lack of enough strong photoperiod in this region. So we have to breed some cultivars for adaption to condition in China.

The first public rapeseed program in China was initiated in 1980. The first Chinease double low cultivar Yuyou No. 2 in *Brassica napus* was released in 1985. Since then, a series of cultivars with improvement in yield, resistance to diseases, quality and agronomic type, have been released. Now, there are about 144 double and single low cultivars registered officially in China during 1985 – 2002, of which 67 are OP's cultivars, and 77 are hybrids. The potential yield of the double low OP's cultivars is about 5% higher than that of the common quality cultivars (check, double high).

3 Application of Heterosis

The development of F1 hybrids in maize, sorghum and sunflower gave dramatic increasee in yield over the open-pollinated varieties by exploiting heterosis or hybrid vigour. In the case of sorghum and sunflower the discovery of cytoplasmic male sterility(CMS) systems in each species quickly led to the development and introduction of hybrids. It is expected that a CMS system could be found in *Brassica* that would enable the development of hybrid in double low rapeseed. A good candidate crop for hybrid development should:

– be self pollinated so as to enable the development of inbred lines.

– be capable of cross pollination so as to enable the easy production of hybrid seed.

– have a low seeding rate and therefore permic low cost seed per hectare.

– have good heterosis for yield.

– have a good pollination control system to enable the easy production of F1 hybrids.

Rapeseed (*Brassica napus*) has all these traits but is lacking a good pollination control system to make hybrids. Although a range of different methods has been put forward as means to produce hybrids such as self incompatibility (SI), genic male sterility (GMS) and the use of chemical hybridizing agents(CHA), the successs and simplicity of CMS in other crops suggested that this would be an ideal method to make hybrids. Luckily, in 1972, a new (CMS) system, "polima A", was discovered by professor D. T. FU (Huazhong Agricultural University) in China. Initial work was showed that there was a single dominant gene for restoration which did not occur in normal cultivars. All cultivars behaved as B lines or had some degrees of partial restoration so could be classified as poor maintainers. In fact, some good restorative genes for polima A were discovered in Chine and other countries. Polima system is the first practicable cytoplasmic male sterility systems in the world. It led to the release of the first hybrid , Qinyou No. 2, in 1986. The first single low hybrid, Huaza No. 3, released in 1991. The first double low hybrid, Huaza No. 4, registered in 1994. Since then, a series of cultivars with improvement in yield, resistance to diseases, quality and agronomic type, have been released. Now, there are about 77 double and single low hybrids registered officially in China during 1985 – 2002. The potential yield of the double low hybrids is 15% – 20% higher than that of the normal checks.

Despite of the success of these hybrids, it was very clear that the polima CMS system had limitations. The challenge was to find germplasm which could produce A lines with stable male sterility. It was very difficult to breed A lines with stable male sterility and even the best ones produced some pollen at either low or high temperatures(or both). The petal morphology of the A lines attracted bees to gather nectar but they do poor job of transferring pollen. This means that seed yield in hybrid production fields would be low and unpredictable. To overcome the disadvantage of polima CMS, a range of different methods have been put forward such as GCMS (genic and cytoplasmic male sterility) and dominant genic male sterility gene (DGMS) to im-

prove the stability of the male sterility. Two new GCMS systems (dominant genic and polima CMS male sterility, recessive genic and polima CMS male sterility) have been established. With these new GCMS, the polima line 1141A and its two hybrids (Huaza No. 3, Huaza No. 4) have been improved. The genetically improved A line has more stable male sterility. The genetically improved two hybrids (Huaza No. 3, Huaza No. 4) have higher yield, better quality and better tolerance to the disease of *Sclerotinia*. The DGMS has been used to establish a random-mating population of polima CMS maintainers by using some polima CMS maintainers to cross twice with the DGMS.

4 Future Direction

(1) The planting acreage might reach 7 – 8 million hectares in the coming 5 – 10 years. The acreage of transplanting rapeseed will decrease because the cost of labour is going up. So the raise of total production would be limited.

(2) Double low cultivars will replace double high cultivars in 3 – 5 years. The breeding goal is to increase oil and protein content, resistance to diseases, higher yield and decrease the glucosinolates content.

(3) The breeding of yellow seed coat has been in a great advance in many institutions. It is predicated that the acreage of double low cultivars with yellow seed coat will be extended widely in 3 – 5 years.

(4) The major breeding goal is to utilize heterosis with good quality. Cytoplasmic male sterility and genic male sterility are still two important systems for hybrid breeding . The planting acreage of hybrids will be over 75% in 5 – 10 years.

(5) The studies on transgenic rapeseed will become important. At present the nation still limits the extension of the transgenic plant. If the nation could approve genetic modification of rapeseed, herbicide tolerant varieties would be the first transgenic rapeseed cultivars in market.

(6) The processing level of rapeseed will be improved greatly by introducing equipment and improving technology.

Correspondence to:
Baoming Tian
Department of Bioengineering
Zhengzhou University
Zhengzhou, Henan 450001, China
Telephone: 86-371-6778-3235
Email: tianbm@zzu.edu.cn

References

1. Fu Tingdong, Yang Guangsheng, Tu Jinxing, et al. Rapeseed production and variety improvement in China. Journal of Huazhong Agricultural University 1999; 18 (6): 501 – 4.
2. Yang Guangsheng, Fu Tingdong. Study on the cytoplasmic male sterility types in *B. napus* rapeseed. Heredity 1988; 10(5): 8 – 10.
3. Yang Guangsheng, Fu Tingdong. Preliminary study on the restoring and maintaining relationship of cytoplasmic male sterility in *B. napus*. Journal of Crops 1990; 17 (2): 151 – 6.

Received November 5, 2005

Determination of the Equilibrium, Kinetic and Thermodynamic Parameters of the Batch Biosorption of Copper(Ⅱ) Ions onto Chaff

Runping Han[1], Jinghua Zhang[2], Lu Zhu[1], Weihua Zou[1], Jie Shi[1]

1. Department of Chemistry, Zhengzhou University, Zhengzhou, Henan 450052, China

2. Department of Chemistry, Huanghuai University, Zhumadian, Henan 463000, China

Abstract: A new sorbent system for removing copper ions from aqueous solutions has been investigated. This new sorbent is cereal chaff, an agriculture product in middle-west region in China. Variables of the system include sorption time, pH, chaff dose and solution temperature. The experimental results were fitted to the Langmuir, Freundlich model isotherms to obtain the characteristic parameters of each model. Both the Langmuir and Freundlich isotherms were found to represent the measured sorption data best. According to the evaluation with the Langmuir equation, the maximum sorption capacities of copper ion onto chaff increased from 4.46 to 5.62 $mg \cdot g^{-1}$ with temperature increasing from 293 K to 303 K. Using the thermodynamic equilibrium coefficients obtained at different temperatures, various thermodynamic parameters, such as ΔG^0, ΔH^0 and ΔS^0, were calculated. The thermodynamics of copper ion/chaff system indicates spontaneous and endothermic nature of the process. The pseudo first-order and pseudo second-order kinetic models were also applied to experimental data assuming that the external mass transfer limitations in the system can be neglected and biosorption is sorption controlled. The results showed that copper(Ⅱ) uptake process followed the second-order rate expression and adsorption rate constants increased with temperature. Using the second-order kinetic constants, the activation energy of biosorption was also evaluated. [Life Science Journal. 2006;3(1):81-88] (ISSN: 1097-8135).

Keywords: biosorption; copper(Ⅱ); chaff; equilibrium isotherms; kinetics

1 Introduction

Sorption has been an effective separation process for a wide variety of applications. Since applicating traditional treatment techniques need enormous cost and continuous input of chemicals, which become impracticable, uneconomical, an alternative inexpensive sorbent able to drastically reduce the cost of a sorption system has always been searched. The process of heavy metal removal by biological material is called biosorption. The major advantages of biosorption include: (1) low cost, (2) high efficiency of heavy metal removal from diluted solutions, (3) regeneration of the biosorbent and the possibility of metal recovery. Other advantages of biosorption are that it avoids the generation of toxic sludge and can be used under a broad range of operating conditions (pH, temperature, metal concentration, presence of other ions in the solution, etc). These demands led to increasing interest in biosorption (Drake, 1996; Han, 2000).

In recent years, agricultural by-products such as wheat shell, rice husk, tree fern have been widely studied for metal removal from wastewater (Teixeira, 2004; Ho YS, 2003; Basci, 2004). In this article, we selected cereal chaff as the biosorbent to adsorb copper(Ⅱ) from the aquatic systems. Firstly, chaff contains abundant floristic fiber, protein and some functional groups such as carboxyl, hydroxyl and amidogen etc, which make adsorption processes possible (Han, 2004). Secondly, obtained from agriculture as a byproduct, the chaff yield is vast. Usually, chaff is fed to livestock and poultry and did not have any other use. Biosorption for lead(Ⅱ) from aqueous solution by chaff in batch mode has been studied and the chaff can be as a adsorbent to removal lead from aqueous solution (Han, 2005).

The aim of this work was to study the possibility of the utilization of chaff for sorption of copper ions from aqueous solutions. The system variables studied included pH, biomass dose and the initial metal ions concentration at different temperature. The isotherm constants for the Langmuir, Freundlich model have been determined. The ther-

modynamics and kinetic parameters, such as ΔG^0, ΔH^0, ΔS^0 and E_a, k_1, k_2 and so on have been calculated.

2 Materials and Methods

2.1 Preparation of biomass

Fresh biomass of chaff was collected from its natural habitats on the dead millet in the farmland, Luoyang City, Henan Province, China. The raw chaff was washed a few times with distilled water, and dried in an oven at 373 K for a period of 24 hours, then ground and screened through a set of sieves to get different geometrical sizes 104 – 120 μm. This produced a uniform material for the complete set of biosorption tests, which was stored in an air-tight plastic container for all investigations.

2.2 Metal solution

The chemicals used for study were analytical grades of copper nitrate ($Cu(NO_3)_2$), and nitric acid supplied by Luoyang Chemical Reagent Company (China). The stock solution (1000 $mg \cdot l^{-1}$) of copper was prepared by dissolving the salts in distilled water.

2.3 Methods of adsorption studies

The process of experiment was as following: put a certain mass of chaff into conical flasks, added the solute of metals of copper, vibrated for some time, when reaching the biosorption equilibrium, took out the conical flasks, and filtrated to separate the chaff and the solution. The concentration of the free metal ions in the filtrate was analyzed using flam atomic absorption spectrometer (AAS) (AAanalyst 300, Perkin Elmer, USA). Each procedure was repeated three times and the results given were the average values.

The data obtained in batch model studies was used to calculate the equilibrium metal uptake capacity. It was calculated for each sample of copper by the following equation:

$$q_e = \frac{V(c_0 - c_e)}{m} \quad (1)$$

Where: q_e is the biomass biosorption equilibrium metal ion uptake amount in $mg \cdot g^{-1}$, V is the sample volume in ml, c_0 is the initial metal ion concentration in $mg \cdot l^{-1}$, c_e is the equilibrium metal ion concentration in $mg \cdot l^{-1}$, and m is the dry weight of the biomass in g.

3 Results and Discussion

3.1 The effect of biosorption time

In this part of experiment, in order to find the time of equilibrium, we studied the effect of time to adsorb copper on chaff. Take 0.08 g chaff to several conical flasks, added contenting metal ions solution 10 ml separately. The concentration of copper was 20 $mg \cdot l^{-1}$. Then in different intervals we analyzed the concentration of metal ions in the solution. The results were shown in Figure 1. A two-stage kinetic behavior was evident: a very rapid initial sorption over a few minutes, followed by a long period of much slower uptake. As seen from Figure 1, with the beginning of biosorption the uptake of metal ions increased quickly, then 10 minutes later, the change slowed down. So the adsorption of copper on chaff was speedy, and in ten minutes, the reaction of sorption nearly reached equilibrium. After this equilibrium period, the amount of adsorbed metals ions did not significantly change with time. So the removal efficiency was high. Furthermore the adsorption capacity of copper attained 1.78 $mg \cdot g^{-1}$ (0.028 $mmol \cdot g^{-1}$). Hence in the following studies, we selected 30 minutes as the time of adsorption equilibrium.

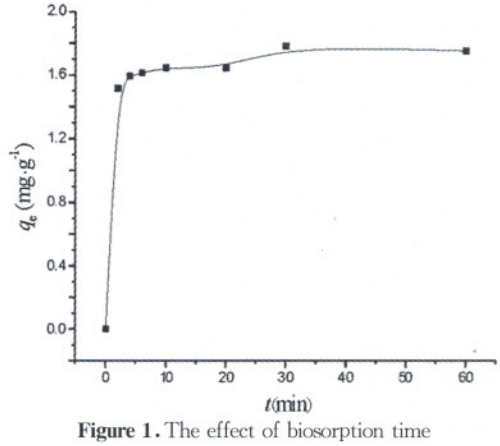

Figure 1. The effect of biosorption time

3.2 The effect of biomass dose

In order to find out the effect of biomass dose on biosorption of copper on chaff, studies were carried out in stirred batch experiments using known quantities of the chaff. We did the following experiments. Put different weight chaff into conical flasks, then added the solute of metals in the same concentration, which copper was 20 $mg \cdot l^{-1}$, and vibrated for 30 minutes. The influence of adsorbent dosage in equilibrium uptake and copper removal is depicted in Figure 2.

The increase in adsorbent dosage from 2 – 12 $g \cdot l^{-1}$ resulted in an increase from 50.7% to 77.0% in adsorption of copper(Ⅱ) ions. This was because of the availability of more and more binding sites for complexation of copper(Ⅱ) ions. However, copper uptakes showed a reverse trend to the percentage adsorptions (Figure 2). With increasing

adsorbent dosage from 2 to 12 $g \cdot l^{-1}$, the adsorption of copper(Ⅱ) ion per unit weight of adsorbent decreased from 5.1 to 1.2 $mg \cdot g^{-1}$. There were many factors, which contributed to this adsorbent concentration effect. The first and most important factor was that adsorption sites remain unsaturated during the adsorption reaction. This was due to the fact that as the dosage of adsorbent is increased, there was less commensurate increase in adsorption resulting from the lower adsorptive capacity utilization of the adsorbent. The second cause may be the aggregation/agglomeration of sorbent particles at higher concentrations, which would lead to a decrease in the surface area and an increase in the diffusional path length. Put together, the following experiments were carried as the selected concentration of biosorbent 8 $g \cdot l^{-1}$.

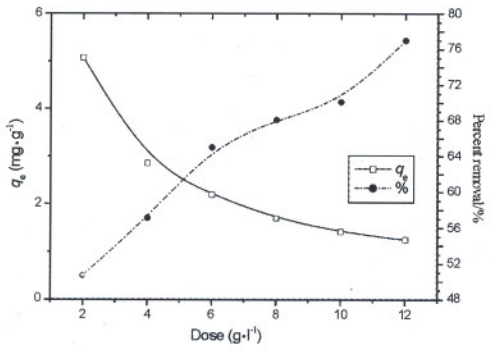

Figure 2. The effect of biomass dose

3.3 The effect of pH values

The most important single parameter influencing the biosorption rate and capacity is the pH of the biosorption medium. In order to examine the pH variation as well as its effect on metal ions biosorption in batch, copper ions adsorption experiments were done in the pH ranging from 2.0 to 6.5 at 293 K. The concentration of copper was 20 $mg \cdot l^{-1}$. The adsorptive time was 30 minutes. Figure 3 showed the effect of pH values on adsorption of copper by chaff.

From Figure 3, we observed that the adsorption capacities increased with pH value at the range of 1.8 to 5.2. While, when the value of pH was higher than 5.2, the decrease of adsorption capacities were observed. The reason may be as follows: at very low pH values, the surface of adsorbent would also be surrounded by the hydrogen ions which competed with metal ions binding the sites of the biosorbent. While with the pH values increased, especially when the pH value was above 3.0, and the concentration of proton was very low, the carboxylic acid sites can be appreciably deprotonated, the effect of proton competition was feeble, and metal ions removal was increased. As for the decrease of adsorption capacities after the pH value of 5.2, it was because when above this pH value, copper ions in solution were in two forms: Cu^{2+} and $(CuOH)^+$. Since in the later state copper in solution would present a larger size that it would be adsorbed less easily and therefore a diminution in the biosorption capacity would be expected. Furthermore, if the pH value was over 7.0, the ions of copper would deposit, so in the course of experiment, we selected that the pH values near 5.0. Similar results were reported using wheat shell as the biosorbent at pH 2−7 (Basci, 2004).

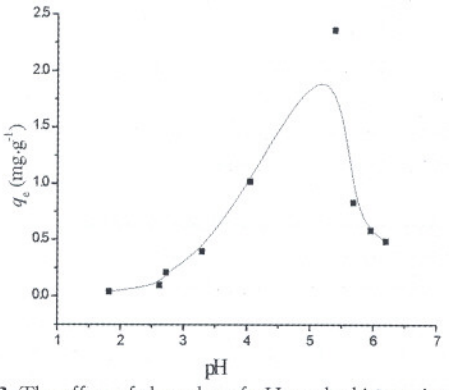

Figure 3. The effect of the value of pH on the biosorption of copper on chaff

3.4 The effect of initial copper concentration on temperature-dependent biosorption

The biosorption of copper by chaff at the biomass concentration of 8 $g \cdot l^{-1}$ was studied at several different initial metal concentrations ranging from 5 $mg \cdot l^{-1}$ to 30 $mg \cdot l^{-1}$ of copper at pH 5.0 and 293 K. The result was shown in Figure 4. As seen from Figure 4, equilibrium uptake increased with the increasing of initial metal ions concentrations at the range of experimental concentration. This was a result of the increase in the driving force from the concentration gradient, as an increase in the initial copper(Ⅱ) ion concentrations. In the same conditions, if the concentration of metal ions in solution was higher, and the active sites of chaff were surrounded by much more metal ions, the reaction of adsorption would be carried out more sufficiently. So as it was observed, the biosorption amount for copper increased with the increase of initial metal ion concentrations.

The equilibrium uptake at different temperatures were also showed in Figure 4 with respect to initial metal ion concentration (5−30 $mg \cdot l^{-1}$). It was clear that the uptake increased with increasing temperature. The increase of the equilibrium up-

take at increased temperature indicated that the adsorption of copper(Ⅱ) ions to chaff was endothermic by nature. The endothermic nature of metal adsorption has also been reported previously for adsorptive removal of copper(Ⅱ) by tree fern (Ho YS, 2003) and wheat shell (Basci, 2004).

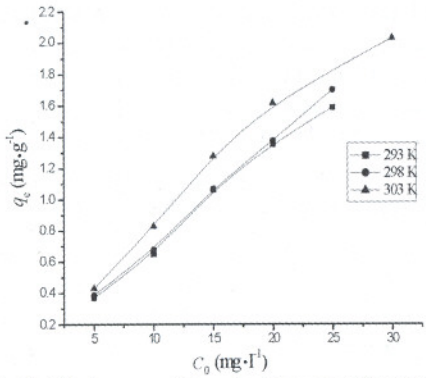

Figure 4. Equilibrium quantities of copper at different initial concentrations at different temperature

3.5 Application of adsorption model

Adsorption isotherms show the distribution of solution between the liquid and solid phases. Many different isotherm models have been proposed for the adsorption of solutes in a liquid solution on a solid surface. And it can be described by several mathematical relationships such as the standard Langmuir and Freundlich models. In this article, Langmuir and Freundlich models were both applied to the adsorption data.

Langmuir model is probably the most popular isotherm models due to its simplicity and its good agreement with experimental data. It can be described by the linearized form (Langmuir I, 1916):

$$\frac{1}{q_e}=\frac{1}{K_L q_{max}}\cdot\frac{1}{c_e}+\frac{1}{q_{max}} \quad (2)$$

Where q_{max}(mg·g^{-1}) is the maximum amount of metal ion per unit weight of chaff and K_L is the equilibrium adsorption constant. c_e is the equilibrium metal ion concentration in mg·l^{-1} and q_e is the biomass biosorption equilibrium metal ion uptake capacity in mg·g^{-1}. By plotting $1/q_e$versus $1/c_e$, q_{max} and K_L can be determined.

As to Freundlich model, the equilibrium established between the adsorbed metal ions (q_e) and that remained free in the solution (c_e) is represented by the Freundlich adsorption isotherm, which has the general form (Freundlich, 1906),

$$q_e=K_F\cdot c_e^{1/n} \quad (3)$$

A linear plot of this equation is as the following form,

$$\ln q_e=\ln K_F+\frac{1}{n}\ln c_e \quad (4)$$

This equation gives an intercept K_F denoting the adsorption and slope, the value of $1/n$ indicating the intensity of adsorption.

The data obtained in different temperature were applied to the Langmuir and Freundlich model and the results were shown in Table 1. *SD* is the residual standard deviation of regressive lines.

Table 1. The application of Langmuir and Freundlich model to the adsorption of copper on chaff at different temperatures

T/(K)	Langmuir constant				Freundlich constant			
	K_L (l·mg^{-1})	q_{max} (mg·g^{-1})	R	SD	K_F	n	R	SD
293	0.0437	4.46	0.987	0.160	0.188	1.130	0.990	0.097
298	0.0484	4.51	0.982	0.180	0.210	1.134	0.976	0.153
303	0.0533	5.62	0.996	0.074	0.344	1.359	0.975	0.155

From Table 1, as the $R>0.97$ and $SD<0.2$, it could be concluded that the adsorption of copper on chaff was both fitted well to Langmuir model and Freundlich model. It could be observed that with the temperature increasing, the value of equilibrium adsorption constant became bigger and the maximum amount of metal ion per unit weight of chaff increased, too. When the temperature was lower than 300 K, the adsorption capacity rose with temperature increase. It could also be observed that with the temperature increasing, the values of K_F and n rose. This also indicated that with the temperature increasing, the ability of adsorption increased. It was consistent with the result obtained from Langmuir model.

K_F, one of the Freundlich constants has been used as a relative measure of adsorption capacity, n, the other Freundlich constant was related to intensity of adsorption. From Table 1, all measured values of K_F showed easy uptake of copper with high adsorptive capacity of chaff and significant differences in sorption capacities due to temperature. In general, the values of K_F increased with temperature from 293 K to 303 K. The obtained values of

n indicated a higher adsorb ability of the copper at all temperatures studied.

While the Freundlich model does not describe the saturation behaviour of the sorbent, q_{max}, the mono-component Langmuir constant represents the monolayer saturation at equilibrium or the total capacity of chaff for copper. From Table 1, the values of q_{max} increased with temperature till 303 K. At 303 K, the maximum loading capacities of chaff was determined as 5.62 $mg \cdot g^{-1}$. The other mono-component Langmuir constant K_L indicated the affinity for the binding of copper. Its value was the reciprocal of the concentration at which half of the saturation of the adsorbent was attained (or copper amount of $q_{max}/2$ was bound). A high K_L value indicates a high affinity. The higher values of K_L obtained at 303 K also implied the strong bonding of copper to chaff at this temperature. But for adsorption Pb(Ⅱ) on chaff, the results were inverse to the effect of temperature. The adsorptive capacity decreased which implied the weaker bonding of lead to chaff with temperature increasing (Han, 2005).

3.6 Estimation of the specific surface area *S* of chaff

The solubility of a metal is an essential property to enable the metal to penetrate into the porous structure of chaff. The concentrations of metal species (i. e. $CuOH^-$, $Cu(OH)_2$, $Cu(OH)_3^-$, and $Cu(OH)_4^{2-}$) were too small to affect the concentrations of Cu^{2+} in this study. Although many metal species can be viewed as potential adsorbates in the uptake of Cu^{2+} from solution, the data presented in this study suggested that, under experimental conditions (pH = 5.0), the species responsible for the adsorptive removal of Cu^{2+} was the predominant one in the species distribution, namely the Cu^{2+} (Ho YS, 2003; Basci, 2004). Thus, biosorption could be explained by elucidating the mechanism whereby the Cu^{2+} molecules were accommodated by chaff surface.

Monolayer coverage of the surface by the metal ions can be used for the calculation of the specific surface area S according to following equation (Ho YS, 2003):

$$S = \frac{q_{max} NA}{M} \quad (5)$$

where S is the specific surface area, $m^2 \cdot g^{-1}$ chaff; q_{max} is monolayer sorption capacity, gram metal per gram chaff; N is Avogadro number, 6.02×10^{23}; A is the cross sectional area of metal ion, m^2; M is molecular weight of metal. For Cu^{2+} ion, the molecular weights are 63.5 and the cross sectional area Cu^{2+} has been determined to be 1.58Å^2 (Cu^{2+} radius is 0.71Å) in a close packed monolayer. Therefore, the specific surface areas can be calculated for Cu^{2+}. Table 2 listed the S values at three different temperatures.

Table 2. Specific surface areas for copper ion

T(K)	q_{max}(mg)	S($m^2 \cdot g^{-1}$)
293	4.46	0.67
298	4.51	0.68
303	5.62	0.69

From Table 2, the maximum specific surface area of chaff towards Cu^{2+} binding was 0.67 $m^2 \cdot g^{-1}$, 0.68 $m^2 \cdot g^{-1}$, 0.69 $m^2 \cdot g^{-1}$ with the temperature 293 K, 298 K, 303 K, respectively.

3.7 K_R values at different initial concentrations

The effect of isotherm shape can be used to predict whether a sorption system is 'favourable' or 'unfavorable' (Ho YS, 2003). The essential features of the Langmuir isotherm can be expressed in terms of a dimensionless constant separation factor or equilibrium parameter K_R, which is defined by the following relationship(Ho YS, 2003):

$$K_R = \frac{1}{1 + K_L c_0} \quad (6)$$

where K_R is a dimensionless separation factor, c_0 is initial concentration ($mg \cdot l^{-1}$ and K_L is Langmuir constant ($l \cdot mg^{-1}$). The parameter K_R indicates the shape of the isotherm accordingly:

Values of K_R	Type of isotherm
$K_R > 1$	Unfavorable
$K_R = 1$	Linear
$0 < K_R < 1$	Favorable
$K_R = 0$	Irreversible

The values of K_R at 293 K, 298 K and 303 K were given in Table 3. The K_R values indicate that sorption was more favorable for the higher initial copper concentrations than for the lower ones. It was apparent that the sorption of copper on chaff was favorable with the conditions used in this study.

3.8 Thermodynamic parameters of biosorption

The original concepts of thermodynamics assumed that in an isolated system, where energy cannot be gained or lost, the entropy change was the driving force. In environmental engineering practice, both energy and entropy factors must be considered in order to determine what processes will occur spontaneously. The Gibbs free energy change, ΔG^0, is the fundamental criterion of spontaneity. Reactions occur spontaneously at a given temperature if ΔG^0 is a negative quantity.

Table 3. K_R values based on the Langmuir isotherm

C_0(mg·l^{-1})	293 K	298 K	303 K
5	0.821	0.805	0.790
10	0.696	0.674	0.652
15	0.604	0.579	0.556
20	0.534	0.508	0.484
25	0.478	0.452	0.429
30	0.433	0.408	0.385

Value of ΔG^0 can be determined from the following equation (Ho YS, 2003; Tewari, 2005)

$$\Delta G^0 = -RT\ln K_L \quad (7)$$

The change of enthalpy (ΔH^0) and entropy (ΔS^0) can be obtained from the slope and intercept of a van't Hoff equation of ΔG^0 versus T (Tewari, 2005; Aksu, 2002),

$$\Delta G^0 = \Delta H^0 - T\Delta S^0 \quad (8)$$

Where ΔG^0 is standard free energy change, J; R is universal gas constant, 8.314 J·mol^{-1}·K and T is absolute temperature, K.

Values for the biosorption process obtained from Eq. (7) and Eq. (8) are listed in Table 4.

Table 4. The ΔG^0, ΔH^0 and ΔS^0 values of copper and copper adsorption on chaff at different temperatures

T/K	293	298	303
ΔG^0(kJ·mol^{-1})	−19.3	−19.9	−20.5
ΔH^0(kJ·mol^{-1})		14.6	
ΔS^0(kJ·mol^{-1} K^{-1})		0.116	

The negative values of ΔG^0 confirm the feasibility of the process and the spontaneous nature of sorption with high preference of copper (Ⅱ) on chaff. The value of ΔH^0 is positive, indicating that the sorption reaction is endothermic. The positive value of ΔS^0 reflects the affinity of the chaff for copper ion and suggests some structural changes in copper and chaff (Gupta, 1998). In addition, positive value of ΔS^0 shows the increasing randomness at the solid/liquid interface during the sorption of copper ion on chaff.

3.9 Kinetic parameters of biosorption

In order to calculate the kinetic parameters, the change of the amount of metal ion per unit weight of chaff with adsorbing time increasing at different temperatures was shown in Figure 5.

From Figure 5, we observed that the value of q_e increased with time and in the same condition of adsorption, the higher temperature was, the higher of the capacity quantities of chaff were. Hence as to copper adsorption, it took advantage of higher temperature.

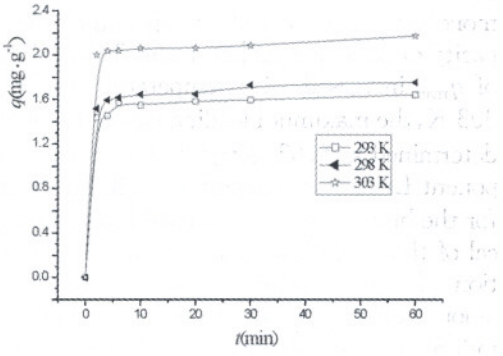

Figure 5. The effect of temperature and time on biosorption of copper

3.9.1 Kinetic modeling

There were several reports on the use of different kinetic models to adjust the experimental data of heavy metals adsorption on biomass. One of them was the pseudo-first-order Lagergren model that considered that the rate of occupation of adsorption sites was proportional to the number of unoccupied sites (Aksu, 2005):

$$\frac{dq}{dt} = k_1(q_e - q) \quad (9)$$

Where q_e and q are the amounts of adsorbed metal ions on the biosorbent at equilibrium and at any time t, respectively, and k_1 is the Lagergren rate constant of the first-order biosorption. The range of t is from 0 to t and q is from 0 to q_e. It can be described by the linearized form as following:

$$\log(q_e - q) = \log q_e - \frac{k_1}{2.303}t \quad (10)$$

Linear plots of $\log(q_e - q)$ versus t indicate the applicability of this kinetic model. However, before application Eq. (10), the value of q_e must be preestimated by extrapolating the experimental data to $t = \infty$.

The second model is the pseudo-second-order model reaction. The observed kinetics can be modeled that the rate of occupation of adsorption sites is proportional to the square of the number of unoccupied sites (Ho YS, 1999):

$$\frac{dq}{dt} = k_2(q_e - q)^2 \quad (11)$$

Where k_2 is the rate constant of second-order biosorption (g·mg^{-1}·min^{-1}), which corresponds to the integrated rate law for a second-order reaction, is obtained:

$$\frac{1}{q_e - q} = \frac{1}{q_e} + k_2 \cdot t \quad (12)$$

Eq. (12) can be rearranged and linearized to obtain:

$$\frac{t}{q} = \frac{1}{k_2 q_e^2} + \frac{1}{q_e} t \quad (13)$$

The plot t/q versus t should give a straight line if second-order kinetics is applicable and k_2 and q_e can be determined from the slop and intercept of the plot, respectively. Furthermore, the value of q_e may not be known.

3.9.2 Kinetic parameters

Aiming at evaluating the biosorption kinetics of copper and copper ions on chaff, the pseudo-first-order kinetic model and pseudo-second-order model were used to fit the experimental data. The initial concentration of copper and copper was 20 $mg \cdot l^{-1}$. The result was shown in Table 5.

Table 5. The application of kinetic model to the biosorption of copper on chaff

T(K)	First-order kinetic model			Second-order kinetic model		
	$k_1(min^{-1})$	$q_e(mg \cdot g^{-1})$	R	$k_2(g \cdot mg^{-1} \cdot min^{-1})$	$q_e(mg \cdot g^{-1})$	R
293	0.0260	0.27	0.980	0.939	1.65	1.000
298	0.0286	0.23	0.951	1.305	1.73	1.000
303	0.0316	0.20	0.940	3.685	2.09	1.000

From Table 5 we came to a conclusion that the biosorption data of copper on chaff was perfectly fitted the second-order kinetic model. The linear coefficients were all 1.000, which indicated that the linearity was good. Furthermore the value of q_e obtained from the Eq. (13) fitted the experiment data well. The value of k_2 was increased with the increased temperature, which indicated that the rate of reaction became speedy.

According to the Arrhenius-type correlation (Tewari, 2005; Aksu, 2002; Ho YS, 1999):

$$k = k_0 \exp(\frac{-E_a}{RT}) \quad (14)$$

where k_0 is the temperature independent factor in $g \cdot mg^{-1} \cdot min^{-1}$, E_a is the activation energy of the reaction of biosorption in $kJ \cdot mol^{-1}$, R is the gas constant, 8.314 $J \cdot mol^{-1} \cdot K^{-1}$ and T is the sorption absolute temperature, K. The linear form is:

$$\ln k = -\frac{E_a}{RT} + \ln k_0 \quad (15)$$

Linear plots of $\ln k$ versus $1/T$ should give a straight line. The value of E_a can be obtained from the slope of the line. According to the Eq. (15), the activation energy of biosorption of copper on chaff was evaluated as 100.3 $kJ \cdot mol^{-1}$ by the value of the rate constant of second-order biosorption. This value was of the same magnitude as the activation energy of activated chemisorption. The result also suggested that the process of the chaff adsorbing copper was endothermic.

4 Conclusion

The Freundlich and Langmuir adsorption models were used for the mathematical description of the biosorption equilibrium of copper(Ⅱ) ions to chaff depending on temperature. The isotherm constants evaluated from the isotherms were used to compare the biosorptive capacity of the dried biomass. It was seen that the isotherm constants decreased with temperature increasing. The obtained results showed that the adsorption equilibrium data fitted very well to both the models in the studied concentration range at all the temperatures studied. The equilibrium sorption of copper ions was determined from the Langmuir equation and was found to be 5.62 $mg \cdot g^{-1}$ at 303 K. Various thermodynamic parameters, such as ΔG^0, ΔH^0 and ΔS^0, were calculated. The suitability of the pseudo first and second order kinetic models for the sorption of copper(Ⅱ) ions onto biomass was also discussed. It was decided that the biosorption kinetics of copper (Ⅱ) ions to chaff obeyed the psendo second-order adsorption kinetics. with the pseudo second-order kinetic constants increasing with temperature, the activation energy of biosorption was evaluated as 100.3 $kJ \cdot mol^{-1}$. The thermodynamics and kinetics of copper ion/chaff system indicated spontaneous and endothermic nature of the process.

Acknowledgments

The authors express their sincere gratitude to the Bureau of Science and Technology of Henan Province in China, for the financial support of this study.

Correspondence to:
Runping Han
Department of Chemistry

Zhengzhou University
Zhengzhou, Henan 450052, China
Telephone: 86-371-6776-3707
Email: rphan67@zzu.edu.cn

References

1. Aksu Z. Application of biosorption for the removal of organic pollutants: a review. Process Biochem 2005; 40(3-4): 997-1026.
2. Aksu Z. Determination of the equilibrium, kinetic and thermodynamic parameters of the batch biosorption of lead(Ⅱ) ions onto Chlorella vulgaris. Process Biochemistry 2002; 38(1): 89-99.
3. Basci N, Kocadagistan E, Kocadagistan B. Biosorption of lead (Ⅱ) from aqueous solutions by wheat shell. Desalination 2004; 164(2): 135-40.
4. Drake LR, Rayson GD. Plant-deprived materials for metal ion-selective binding and preconcentration. Anal Chem 1996; 68: 22A-27A.
5. Freundlich HMF. Uber die adsorption in lasungen. Z Phys Chem 1906; 57: 385-470.
6. Gupta VK. Equilibrium uptake sorption, dynamics process, development, column operations for the removal of copper and nickel from aqueous solution and wastewater using activated slag, a low-cost adsorbent. Ind Eng Chem Res 1998; 37(1): 192-202.
7. Han RP, Shi J, Li JJ, et al. Biosorption and preconcentration of heavy metals by biomaterial. Hua Xue Tong Bao (Chemistry, Chinese) 2000; 63(7): 25-8.
8. Han RP, Yin JS, Li HQ, et al. Analysis and comparison of infrared spectra of native cereal chaff and pyrolysis products. Spectrosc Spect Anal 2004; 24(11, Suppl): 187-8.
9. Han RP, Zhang JH, Zou WH, et al. Equilibrium biosorption isotherm for lead ion on chaff. J Hazard Mater 2005; B125(1-3): 266-71.
10. Ho YS, McKay G. Pseudo-second-order model for sorption processes. Process Biochem 1999; 34(5): 451-65.
11. Ho YS. Removal of copper ions from aqueous solution by tree fern. Water Research 2003; 37(10): 2323-30.
12. Langmuir I. The constitution and fundamental properties of solids and liquids. J Am Chem Soc 1916; 38: 2221-95.
13. Teixeira Tarley CR, Zezzi Arruda MA. Biosorption of heavy metals using rice milling by-products: Characterization and application for removal of metals from aqueous effluents. Chemosphere 2004; 54(7): 987-95.
14. Tewari N, Vasudevan P, Guha BK. Study on biosorption of Cr(Ⅵ) by Mucor hiemalis. Biochem Eng J 2005; 23(2): 185-92.

Received October 24, 2005

Effects of Marriage Quality upon the Mental Health of Parents and Their Adult Offspring

Ronghua Wei[1], Yuzhong Wang[2], Bangli Liu[3]

1. *Henan Provincial Communications Polytechnic Institute, Zhengzhou, Henan 450052, China;*
2. *Psychology Department, School of Education, Zhengzhou University, Zhengzhou, Henan 450052, China*
3. *School of Foreign Languages, Zhengzhou University, Zhengzhou, Henan 450052, China*

Abstract: Aim. To probe into the effects of marriage quality upon the mental health of parents themselves and their adult offspring. **Methods.** The Symptom Checklist-90 (SCL-90) is applied to and marriage quality questionnaire is carried out among 255 college students, and results have been analyzed. **Results.** Marriage quality appraised by parents themselves is negatively correlated to most of their factors in SCL-90 ($P<0.05, P<0.01$). Marriage quality appraised by father shows negative correlation with mother's total score and her most factors in SCL-90 ($P<0.01$, $P<0.001$). Marriage quality of parents also shows negative correlation with the total score and most factors of their adult offspring in SCL-90 ($P<0.05, P<0.01$). Marriage quality of parents during the earlier years of their married life is more negatively correlated to their factors in SCL-90 than the marriage quality at present ($P<0.05$, $P<0.01$). **Conclusion.** The mental health of middle-aged couples is correlated to their marriage quality. Husbands normally feel that marriage quality exerts greater influence on the mental health of wives. Marriage quality of parents may also have effects upon the mental health of their adult offspring, and particularly the marriage quality of parents during the earlier stage of their married life may produce greater influence upon the mental health of their adult offspring. [Life Science Journal. 2006;3(1):89-93] (ISSN: 1097-8135).

Keywords: parents' marriage quality; adult offspring; mental health; effects

1 Introduction

The stress theory in medical psychology is a theory about the psychosomatic relationship. It emphasizes the effect brought about by stress life events upon a person's mental health. Then, what stress life events will exert significant effects upon man's mental health? In the Social Readjustment Rating Scale (SRRS) worked out by Holmes and Rahe, which contains 43 life events, 16 life events belong to categories of family, marriage and sexual life(Rabin, 1976). In the Life Events Scale(LES) which covers 50 kinds of life events and is prepared by Yang Desen et al, 28 items relate to marriage and family (Yang, 1990). This indicates that family and marriage are major stress factors which produce great effects upon people's mental health. To modern people who normally work outside, family could serve as a base camp which may help stabilize one's mentality psychologically.

Some studies of mental health and marriage quality had been conducted during the early 1980s (Dobson, 1987). These studies have found that the female shows more mental symptoms in miserable marriages, and in general, wives are more likely to be affected by marriage changes than husbands, thus mental problems are more likely to occur among wives (Moffit, 1986). In the 1990s some investigations and analyses had been conducted by Liu Peiyi and others among 118 intellectual couples. Results showed that mental health only correlated to the self-rated marriage happiness, and it did not correlate to the marriage happiness appraised by others. As to the effects of the couple's marriage quality upon the mental health of their offspring, most efforts, in terms of the age of their offspring, have been made on the study of effects upon infants and school-aged children. Yu Guoliang and others have discovered that marriage relationship is quite positively correlated to parenthood (Yu, 2003). In terms of influence ways of marriage, studies have been concentrated on the effects of divorce upon the offspring's mentality and personality (Li, 1999). After all, divorced couples are of minority in China. The majority of couples have their marriage kept. What effects does the quality of their marriage have on the mental health of themselves and their children? Do such effects still exist when their children have left home for college study? These questions will be discussed in this paper.

2 Objects and Methods

2.1 Measuring tool and questionnaire designing

Symptom Checklist-90 (SCL-90), the most popular measuring tool for mental hygiene applied both at home and abroad, is used to check the objects' mental health level through the total score and the scores of 10 factors. Meanwhile, principal subjects concerning marriage quality have been chosen and a questionnaire been designed. The questionnaire includes, among other things, satisfaction of sexual life self-rated by the couple themselves, their feelings about the satisfaction and stability of their marriage. Furthermore, both the parents and their children are encouraged to evaluate the satisfaction and stability of the marriage so as to understand its objectivity and reality.

2.2 The selection of samples under study

As many as 280 students majoring respectively in liberal arts, science, engineering and medical science were randomly selected at a comprehensive university, and an investigation was conducted by questionnaire among them about their mental health. In accordance with their registered home addresses, a sealed questionnaire about adults' marriage affairs and SCL-90 were mailed to the students' parents. Each student's response to the investigation was put as a set together with the returned questionnaire from the parents (510 copies altogether, making 255 pairs). 255 copies of valid answers from students were obtained, thus we got 255 sets ($255 \times 3 = 765$).

2.3 General conditions of samples under study

2.3.1 Gender of college students: 104 male, accounting for 40.78%; 151 female, making up 59.22%.

2.3.2 Age of parents: The average age of sampled parents is 46.70 ± 6.73, among which the average age of father is 47.15 ± 6.55 and that of mother is 46.34 ± 6.17.

2.3.3 Life background of samples investigated: Parents of 113 students come from the countryside, accounting for 44.3%; 52 couples are from county seats, accounting for 20.4%; 56 couples are from medium- and small-sized cities, accounting for 22.0%; and 34 couples are from provincial capital cities or municipalities directly under the central government, accounting for 13.3%. The life background of the students was the same as that of their parents before they came to the university.

2.3.4 Education background of parents: 25 persons are illiterate, accounting for 4.9%; 70 people have received primary education, accounting for 13.87%; 135 persons have graduated from junior middle schools, making up 26.5%; 134 persons have finished senior middle school, accounting for 26.3%; 47 people are two-year-college graduates, 9.2%; 61 persons are three-year-college graduates, 12%; 36 persons have got bachelor degrees, 7.1%; 2 persons have respectively held a master degree and a doctorate degree, accounting for 0.39%; with 510 persons in all.

Statistic analysis has been conducted to those returned questionnaires by way of SPSS 10.1.

3 Results

By marriage quality we mean here the one respectively evaluated by father, mother and the offspring. Results show that there is no significant difference between the evaluation made by parents and that by the offspring, which indicates the index is true.

The marriage quality self-rated by both the father and mother may exert influence not only on their own psychological symptoms, but also on those of their spouse and offspring. Therefore, correlated analyses have been made not only of the self-rated marriage quality, their own factors in SCL-90 and the total score, but also of the self-rated marriage quality, the factors of the their spouse and offspring in SCL-90 and the total score. Marriage quality also includes the evaluated quality of marriage during the early stage of married life and the marrige quality rated at the time of questionnaire.

3.1 Analyses of the correlation of parents' marriage quality with their psychological symptom level

3.1.1 Analysis of the correlation of the father's psychological symptom level with the marriage quality evaluated by the father: From the statistic results we can see that the earlier stage of marriage satisfaction rated by the father bears significantly and highly significantly negative correlation with most of his own factors in SCL-90 (except the marriage satisfaction and factors 3 and 6, marriage stability and factor 10, sexual life and factors 3,5,6, and 10). The marriage satisfaction evaluated by father at present shows significantly and highly significantly negative correlation with his own factors 4, 7, 8 and 9 and the total score in SCL-90. The marriage stability and sexual satisfaction self-rated by the father bear significantly and highly significantly negative correlation with the total score and all factors except factors 6 and 10.

3.1.2 Analysis of the correlation of the marriage quality evaluated by the father with the mother's psychological symptom level: Generally speaking,

marriage quality evaluated by the father bears high correlation with the wife's factors in SCL-90. Apart from the fact that there exists no significant correlation between the marriage quality at the early stage of married life and factor 1 in SCL-90, between sexual satisfaction at the early stage of married life and factor 10 in SCL-90, and between the marriage satisfaction at present and factor 2 in SCL-90, the rest factors in SCL-90 and the total score bear significantly or highly significantly negative correlation with the marriage quality both at the early stage of married life and at present, indicating that the marriage quality evaluated by the father exerts greater psychological influence upon the wife than upon himself.

3.1.3 Analysis of the correlation of the marriage quality evaluated by the mother with her own psychological symptom level: The marriage quality evaluated by the mother is correlated with only a few of her own factors in SCL-90. For instance, her marriage satisfaction at the early stage of married life bears highly significantly negative correlation with only factors 4 and 6 in SCL-90; her sexual satisfaction at the early stage of married life has significantly or highly significantly negative correlation with factors 3, 4, 6 and 7 in SCL-90. The marriage stability possesses no significant correlation with every factor in SCL-90. But the mother's marriage satisfaction at present shows significantly negative or highly significantly negative correlation with factors 2, 4 and 6 in SCL-90; the marriage stability has significantly negative or highly significantly negative correlation with factors 1, 2, 4, 6, 8 and 9 in SCL-90; whereas the sexual satisfaction bears significantly negative or highly significantly negative correlation with the total score and all factors except factor 7.

3.1.4 Analysis of the correlation of the marriage quality evaluated by the mother with the father's psychological symptom level: The marriage satisfaction and stability at the early stage of married life evaluated by the mother bear no significant correlation with any of father's factors in SCL-90. But sexual satisfaction has significantly negative or highly significantly negative correlation with factors 6 and 10. Only factor 2 bears significantly negative or highly significantly negative correlation with mother's present marriage satisfaction, stability and sexual satisfaction.

3.2 Analysis of the correlation of parents' marriage quality with the psychological symptom level of their adult offspring

3.2.1 Analysis of the correlation of the marriage quality evaluated by the father with every factor of their adult offspring in SCL-90: From Table 1 we can see that the marriage quality at the early stage evaluated by father has significantly negative or highly significantly negative correlation with the total score and most of their offspring's factors in SCL-90 (except that marriage satisfaction does not correlate to factors 5, 8 and 10, nor does marriage stability correlate to factors 7, 8 and 10, nor sexual life to factors 6, 8 and 10). However, the present marriage satisfaction bears significantly negative or highly significantly negative correlation with only factor 10 and the total score; the present marriage stability shows significantly negative or highly significantly negative correlation with nine factors in SCL-90 (except for factor 10 and the total score); the present sexual life also bears significantly negative or highly significantly negative correlation with the total score and most factors (except for factors 1, 3 and 6).

3.2.2 Analysis of the correlation of the marriage quality evaluated by mother with every factor of the offspring in SCL-90: Comparatively speaking, marriage quality evaluated by mother correlates with fewer number of factors and total score in SCL-90 than that of father, but her correlation shows higher degree in significance than that of father's. The marriage satisfaction and stability at the early stage of married life evaluated by mother have significantly negative or highly significantly negative correlation with the total score and most of her offspring's factors in SCL-90 (except that her marriage satisfaction does not correlate with her offspring's factors 4, 6 and 9; nor does her marriage stability correlate to her offspring's factors 8 and 10). Whereas her sexual life shows significantly negative or highly significantly negative correlation with only the total score and factors 4 and 5. Her marriage satisfaction at present, just like that of father's, bears highly significantly negative correlation with only factor 10 and the total score. Mother's marriage stability at present has significantly negative or highly significantly negative correlation with all factors in SCL-90 except for factors 2, 7, 10 and the total score. The sexual life at present evaluated by mother only possesses significantly negative or highly significantly negative correlation with factors 5, 8, 9 and the total score.

4 Conclusion

Marriage change is the most important stress life event of people. It will surely produce some effects upon the mental health of the couple concerned and their offspring. Some meaningful conclusions have been reached in this study.

Table 1. The correlation of the couple's factors in SCL-90 with their marriage quality

SCL-90 / Marriage Quality	1	2	3	4	5	6	7	8	9	10	Total Score
Correlation of marriage quality evaluated by father with his factors in SCL-90:											
A	−.196**	−.161*	−.065	−.241***	−.132*	−.106	−.191**	−.126*	−.164*	−.112*	−.155*
B	−.165*	−.191**	−.160*	−.248***	−.186**	−.116	−.205**	−.217***	−.245***	−.140*	−.228**
C	−.124*	−.148*	−.077	−.193**	−.073	−.044	−.188**	−.117*	−.121*	−.052	−.124*
D	−.117*	−.115*	−.104	−.189**	−.108	−.079	−.156*	−.159*	−.139*	−.065	−.129*
E	−.180**	−.158*	−.178**	−.200**	−.192**	−.113	−.172**	−.186**	−.198**	−.116	−.211**
F	−.239***	−.283***	−.168*	−.225***	−.152*	−.119	−.158*	−.138*	−.180**	−.148*	−.250***
Correlation of marriage quality evaluated by father with mother's factors in SCL-90:											
A	−.105	−.161*	−.154*	−.261***	−.250***	−.210***	−.194*	−.250***	−.269***	−.180**	−.275***
B	−.066	−.191**	−.200**	−.230***	−.245***	−.151*	−.140*	−.221***	−.229***	−.138*	−.239***
C	−.109	−.148*	−.150*	−.240***	−.252***	−.223***	−.123*	−.219***	−.185**	−.118	−.258***
D	−.018	−.115*	−.125*	−.261***	−.171**	−.171**	−.128*	−.187**	−.178**	−.161*	−.171*
E	−.077	−.158*	−.181**	−.282***	−.239***	−.234***	−.140*	−.223***	−.229***	−.157*	−.215**
F	−.224***	−.283***	−.207**	−.311***	−.251***	−.346***	−.163*	−.273***	−.239***	−.254***	−.374***
Correlation of marriage quality evaluated by mother with her own factors in SCL-90:											
A	−.061	−.075	−.053	−.204**	−.076	−.145**	−.042	−.120*	−.037	−.086	−.144*
B	.024	−.035	−.095	−.125	−.089	−.066	−.010	−.066	−.047	−.077	−.087
C	−.093	−.106	.426***	−.192**	−.124*	−.163*	−.433***	−.026	−.007	.110	−.127*
D	−.084	−.152*	−.109	−.278***	−.077	−.135*	−.006	−.121	−.085	−.123	−.097
E	−.141**	−.212**	−.128*	−.230***	−.130	−.131*	.032	−.180**	−.171**	−.097	−.110
F	−.178**	−.266**	−.137*	−.331***	−.186**	−.258***	−.109*	−.224***	−.216***	−.185**	−.244***
Correlation of marriage quality evaluated by mother with father's factors in SCL-90:											
A	−.039	−.075	−.005	−.125*	−.028	−.032	−.067	−.073	−.057	.001	−.067
B	−.068	−.035	−.023	−.096	−.021	−.067	−.081	−.023	−.096	.006	−.104
C	−.023	−.106	−.025	−.032	−.021	−.416***	.006	.000	−.027	−.156*	−.034
D	.033	−.152*	.063	−.021	.052	−.007	.092	−.014	.006	.028	.006
E	−.092	−.212**	−.061	−.117*	−.068	−.114*	−.021	−.063	−.123*	−.061	−.125*
F	−.080	−.215**	.040	−.045	.022	.023	.065	−.006	−.073	.022	−.077
Correlation of marriage quality evaluated by father with offspring's factors in SCL-90:											
A	−.142*	−.164**	−.133*	−.160**	−.108	−.139*	−.151**	−.082	−.286**	−.034	−.182**
B	−.163**	−.164**	−.182**	−.141*	−.126*	−.115*	−.109	−.065	−.169**	.055	−.189**
C	−.113*	−.110*	−.151**	−.162*	−.131*	−.103	−.196**	−.061	−.212**	−.079	−.185**
D	−.099	−.095	−.078	−.041	−.089	−.082	−.085	−.097	−.045	−.183**	−.124*
E	−.184**	−.127*	−.170**	−.159*	−.146**	−.136*	−.112*	−.117*	−.117*	.087	−.053
F	−.104	−.146**	−.091	−.131*	−.130*	−.078	−.135*	−.113*	−.224**	−.230**	−.161**
Correlation of marriage quality evaluated by mother with offspring's factors in SCL-90:											
A	−.125*	−.149*	−.160**	−.078	−.156**	−.105	−.096	−.202***	−.094	−.164**	−.114*
B	−.227***	−.193**	−.199**	−.180**	−.152**	−.130*	−.223***	−.090	−.218**	.038	−.178**
C	−.035	−.039	.007	−.115*	−.405***	−.009	−.038	−.028	−.033	−.044	−.294**
D	−.039	−.075	.009	−.069	.001	.004	−.006	−.052	−.063	−.178**	−.185**
E	−.157**	−.083	−.196**	−.123*	−.111	−.177**	−.099	−.125*	−.126*	.031	−.094
F	−−.072	−.102	−.066	−.112	−.121*	−.075	−.101	−.140*	−.202**	−.084	−.148*

Notice: The numbers 1 to 10 and letters A to F respectively stand for as follows: 1: Somatization; 2: Obsessive-Compulsive; 3: Interpersonal sensitivity; 4: Depression; 5: Anxiety; 6: Hostility; 7: Photic anxiety; 8: Paranoid ideation; 9: Psychoticism; 10: Others. A: Marriage satisfaction at the early stage of married life; B: Marriage stability at the early stage of married life; C: Sexual life at the early stage of married life; D: The present marriage satisfaction; E: The present marriage stability; F: The present sexual life.

Firstly, couple's subjective feeling about their own marriage, which sensitively indicates their marital changes, may serve as an index of marriage quality. There is no significant difference between the assessment made by the couple and that made by their offspring, which shows that such an index is subjective, true and objective as well.

Secondly, the psychological symptom level of a couple (i. e., most factors and the total score in SCL-90) respectively bears significantly negative or highly significantly negative correlation with the self-rated marriage quality (consisting of marriage satisfaction, stability and sexual satisfaction). This indicates that the subjective feelings of a couple

about their marriage may affect their own psychological symptom level, especially their depressive feeling and hostility. It is significant to notice that the sexual satisfaction respectively felt by husband and wife has significantly negative or highly significantly negative correlation with psychological symptom (most factors and the total score in SCL-90). This shows that sexual satisfaction is indeed a major factor which affects psychological symptom level (Locke, 1959). Great attention should be attached to this point in psychological consultation.

Thirdly, according to the study made by Liu Peiyi et al, mental health is only related to self-rated marriage happiness(Liu, 1991). In this study, we have found that the father's psychological symptom level is related to the self-rated marriage quality, but has no relation with the marriage quality evaluated by the mother, which agrees to the results of Liu Peiyi's study. However, we have discovered that mother's psychological symptom level is significantly related to the marriage quality evaluated by father (it bears significantly negative or highly significantly negative correlation with almost every factor in SCL-90 and the total score). Such result indicates that father is not sensitive to mother's mental feelings about the marriage, but mother is quite sensitive to father's mental feelings about the marriage. This, on one hand, is perhaps because the male is, comparatively speaking, not very sensitive; on the other hand, the male is likely to get some compensation from other aspects. The above discoveries have provided theoretic foundation for psychological consultation about marriage and sensitivity training of couples.

Fourthly, parents' marriage quality will exert some influence upon the mental health level of their offspring who have left home for college. Overall, effects of parents' marriage quality on the mental health level of the offspring is not so great as on that of parents themselves, but they are greater than the mother's on the father. This indicates that the children, though left home already, are still very sensitive to marital changes of their parents. Further analyses show that parent's marriage satisfaction and stability at the early stage will bring about greater influence upon their children's mentality than their marriage quality at present; the psychological influence of parents' marriage stability upon the children is much greater than that of marriage satisfaction and sexual satisfaction, the marriage stability evaluated by mother in particular. This proves that family life experiences in one's childhood still have influences on people after they have grown up, and that maintenance of marriage provides protection for offspring's mental health. Besides, marriage quality of parents, judged from relative factors in SCL-90, will exert comprehensive influence upon psychological symptoms of the offspring.

Further efforts should be made to study the mechanism so as to understand better how marriage quality influences the mental health of couple themselves and their children.

Acknowledgments

This study is part of the key planned reasearch pro; ect of Social Science of Henan Province (No. 2004FSH006)

Corresppondence to:
Yuzhong Wang
Psychology Department, School of Education
Zhengzhou University
Zhengzhou, Henan 450052, China
Telephone: 86-371-6742-8778
Email: wyz7941391@126.com

References

1. Chen Changhui. Symptom checklist 90 (SCL-90), rating scales for mental health, edited by Wang Xiangdong, et al. Chinese Mental Health Journal 1999 (revised and enlarged edition): 31 – 9.
2. Dobson KS. Marital and social adjustment in depressed and remarried women. Journal of Clinical Psychology 1987; 43(2): 261 – 5.
3. Li Youhui, Li Hua, Wo Min. Paired study of personality characteristics of children from divorced families. Chinese Mental Health Journal 1999; 13(5): 302 – 3.
4. Liu Peiyi, He Mutao. Marriage, family and mental health — an analysis of 118 couples of young intellectuals. Chinese Mental Health Journal 1991; 5(5): 193 – 5.
5. Locke HJ, Wallace KM. Short marital-adjustment and prediction test: their reliability and validity. Marriage and Family 1959: 160 – 78.
6. Moffit PF. Mental health in marriage: the roles of need for affiliation, sensitivity to rejection and other factors. Journal of Clinical Psychology 1986; 42(11): 68 – 72.
7. Rabin JG. Life events stress and illness. Science 1976; 194: 1013.
8. Yang Desen, Zhang Yalin. Life Events Scales: Behavioral Medicine. Hunan Normal University Press, Changsha, Hunan, China. 1990: 285 – 301.
9. Yu Guoliang, Jin Donxian. Effects of marital and generational relations upon psychological behavior of 3-6-year-old children. Psychology Science 2003; 26(4): 508 – 610.

Received September 22, 2005

Author Index

Subject Index

Instructions to Authors

1. General Information

(1) **Goals**: As an international journal published both in print and on internet, *Life Science Journal* is dedicated to the dissemination of fundamental knowledge in all areas of life science. The main purpose of *Life Science Journal* is to enhance our knowledge spreading in the world under the free publication principle. It publishes full-length papers (original contributions), reviews, rapid communications, and any debates and opinions in all the fields of life science.

(2) **Categories of publication**: Research articles, reviews, objective descriptions, research reports, opinions/debates, news, letters to editor, meeting report.

(3) **Cover feature**: The covers of *Life Science Journal* feature illustrations the Editor-in-Chief selects from the articles scheduled for publication in that issue. Authors whose articles are chosen for a cover feature will be asked to provide a high-quality version of the selected illustration as well as a brief legend (four to five sentences) describing the significance of the image. In light of the rapid production schedule for journal covers, authors are expected to provide the requested material within 3 days.

(4) **Publication costs**: US $ 30 per printed page of an article to defray costs of the publication will be paid by the authors when it is accepted. Extra expense for color reproduction of figures will be paid by authors (estimate of cost will be provided by the publisher for the author's approval). For the starting, publication fee will be waived for the current issues and they will be supported by Zhengzhou University.

(5) **Journal copies to authors**: Two hard copies of the journal will be provided free of charge for each author.

(6) **Additional copies bought by authors**: Additional hard copies could be purchased with the price of US $ 4/issue (mailing and handling cost included).

(7) **Distributions**: Web version of the journal is freely opened to the world without payment or registration. The journal will be distributed to the selected libraries and institutions for free. US $ 5/issue hard copy is charged for the subscription of other readers.

(8) **Advertisements**: The price will be calculated as US $ 400/page, i. e. US $ 200/a half page, US $ 100/a quarter page, etc. Any size of the advertisement is welcome.

2. Manuscripts Submission

(1) **Submission methods**: Electronic submission through email is encouraged and hard copies plus an IBM formatted computer diskette would also be accepted.

(2) **Software**: The Microsoft Word file will be preferred.

(3) **Font**: Normal, Times New Roman, 10 pt, single space.

(4) **Indent**: Type 4 spaces in the beginning of each new paragraph.

(5) **Manuscript**: Do not use "Footnote" or "Header and Footer".

(6) **Title**: Use Title Case in the title and subtitles, e. g. **"Debt and Agency Costs"**.

(7) **Figures and tables**: Use full word of figure and table, e. g. "**Figure** 1. Annul income of different groups", **Table** 1. Annual increase of investment".

(8) **References**: Number the references in the order of their first mention in the text. References should include all the authors' last names and initials, title, journal, year, volume, issue, and pages etc.

***Reference examples*:**

Journal article: Hacker J, Hentschel U, Dobrindt U. Prokaryotic chromosomes and disease. Science 2003;301(34):790 – 3.

Book: Berkowitz BA, Katzung BG. Basic and clinical evaluation of new drugs. In: Katzung BG, ed. Basic and Clinical Pharmacology. Appleton & Lance Publisher. Norwalk, Connecticut, USA. 1995:60 – 9.

(9) **Submission address**: America: lifesciencej@gmail.com, Marsland Press, P. O. Box 21126, Lansing, Michigan 48909, USA.

China: lifesciencej@zzu. edu. cn, Zhengzhou University, 100 Science Road, Zhengzhou, Henan 450001, China

(10) **Reviewers**: Authors are encouraged to recommand 2 – 8 competent reviewers with their names and email addresses.

3. Manuscript Preparation

Each manuscript is suggested to include the following components but authors can do their own ways:

(1) Title. Including each author's full name; institution (s) with which each author is affiliated, with city, state/province, zip code, and country.

(2) Abstract. Including Background, Materials and Methods, Results, and Discussion.

(3) Keywords.

(4) Abbreviations. All abbreviations needed are listed here, so that they could be used directly in the article.

(5) Introduction.

(6) Materials and Methods.

(7) Results.

(8) Discussion.

(9) Acknowledgments.

(10) Correspondence. Correspondence author's full name, institution, city, state/province, zip code, country, telephone number, facsimile number (if available), and email address are listed here.

(11) References.

4. Copyright and Permissions

Life Science Journal

Acta Zhengzhou University Overseas Edition

Volume 3 Number 1, January 2006

Published by:
Zhengzhou University
Marsland Press

Sponsor:
North American Branch of Zhengzhou University Alumni

Zhengzhou University
100 Science Road
Zhengzhou, Henan 450001, China
Telephone: 86-371-6778-1272
Email:lifesciencej@zzu.edu.cn
Website:http://life.zzu.edu.cn

Marsland Press
P. O. Box 21126
Lansing, Michigan 48909, USA
Telephone: 517-980-4106
Email: lifesciencej@gmail.com
Website: http://www.sciencepub.org

ISSN 1097-8135

Life Science Journal
Volume 3 Number 1 January 2006